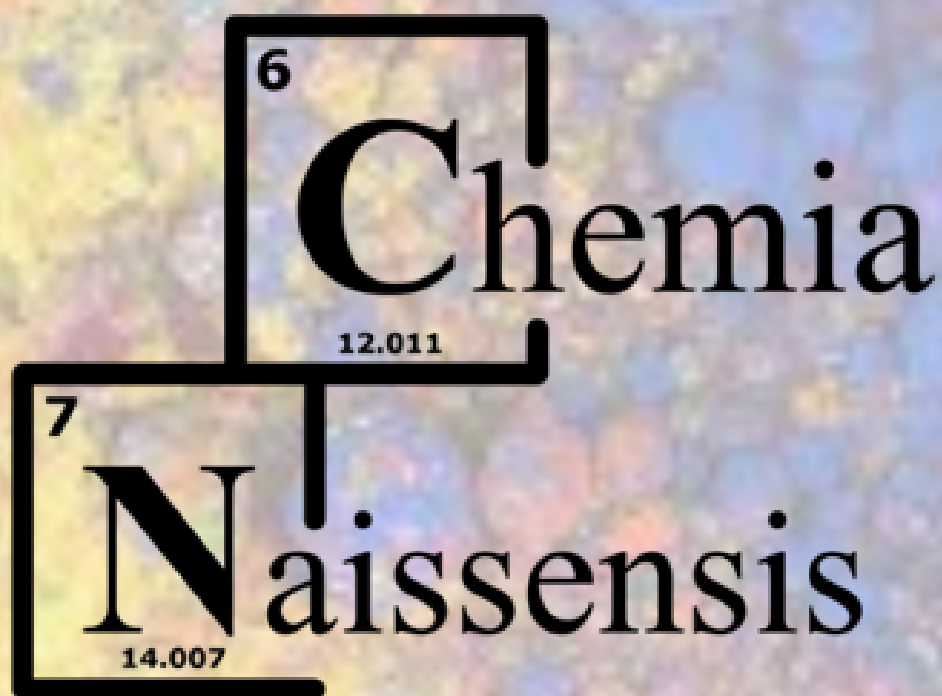


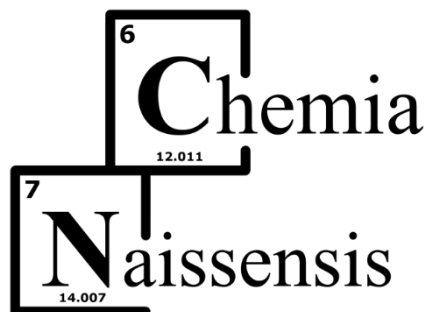
September 2021 Volume 4, Issue 1

www.pmf.ni.ac.rs/chemianaissensis



ISSN 2620-1895

University of Niš, Faculty of Sciences and Mathematics



ISSN 2620-1895

Volume 4, Issue 1

September 2021

Category: M54

https://kobson.nb.rs/upload/documents/MNTR/Kategorizacija_casopisa/2019/MNTR2019_hemija.pdf

Publisher:

Faculty of Sciences and Mathematics, University of Niš

Editor-in-Chief:

Dr Vesna Stankov Jovanović, Department of Chemistry, Faculty of Sciences and Mathematics, University of Niš, Republic of Serbia

Deputy Editor:

Dr Biljana Arsić, Department of Chemistry, Faculty of Sciences and Mathematics, University of Niš, Republic of Serbia

Editors:

Analytical Chemistry

Dr Aleksandra Pavlović, Department of Chemistry, Faculty of Sciences and Mathematics, University of Niš, Republic of Serbia

Physical Chemistry

Dr Snežana Tošić, Department of Chemistry, Faculty of Sciences and Mathematics, University of Niš, Republic of Serbia

Organic Chemistry and Biochemistry

Dr Aleksandra Đorđević, Department of Chemistry, Faculty of Sciences and Mathematics, University of Niš, Republic of Serbia

Inorganic Chemistry

Dr Dragan Đorđević, Department of Chemistry, Faculty of Sciences and Mathematics, University of Niš, Republic of Serbia

Chemical Engineering

Dr Marjan Randelović, Department of Chemistry, Faculty of Sciences and Mathematics,
University of Niš, Republic of Serbia

Chemical Education

Dr Vesna Stankov Jovanović, Department of Chemistry, Faculty of Sciences and Mathematics,
University of Niš, Republic of Serbia

Language Editors:

1. **Dr Selena Stanković**, Department of French Language and Literature, Faculty of Philosophy,
University of Niš, Republic of Serbia (French)
2. **Jovana Golubović** (French)
3. **Dr Nikoleta Momčilović**, Department of German Language, Faculty of Philosophy,
University of Niš, Republic of Serbia (German)
4. **Katarina Stamenković**, Department of German Language, Faculty of Philosophy, University
of Niš, Republic of Serbia (German)
5. **Dr Nadežda Jović**, Department of Serbian language and literature, Faculty of Philosophy,
University of Niš, Republic of Serbia (Serbian)
6. **Jelena Stošić**, Department of Serbian language and literature, Faculty of Philosophy,
University of Niš, Republic of Serbia (Serbian)

PR Manager:

Dr Radomir Ljupković, Department of Chemistry, Faculty of Sciences and Mathematics,
University of Niš, Republic of Serbia

Technical Secretary:

1. **Dr Jelena Nikolić**, Department of Chemistry, Faculty of Sciences and Mathematics,
University of Niš, Republic of Serbia
2. **Milica Nikolić**, Department of Chemistry, Faculty of Sciences and Mathematics, University
of Niš, Republic of Serbia

IT Support:

Predrag Nikolić, Haed of the Informational&Computational Center of Faculty of Science and
Mathematics, University of Niš, Republic of Serbia

Cover design:

Dr Vesna Stankov Jovanović

CONTENT

Review article

Danijela Kostic, Nenad Krstic and Marina Blagojevic

Alternative Periodic System of the Elements 1

Alternativni periodni sistem elemenata 14

Tableau périodique alternatif des éléments 15

Альтернативные периодические системы элементов 16

Alternative Periodensysteme der Elemente 17

Research articles

Jelena M. Purenović, Milovan M. Purenović and Marjan S. Ranđelović

The Influence of Metal Microelements, Colloids and Organic Phase on Physical-chemical Properties and Processes in Peloids 18

Utica j metalnih mikroelemenata, koloida i organske faze na fizičko-hemijska svojstva i procese u peloidima 36

L'influence des microéléments métalliques, des colloïdes et de la phase organique sur les propriétés et les processus physico-chimiques des péloïdes 37

Влияние металлических микроэлементов, коллоидов и органической фазы на физико-химические свойства и процессы в пелоидах 38

Der Einfluss von metallischen Mikroelementen, Kolloiden und der organischen Phase auf physikalisch-chemische Eigenschaften und Prozesse in Peloiden 39

Emilija Pecev-Marinković, Ana Miletić, Aleksandra Pavlović and Vidoslav Dekić

Development and application of kinetic-spectrophotometric method for analysis of diflubenzuron in soil samples using SPE followed by HPLC method 40

Razvoj i primena kinetičko-spektrofotometrijske metode za analizu diflubenzurona u uzorcima zemljišta primenom SPE praćene HPLC metodom 62

Développement et application d'une méthode cinétique-spectrophotométrique pour l'analyse du diflubenzuron dans des échantillons de sol à l'aide de la SPE suivie de la méthode HPLC 63

Разработка и применение кинетико-спектрофотометрического метода анализа дифллубензурана в образцах почвы с использованием ТФЭ с последующей ВЭЖХ 64

Entwicklung und Anwendung einer kinetisch-spektrophotometrischen Methode zur Analyse von Diflubenzuron in Bodenproben mittels SPE gefolgt von HPLC-Methode 65

Todosijević Anka, Jančić Minić Aleksandra, Mihailović Vladimir and Srečković Nikola

Synthesis, characterization, and antimicrobial activity of novel 2-ferrocenyl-1,3-thiazolidin-4-thiones 66

Sinteza, karakterizacija i antimikrobna aktivnost novih 2-ferocenil-1,3-tiazolidin-4-tiona 85

Synthèse, caractérisation et activité antimicrobienne de nouvelles 2-ferrocényl-1,3-thiazolidine-4-thiones 86

Синтез, характеристика и антимикробная активность новых 2-ферроценил-1,3-тиазолидин-4-тионов 87

Synthese, Charakterisierung und antimikrobielle Aktivität von neuartigen 2-Ferrocenyl-1,3-Thiazolidin-4-thionen 88

Necati MENEK, Serpil ZEYREKLİ and Yeliz KARAMAN

Investigation of Electrochemical Behavior of Mordant Dye (C.I. 17135) at Glassy Carbon and Silver Electrodes 89

Istraživanje elektrohemijskog ponašanja Mordant boje (C.I. 17135) na staklenim ugljeničnim i srebrnim elektrodama 105

Enquête sur le comportement électrochimique du colorant Mordant (C.I. 17135) aux électrodes de carbone vitreux et d'argent 106

Исследование электрохимического поведения красителя протравы (C.I. 17135) на стеклогуглеродных и серебряных электродах 107

Untersuchung zum elektrochemischen Verhalten von Mordant-Farbstoff (C.I. 17135) an Glaskohlenstoff- und Silberelektroden 108

Alternative Periodic System of the Elements

Danijela Kostic¹*, Nenad Krstic¹, Marina Blagojevic¹

1- University of Niš, Faculty of Sciences and Mathematics, Department of Chemistry, Višegradska 33, 18000 Niš, Serbia

ABSTRACT

For more than 150 years since the discovery of the periodic table of elements, there has been a need for its constant supplementation and improvement. As a result, today there are over 700 different periodic systems that aim to present the position of the elements more simply, effectively in the periodic table, their interrelationships and the possibility of building different compounds. In addition to two-dimensional, both three- and four-dimensional systems of elements have appeared. All of them, in addition to their great didactic significance, also have great scientific significance and represent guidelines for scientists in various multidisciplinary research. The exploration of new elements of both a more perfect and a comprehensive periodic table continues.

Keywords: Periodic system, modern forms of the Periodic system, alternative forms of the Periodic systems

Danijela Kostic*: danijelaakostic@yahoo.com
Nenad Krstic: nenad.krstic84@yahoo.com
Marina Blagojevic: marina.blagojevic2631@gmail.com

Introduction

The periodic elements' table is a tabular arrangement of chemical elements, organized on the basis of their atomic numbers (number of protons in the nucleus), electronic configuration and repetitive chemical properties. The elements are arranged in ascending order of atomic numbers, which is usually indicated by a chemical symbol in each field. It ranges from element 1 (hydrogen H) in the upper left corner to the newly approved element 118 (oganesson Og) in the lower right corner. The standard form of the table consists of a network of elements arranged in 18 columns and 7 rows, with two rows of elements below that table - lanthanides and actinoids (Figure 1). The rows of the table are called periods, and the columns are called groups, and some of the columns have special names such as halogen elements or noble gases. The table can be divided into four rectangular blocks: *s*-block to the left, *p*-block to the right, *d*-block in the middle and *f*-block below it (Mazur, 1974).

Periodic Table of the Elements

1 1IA 11A	2 IIA 2A											13 IIIA 3A	14 IVA 4A	15 VA 5A	16 VIA 6A	17 VIIA 7A	18 VIIIA 8A
1 H Hydrogen 1.00794	2 He Helium 4.00260											3 B Boron 10.811	4 C Carbon 12.011	5 N Nitrogen 14.00644	6 O Oxygen 15.9994	7 F Fluorine 18.998403	8 Ne Neon 20.1797
3 Li Lithium 6.941	4 Be Beryllium 9.01218	5 B Boron 10.811	6 C Carbon 12.011	7 N Nitrogen 14.00644	8 O Oxygen 15.9994	9 F Fluorine 18.998403	10 Ne Neon 20.1797	11 Na Sodium 22.98976928	12 Mg Magnesium 24.304	13 Al Aluminum 26.9815386	14 Si Silicon 28.0855	15 P Phosphorus 30.973762	16 S Sulfur 32.06	17 Cl Chlorine 35.4527	18 Ar Argon 39.948		
19 K Potassium 39.0983	20 Ca Calcium 40.078	21 Sc Scandium 44.955912	22 Ti Titanium 47.88	23 V Vanadium 50.9415	24 Cr Chromium 51.9961	25 Mn Manganese 54.938	26 Fe Iron 55.847	27 Co Cobalt 58.9332	28 Ni Nickel 58.6934	29 Cu Copper 63.546	30 Zn Zinc 65.39	31 Ga Gallium 69.723	32 Ge Germanium 72.64	33 As Arsenic 74.921595	34 Se Selenium 78.96	35 Br Bromine 79.904	36 Kr Krypton 83.80
37 Rb Rubidium 85.4678	38 Sr Strontium 87.62	39 Y Yttrium 88.90585	40 Zr Zirconium 91.224	41 Nb Niobium 92.90638	42 Mo Molybdenum 95.94	43 Tc Technetium 98.9062	44 Ru Ruthenium 101.07	45 Rh Rhodium 101.065	46 Pd Palladium 106.42	47 Ag Silver 107.8682	48 Cd Cadmium 112.411	49 In Indium 114.818	50 Sn Tin 118.710	51 Sb Antimony 121.757	52 Te Tellurium 127.6	53 I Iodine 126.90447	54 Xe Xenon 131.29
55 Cs Cesium 132.90545196	56 Ba Barium 137.327	57-71 Lanthanide Series	72 Hf Hafnium 178.49	73 Ta Tantalum 180.9479	74 W Tungsten 183.85	75 Re Rhenium 186.207	76 Os Osmium 190.23	77 Ir Iridium 192.22	78 Pt Platinum 195.08	79 Au Gold 196.966569	80 Hg Mercury 200.59	81 Tl Thallium 204.3833	82 Pb Lead 207.2	83 Bi Bismuth 208.98037	84 Po Polonium 209	85 At Astatine 209	86 Rn Radon 222.01758
87 Fr Francium 223	88 Ra Radium 226	89-103 Actinide Series	104 Rf Rutherfordium 261	105 Db Dubnium 262	106 Sg Seaborgium 263	107 Bh Bohrium 264	108 Hs Hassium 265	109 Mt Meitnerium 266	110 Ds Darmstadtium 267	111 Rg Roentgenium 268	112 Cn Copernicium 269	113 Uut Ununtrium 271	114 Fl Flerovium 277	115 Uup Ununpentium 278	116 Lv Livermorium 289	117 Uus Ununseptium 289	118 Uuo Oganesson 289
		57 La Lanthanum 138.90547	58 Ce Cerium 140.12	59 Pr Praseodymium 140.90768	60 Nd Neodymium 144.24	61 Pm Promethium 144.9127	62 Sm Samarium 150.36	63 Eu Europium 151.965	64 Gd Gadolinium 157.25	65 Tb Terbium 158.92534	66 Dy Dysprosium 162.50	67 Ho Holmium 164.93032	68 Er Erbium 167.26	69 Tm Thulium 168.93421	70 Yb Ytterbium 173.04	71 Lu Lutetium 174.967	
		89 Ac Actinium 227	90 Th Thorium 232.0377	91 Pa Protactinium 231.036888	92 U Uranium 238.02891	93 Np Neptunium 237.048173	94 Pu Plutonium 244.06422	95 Am Americium 243.061361	96 Cm Curium 247.07545	97 Bk Berkelium 247.071289	98 Cf Californium 251.083288	99 Es Einsteinium 252.083219	100 Fm Fermium 257.10358	101 Md Mendelevium 258.103868	102 No Nobelium 259.103868	103 Lr Lawrencium 260	
		Alkali Metals	Alkaline Earths	Transition Metals	Basic Metals	Semi-Metals	Nonmetals	Halogens	Noble Gases	Lanthanides	Actinides						

Figure 1. Periodic Table of the Elements

<https://www.thoughtco.com/how-to-use-a-periodic-table-608807>

Mendeleev's Periodic Table has historically expanded and improved with the discovery or synthesis of new elements and the development of new theoretical models.

When the four most recent additions to the table (synthetic elements nihonium, moscovium, tennessine and oganesson) were formally recognized in 2016, the remaining gaps were finally filled. All elements from atomic numbers 1 to 118 have been discovered or synthesized. On December 30, 2015, the International Union of Pure and Applied Chemistry (IUPAC, 2015) confirmed the completeness of the first seven rows of the Periodic Table (Figure 2).

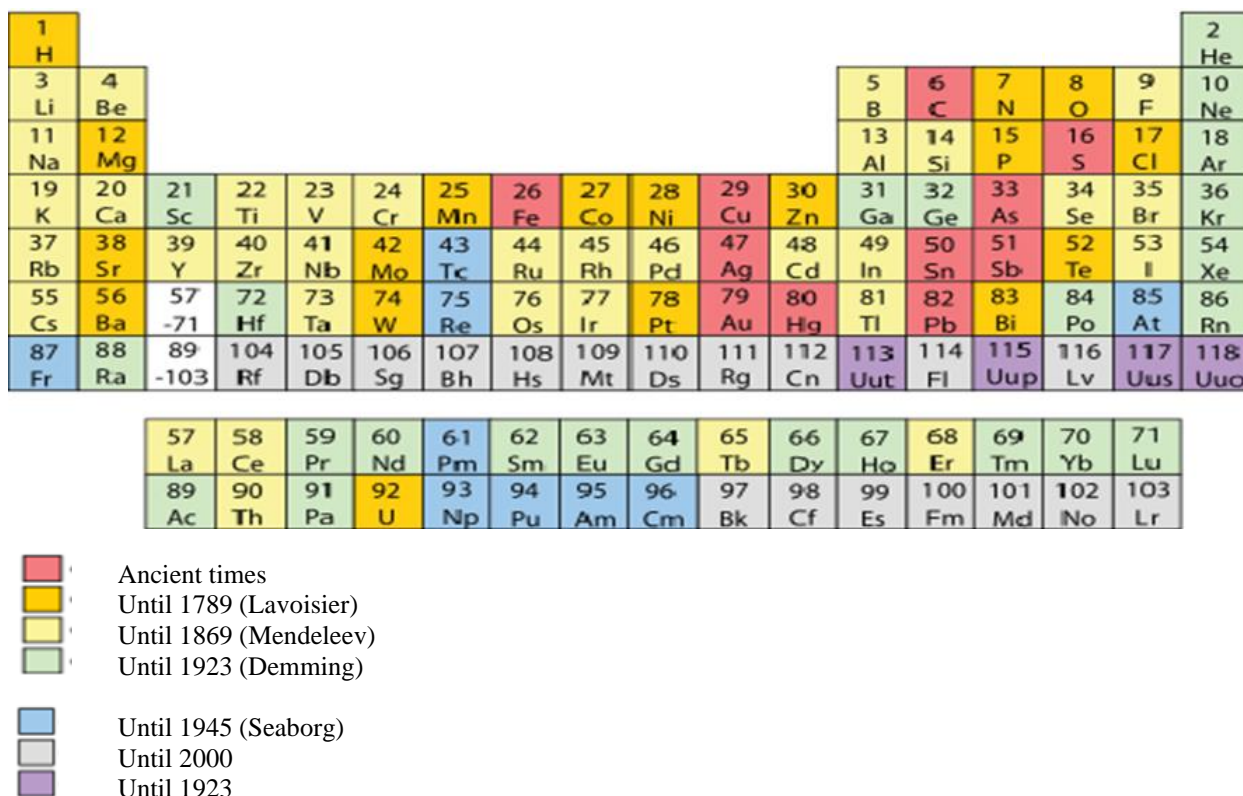


Figure 2. The discovery of chemical elements mapped to significant dates in the development of the periodic table

https://commons.wikimedia.org/wiki/File:Discovery_of_chemical_elements-en.svg

Elements with ordinal numbers up to 81 are stable elements found on Earth and they build most of the objects in the Universe. The next 13 elements are radioactive, but they are also on our planet. Although their half-life is very long, a million or even a billion years, they are rare on Earth, with the origin from meteorites and samples from the Moon. There are 24 more radioactive elements, which are created artificially, in special, laboratory conditions. Unlike naturally occurring radioactive elements, the half-life of this group of elements is much shorter.

The consequence of rapid decay is that these elements cannot be found in nature and are therefore synthesized in laboratories or nuclear reactors. Due to the rapid decay, detecting or determining their properties after production is a real challenge. The first element to be added as a synthetic was neptunium in 1940. (Siborg, 1946)

Alternative periodic systems

The periodic table remained essentially indisputable even after numerous discoveries in the world of science. Of course, there were some changes in the table, although they were relatively small and, in some cases, almost "cosmetic".

One might get the impression that Mendeleev's masterpiece has finally been completed, but the search for element 119 - which would be the first in a new order - is already underway in some laboratories in Japan.

The number of possible elements is not known. A somewhat recent estimate is that the Periodic Table could end shortly after crossing the 'island of stability', which is believed to occur around element 126, because the expansion of periodic and nuclide systems is limited by proton and neutron drop lines. Other significant proposals regarding the end of the Periodic Table include a break in element 128 proposed by John Emsley, a break in element 137 proposed by Richard Feynman, and a break in element 155 proposed by Albert Kazan.

It is not known whether the newly discovered elements will follow the trend of the current Periodic Table as the 8th period or whether additional adjustments and corrections will be necessary. There are currently several competing theoretical models for determining the position of elements with an atomic number less than or equal to 172 (Fricke et al., 1971)

It would be understandable to think that this would be the end of research. However, this is not the case. A simple internet search will reveal different variants of the periodic table.

Many researchers have created hundreds of variations in search of the perfect periodic table. There are short versions, long versions, circular versions, spiral versions, three and even four-dimensional versions. Many of them are certainly simply different ways of conveying the same information, but there are still disagreements about where some elements should be located. Alternative periodic systems are tabular representations of chemical elements that differ significantly from their organization or traditional layout in the Periodic Table. Many such systems have been invented so far, often for didactic reasons, because not all correlations between chemical elements can be effectively represented by a standard Periodic Table.

There are literally hundreds of variations (see Mark Leach's database), and spirals and 3D versions are particularly popular, such as "tongue behind cheek" (Figure 3) or the London Underground (Figure 4). Paul Giguere's 3-D periodic table consists of 4 billboards with the elements written on the front and the back (Giguère, 1965)



Figure 3. 3D 'Mendeleev flower' version of the table

<https://theconversation.com/the-periodic-table-is-150-but-it-could-have-looked-very-different-106899>

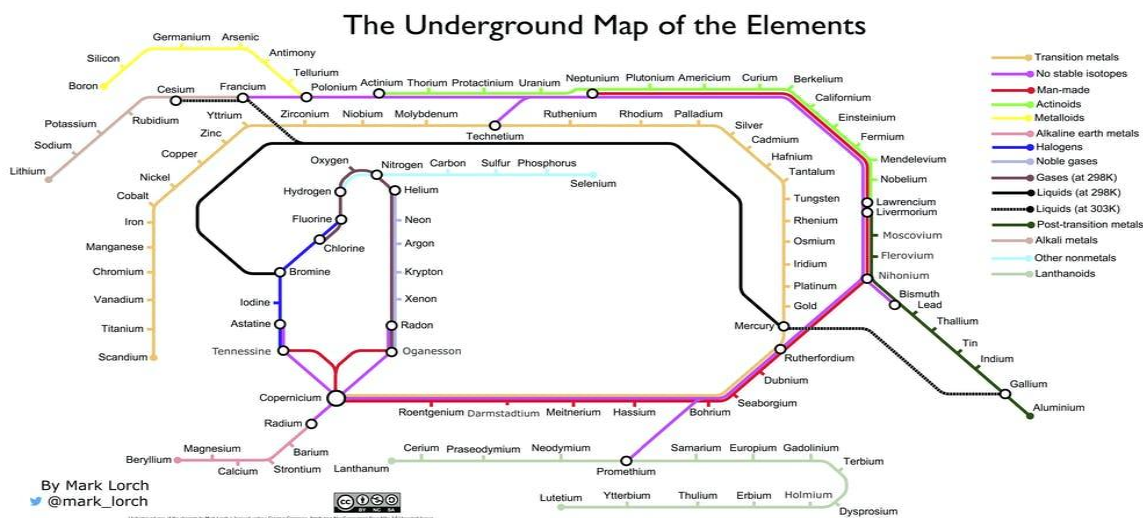
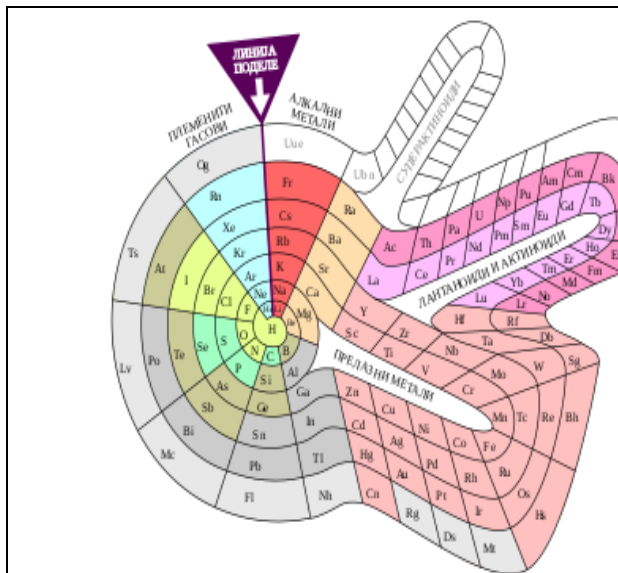


Figure 4. The Mark Lorch's underground map of the elements

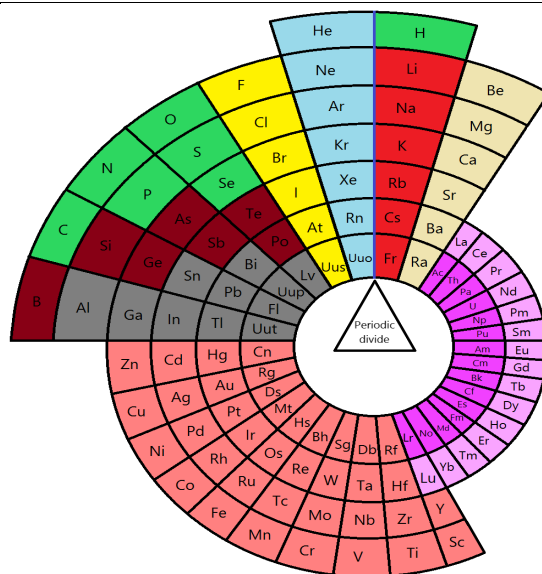
<https://theconversation.com/the-periodic-table-is-150-but-it-could-have-looked-very-different-106899>

Alternative periodic systems are most often developed to emphasize the different chemical and

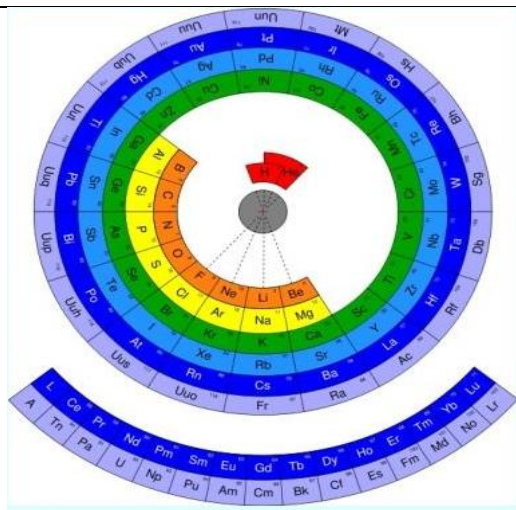
physical properties of elements that are not so obvious in the traditional Periodic Table. Some systems aim to emphasize both the nucleon and electronic structure of atoms. This can be achieved by changing the spatial relationship or arrangement that each element has in relation to the other element in the system (Figure 5).



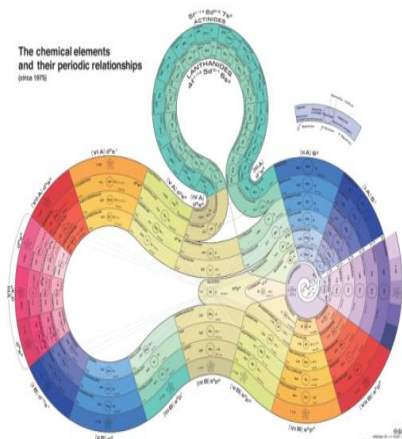
<https://commons.wikimedia.org/w/index.php?curid=27766488>



<https://commons.wikimedia.org/w/index.php?curid=25192173>



<https://commons.wikimedia.org/w/index.php?curid=3113760>



<https://commons.wikimedia.org/w/index.php?curid=54218895>

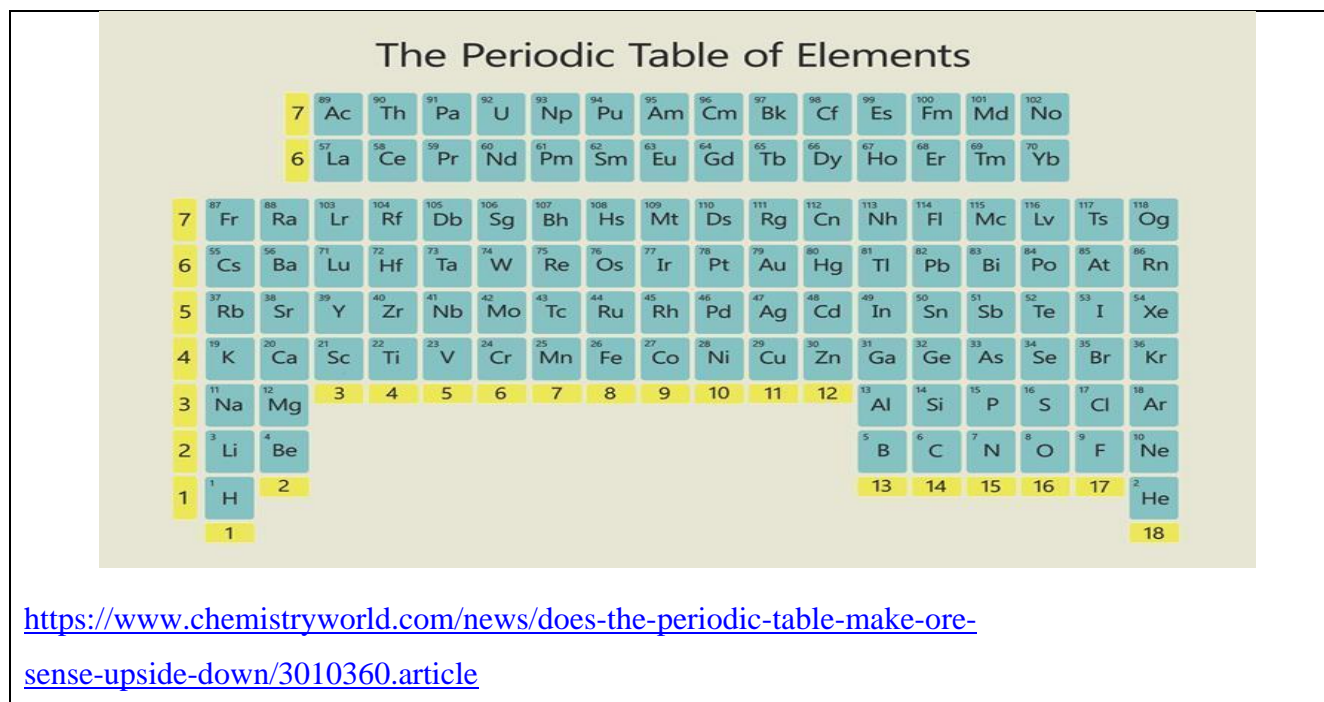


Figure 5. Alternative Periodic Table of the Elements

Other systems have emphasized the isolation of chemical elements throughout history.

Timothy Stowe created the physicist's periodic table. This table is a three-dimensional and the three axes represent the principal quantum number, orbital quantum number, and orbital magnetic quantum number. Helium is again a group 2 element (Bradley, 2011).

In 1984 an idea of a “structure map” was explored by Pettifor, who suggested that a well-structured chemical space could be derived by changing the sequence of the elements in the periodic table. He proposed a chemical scale that determines the “distance” between the elements on an one-dimensional axis and a Mendeleev number (MN): an integer showing the position of an element in the sequence. Pettifor claimed that binary compounds with the same structure type occupy the same region in a two-dimensional map plotted using the MNs (the Pettifor’s map). He evaluated the chemical scale by presenting a map clearly separating 34 different structure types of 574 binary AB compounds (Pettifor, 1984).

Later, Pettifor showed that the MN approach also works for other A_xB_y compounds. Although Pettifor derived the chemical scale and Mendeleev number empirically and based his assessment on only several hundred binary compounds, his study provided a phenomenally successful ordering of the elements confirmed in many later works. In this work, we denote Pettifor’s MN as MNP. We expect that a nonempirical method of finding the MNs would perform even better (Pettifor, 1986).

Villars *et al.* proposed a different enumeration of the elements (called periodic number, PN), emphasizing the role of valence electrons. The atomic number (AN) of the elements together with their 'periodic number' (PN) were found to form an efficient pair for the discussion of metallurgical and structural problems. The periodic number PN represents a different enumeration of the elements, emphasizing the role of the valence electrons. In contrast to the atomic number, PN depends in detail on the underlying Periodic Table of the elements. As a first result we describe the elemental-property parameters 'atomic size SZ_a ' and 'atomic reactivity RE_a ', derived from fits to various experimental and theoretical data sets. We argue that all elemental-property parameter patterns are derived from AN and PN. AN and PN represent fundamental elemental-property parameters independent from each other. Any pattern, which shows well-defined functional behavior within each group number GN, as well as within each main quantum number QN, can be included. On the example of compound formers/non-formers in binary, ternary and quaternary chemical systems we demonstrate that a quantitative link exists between material properties and AN, PN (or simple functions of both) of the constituent element (Villars, 2008).

Glawe *et al.* proposed another sequence of elements (modified MN, in this work, we represent this as MN_m) based on their similarity, defining elements A and B to be similar if they crystallize in the same structure type when combined with other elements of the periodic table. We believe that our proposed 'modified Pettifor scale' can be of use not only for the representation of structure maps, but also as a tool for both theorists and experimentalists to study possible chemical substitutions in the quest for new materials with tailored properties (Glawe, 2016).

In a correctly defined chemical space, closely located materials should have similar properties. The most promising materials will then be clustered in one or a few "islands" in this space. To predict new materials, it could be sufficient to explore these as lands instead of the entire chemical space. The fewer these islands are, the easier it would be to locate and explore them for promising materials. A chemical space containing many small islands is less amenable for the prediction of materials than the one with fewer big islands. Therefore, for evaluating each chemical space, it is useful to have these islands and calculate the number of (similar) materials they cover. For doing this, we used the idea of the clustering algorithm proposed by Rodriguez and Laio and applied it to clustering regions of the chemical space based on their similarity (Rodriguez and Laio, 2014).

The precise placement of certain elements depends on which features we want to emphasize. The last attempt to arrange the elements in this way was recently published in the journal *Physical Chemistry* by scientists *Zahed Allahyari* and *Artem R. Oganov*. Their approach, building on the earlier work of others, is to assign to each element what is called a Mendelian number (MN). There are several ways

to derive such numbers, but the latest study uses a combination of two basic quantities that can be measured directly: the atomic radius of the element and electronegativity (Festschrift, 2020).

In a well-ordered sequence of elements, the atoms with similar properties are close to each other. Therefore, in the two-dimensional chemical space based on such a sequence, the properties of neighboring binary systems should exhibit a close relation. On this premise, we evaluate different MNs: atomic number (AN), Villars' periodic number (PN), Pettifor's Mendeleev number (MNP), modified Mendeleev number (MNm), and Mendeleev numbers obtained in this work-the universal sequence of elements (USE).

Only 1591 binary and 80 unary systems are studied in the database which is about half of the total binary and unary systems that can be created from the combination of 80 elements; in total, 3240 systems can be created.

The number of clusters (*i.e.*, islands) that cover all binary systems in the chemical spaces of the MNs is a good quantitative evaluation of these MNs. The lower the number of clusters is, the better-clustered the chemical space is.

Having a well-defined sequence of the elements (Mendeleev numbers, or MNs), where similar elements take neighboring places, one can produce an organized map of properties for binary or more complex systems that leads to the prediction of new materials by having information on their neighboring systems. A simple, physically meaningful, and universal way to order the elements was defined. MN (USE), in addition to a few previously known MNs such as atomic number (AN), Villars' periodic number (PN), Pettifor's Mendeleev number (MNP), and modified Mendeleev number (MNm), using provided data on binary systems from different databases, such as ICSD and COD, was examined. Two dimensional maps of the hardness, magnetization, enthalpy of formation, and atomization energy were plotted using the provided data in the space of MNs, and it turned out that most of these sequences (except for AN) indeed work well for clustering materials with similar properties. The evaluation of the MNs showed the overall best clustering rate of the chemical spaces produced by USE for target spaces, *i.e.*, hardness, magnetization, and enthalpy of formation. Also, unlike other MNs, USE can be defined at any arbitrary pressure, which is a step forward for the prediction of materials under pressure. Physical meaning of the Mendeleev number (previously defined empirically): it is a collapsed one-number representation of the important atomic properties (such as atomic radius, electronegativity, polarizability, and valence).

If we want to develop replacement materials that omit the use of certain elements, insights from the arrangement of elements according to their MN can prove useful in that search. The importance of the prevalence of elements used in the production of new materials is presented by the example of the

periodic table in the figure below. This table not only illustrates the relative representation of the elements (the larger the framework for each element, the more it has), but also highlights the potential supply issue, relevant to technologies that have become ubiquitous and essential in our daily lives.

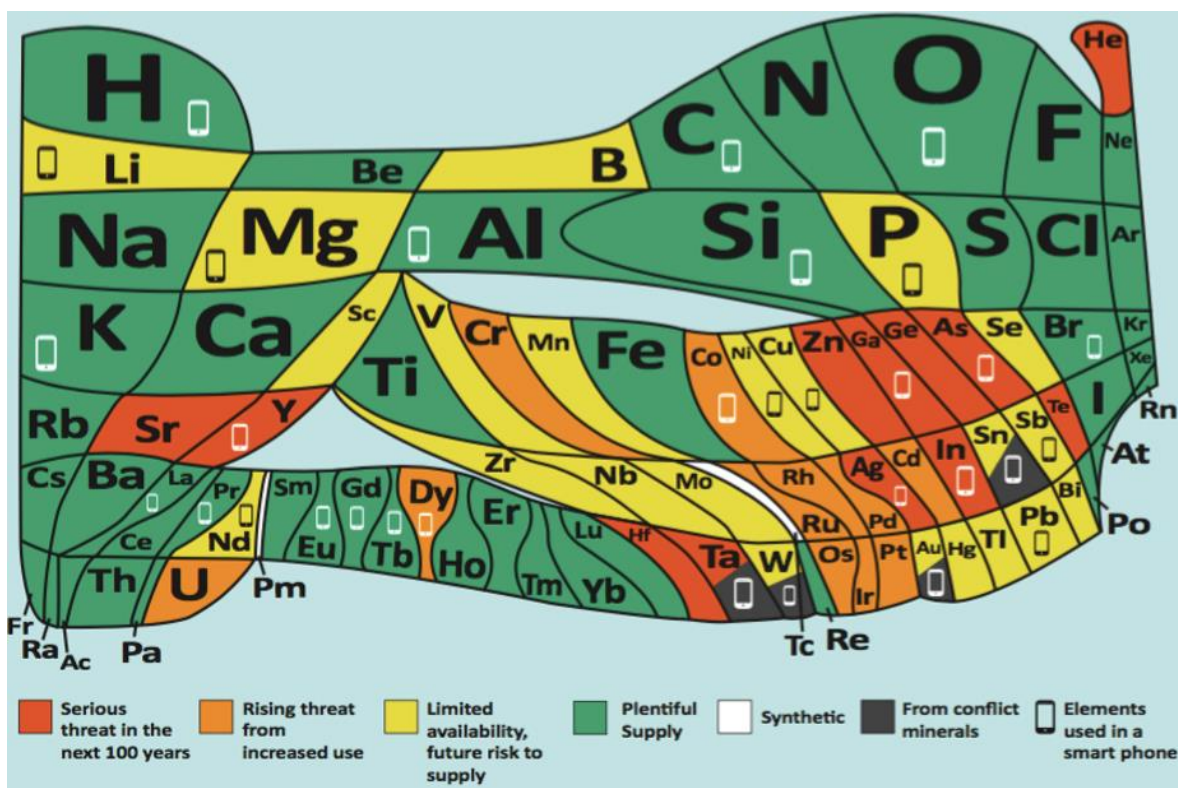


Figure 6. Periodic table showing the relative abundance of elements

<https://theconversation.com/periodic-table-new-version-warns-of-elements-that-are-endangered-110377>

As part of the celebrations, the European Chemical Society published a completely new version of the periodic table (Figure 6).

Each area of the new system is marked with a color that indicates its distribution. In most cases, the elements are not lost, but as we use them, they fall apart and are much easier to recycle. Red indicates that the elements will be much less available in 100 years or less. The orange and yellow surfaces on the new periodic table predict problems caused by the increased use of these elements. Green means that a large amount is available. The four elements - tin (Sn), tantalum (Ta), tungsten (W) and gold (Au) - are colored black because they often originate from “conflicting” minerals; that is, from mines where wars are fought over their ownership. Their color can have a more ethical meaning because it is a reminder that producers must carefully monitor their origin to make sure that people are not harmed to provide the minerals in question.

The three main ways to preserve some elements that are already at a minimum are: replace them

with others, recycle them, or simply reduce their use. Huge efforts are being made to find alternative materials. If we do not take these issues more seriously, many of the items and technologies we take for granted today may be relics of old age after a few generations - or only available to wealthier people. But as the new version of the periodic table underscores, we must do everything in our power to preserve and recycle the first 90 precious elements that make up our wonderfully diverse world (Norman, 2020).

Is the resistance of chemists to changes related to the line boundaries of the standard Periodic Table so great that they cannot accept other solutions, even when other tables offer a better representation of basic chemical principles? Maybe it is just pragmatism. One cynical critic suggested that the compressed version was favored because it fits well on a standard sheet of paper. Aesthetics are important, but they always take the last place in relation to clarity. Ideally, the data in the table should be visible and obvious.

One of the many virtues of the Periodic Table is that it brings simplification and coherence to the world of chemistry. Since the Periodic Table is by definition based on recurring trends, any such table can be used to obtain relationships between the properties of elements or to predict the properties of others. Instead of knowing the properties of all 118 currently known elements, it is enough to gain knowledge about the typical properties of about 10 of them. Therefore, the Periodic Table of the Elements, whether in standard form or in some other variant, provides a useful framework for the analysis of chemical behavior and is widely used in chemistry and other sciences.

Conclusion

Scientific theories are changing. The periodic table contains 118 elements and all rows and columns are filled in. Is it complete and perfect? Laboratories around the world are synthesizing new, even more difficult elements. Synthesis or the discovery of new weights raises the question of how much the 150-year-old Periodic Table of the Elements can be modified to meet any new extensions. After so many years since the creation of the Periodic Table, we can conclude that it is not only a basic educational tool but is useful for researchers looking for new materials. New Periodic Table models should not serve as replacements for previous views. Alternative periodic tables are developed often to highlight or emphasize different chemical or physical properties of the elements which are not so obvious in traditional periodic tables.

Acknowledgement

Authors want to thank Dr Biljana Arsić, Department of Chemistry, Faculty of Sciences and Mathematics, University of Nis, Republic of Serbia for language corrections.

Conflict-of-Interest Statement

None.

References

- Bradley, D., (2011) At Last, A Definitive Periodic Table?, ChemistryViews.org., doi: 10.1002/chemv.201000107
- Festschrift, A. B., Allahyari, Z., Oganov, A. R. (2020), Nonempirical Definition of the Mendeleev Numbers: The Journal of Physical Chemistry virtual special issue, doi:10.1021/acs.jpcc.0c07857
- Fricke, B., Greiner, W., Waber, J. T. (1971). The continuation of the periodic table up to $Z = 172$. The chemistry of superheavy elements". *Theoretica Chimica Acta*. 21 (3), 235– 260.
- Giguère, P. (1965) "The 'new look' for the periodic system". *Chemistry in Canada* vol. 18 (12), 36–39
- Glawe, H., Sanna, A., Gros, E., Marques M. A. L., (2016) The optimal one-dimensional periodic table: a modified Pettifor chemical scale from data mining, *New Journal of Physic*. 18 093011
- IUPAC, Discovery and Assignment of Elements with Atomic Numbers 113, 115, 117 and 118, December 30, 2015
- Mazurs, E. G. (1974) *Graphical Representations of the Periodic System During One Hundred Years*. University of Alabama Press, Alabama
- Norman, N., (2020) Periodic table: scientists propose new way of ordering the elements
- Pettifor, D. G., (1984) A Chemical Scale for Crystal-Structure Maps. *Solid State Commun*. 1984, 51, 31–34.
- Pettifor, D. G., (1986), The Structures of Binary Compounds. I. Phenomenological Structure Maps. *Journal of Physic C: Solid State Physic*. 19, 285–313.
- Rodriguez, A., Laio, A., (2014) Clustering by fast search and find of density peaks, *Science* 344, 1492-1496
- Seaborg, G., (1946), Seaborg Announces Fissionable Neptunium, *Chemical Engineering News*, 24, 20, 2764-2746
- Villars, P., Daams, J., Shikata, Y., Rajan, S., Iwat, A., (2008) A new approach to describe elemental-property parameters, *Chemistry Metal Alloys* 1, 1-23
- <https://www.thoughtco.com/how-to-use-a-periodic-table-608807>
- https://commons.wikimedia.org/wiki/File:Discovery_of_chemical_elements-en.svg
- <https://theconversation.com/the-periodic-table-is-150-but-it-could-have-looked-very-different-106899>

<https://theconversation.com/the-periodic-table-is-150-but-it-could-have-looked-very-different-106899>

<https://commons.wikimedia.org/w/index.php?curid=27766488>

<https://commons.wikimedia.org/w/index.php?curid=25192173>

<https://commons.wikimedia.org/w/index.php?curid=3113760>

<https://commons.wikimedia.org/w/index.php?curid=54218895>

<https://www.chemistryworld.com/news/does-the-periodic-table-make-more-sense-upside-down/3010360.article>

Alternativni periodni sistem elemenata

Danijela Kostić^{1*}, Nenad Krstić¹, Marina Blagojević¹

1- Univerzitet u Nišu, Prirodno-matematički fakultet, Departman za hemiju, Višegradska 33, 18000 Niš, Srbija

SAŽETAK

Više od 150 godina, od otkrića periodnog sistema elemenata, postojala je potreba za njegovim stalnim dopunjavanjem i poboljšavanjem. Kao rezultat toga, danas postoji preko 700 različitih periodnih sistema koji imaju za cilj da jednostavnije i efikasnije predstave položaj elemenata u periodnom sistemu, njihove međusobne odnose i mogućnost građenja različitih jedinjenja. Pored dvodimenzionalnih, pojavili su se i trodimenzionalni i četvorodimenzionalni sistemi elemenata. Svi oni, pored velikog didaktičkog značaja, imaju i veliki naučni značaj i predstavljaju smernice naučnicima u različitim multidisciplinarnim istraživanjima. Istraživanja savršenijih i sveobuhvatnijih periodnih sistema se nastavljaju.

Ključne reči: periodni sistem, savremeni oblik periodnog sistema, alternativni oblik periodnog sistema

Tableau périodique alternatif des éléments

Danijela Kostic^{1*}, Nenad Krstic¹, Marina Blagojevic¹

1- Université de Niš, Faculté des sciences naturelles et des mathématiques, Département de chimie, Višegradska 33, 18000 Niš, Serbie

RÉSUMÉ

Depuis plus de cent cinquante ans, depuis la découverte du tableau périodique des éléments, il a été nécessaire de le compléter et de l'améliorer constamment. En conséquence, il existe aujourd'hui plus de sept cents tableaux périodiques différents qui visent à présenter plus simplement et plus efficacement la position des éléments dans le tableau périodique, leurs interrelations, ainsi que la possibilité de construire les différents composés. En plus des tableaux bidimensionnels, sont apparus aussi des tableaux des éléments tridimensionnels et quadridimensionnels. Tous ces tableaux, outre leur grande importance didactique, possèdent également une grande valeur scientifique et représentent des lignes directrices pour les scientifiques dans les diverses recherches multidisciplinaires. Les explorations des tableaux périodiques plus parfaits et plus complets se poursuivent.

Mots-clés: tableau périodique, forme moderne du tableau périodique, forme alternative du tableau périodique.

Альтернативные периодические системы элементов

Даниела Костич^{1*}, Ненад Крстич¹, Марина Благоевич¹

1- Университет в Нише, Естественно-математический факультет, Кафедра химии, Вишеградска 33, 18000 Ниш, Сербия

АННОТАЦИЯ

Более 150 лет с момента открытия периодической таблицы элементов существовала потребность в ее постоянном дополнении и улучшении. В результате этого, сегодня существует более 700 различных периодических систем, которые стремятся более просто и эффективно представить положение элементов в периодической таблице, их взаимосвязи и возможность построения различных соединений. Помимо двухмерных, появились как трехмерные, так и четырехмерные системы элементов. Все они, помимо большого дидактического значения, также имеют большое научное значение и представляют собой руководящие принципы для ученых в различных междисциплинарных исследованиях. Продолжается поиск более совершенных и всеобъемлющих периодических систем.

Ключевые слова: периодическая система, современная форма периодической системы, альтернативная форма периодической системы.

Alternative Periodensysteme der Elemente

Danijela Kostic^{1*}, Nenad Krstic¹, Marina Blagojevic¹

1- Universität in Niš, Fakultät für Naturwissenschaften und Mathematik, Lehrstuhl für Chemie, Višegradska 33, 18000 Niš, Serbien

ABSTRACT

Seit mehr als 150 Jahren, seit der Entdeckung des Periodensystems der Elemente, besteht die Notwendigkeit, es ständig zu ergänzen und zu verbessern. Infolgedessen gibt es heute über 700 verschiedene Periodensysteme, die das Ziel haben, die Position der Elemente im Periodensystem, ihre Beziehungen untereinander und die Möglichkeit der Bildung verschiedener Verbindungen einfacher und effektiver darzustellen. Neben zweidimensionalen sind auch drei- und vierdimensionale Periodensysteme erschienen. Sie alle haben neben ihrer großen didaktischen auch eine große wissenschaftliche Bedeutung und stellen Leitlinien für Wissenschaftler in verschiedenen multidisziplinären Forschungen dar. Die Forschung nach vollkommeneren und umfassenderen Periodensystemen wird fortgesetzt.

Schlüsselwörter: Periodensystem, moderne Form des Periodensystems, alternative Form des Periodensystems

The Influence of Metal Microelements, Colloids and Organic Phase on Physical-chemical Properties and Processes in Peloids

Jelena M. Purenović^{1*}, Milovan M. Purenović², Marjan S. Randelović²

1-University of Kragujevac, Faculty of Technical Sciences, Svetog Save 65, Čačak, Serbia

2-University of Niš, Faculty of Sciences and Mathematics, Department of Chemistry, Višegradska 33, Niš, Serbia

ABSTRACT

The main emphasis in this study was on the modification of peloid characteristics through maturation processes, physical-chemical analysis of salty geothermal water and intact geomaterial, content of toxic heavy metals, radionuclides, and microorganisms in matured peloid, and physical-chemical processes that occur in a highly heterogeneous and microheterogeneous system solid-water. Main processes were considered to be mass transfer, colloidal processes, adsorption and surface compounding by macro- and micronutrients from salty mineral water with surface groups of intact geomaterial. This study indicated that inorganic and organic components of peloid could be in the form of colloids, suspended macro- and microparticles, ions and molecules. Colloidal silica had special importance in peloids. Due to low maximum solubility of silica, there were a number of processes in which coagulated and flocculated particles were created during maturation, especially in the presence of metal cations (*e.g.*, Fe^{3+} and Al^{3+}) and colloidal metal hydroxides which noticeably reduced the solubility of silica. Single charged alkali metal cations caused coagulation of colloidal silica occupying bridging positions between negatively charged colloidal particles. Colloidal silica in peloid together with other micro- and macro phases, and with the help of numerous microelements, comes in interaction, building a complex surface and occluded compounds. In the multiphase system, very complex organic and inorganic compounds are formed, which are important for therapeutic purposes.

Keywords: Peloid, Macro/micro elements, Thermo mineral water, Colloidal particles.

Jelena M. Purenović: jelena.purenovic@ftn.kg.ac.rs

Milovan M. Purenović: puren@pmf.ni.ac.rs

Marjan S. Randelović: hemija@pmf.ni.ac.rs

Introduction

The term “peloid” usually refers to the natural healing mud, which is a multi-component macro- and micro-heterogeneous system consisting of mineral water, colloidal clay minerals, organic matter, organic-mineral complexes, *etc.* According to The International Society of Medical Hydrology, peloid can be defined as a natural product consisting of a mixture of sea, salt lakes, or mineral-medicinal water (liquid phase), with organic and inorganic material (solid phase) produced by biological action (humus) and geological action (clay minerals). Peloids are used in “pelotherapy” for local or generalized recovering from rheumatism, arthritis, and bone-muscle traumatic damages. The main factors which determine peloid characteristics and its suitability for therapy are: composition, granulometry, geochemistry of mineral water, low-cooling rate, high ion exchange capacity, good adhesivity, ease of handling and pleasant sensation when applied to the skin (Veniale et al., 2004). Today it is known that peloids accelerate blood circulation and metabolism, affect the activity of some endocrine glands, and soothe tension and pain, primarily due to the thermal effect. They also have a beneficial effect on chronic rheumatic diseases, and are used for cosmetic purposes, for example, to remove cellulite. Moreover, some studies have confirmed that peloids possess antimicrobial, antiviral, antineoplastic and anti-inflammatory effects (Suárez et al., 2011).

Primary or secondary mixing of clayey (geo)materials with salty thermo-mineral waters, accompanied by organic materials produced by the metabolic activity of micro-organisms growing during the so-called “maturation” process, is a very common procedure for improving and stabilizing the therapeutic properties of the final product-peloid (Sanchez et al., 2002; Veniale et al., 2007). It is established that the maturation process improves some physical properties of the clay minerals, such as heat retention capacity, rheology, and adhesion. Some studies report that maturation leads to a decrease in grain size, while both mineralogy and chemistry are almost unchanged (Summa and Tateo, 1998).

However, for practical reasons, some studies suggest use of extemporaneous peloids, whose preparation procedure assumes a contact between both phases (clayey material and salty thermo-mineral waters) for around 48 h, instead of several months or up to two years in the case of usual maturation process (Carretero et al., 2006; Gámiz et al., 2009). Organic substances as well as macro- and micronutrient elements present in water are taken up by the peloid during interaction of phases and can be released during application to the human body (Carretero et al., 2010; Gámiz et al., 2009).

Geothermal water from Bujanovačka Spa (south of Serbia) is highly mineralized, hyperthermal (43°C), sodium, hydrogen carbonate, fluoride, sulfate, and carbonic-acid rich (<http://bujanovackabanja.org/>). Uniqueness of this spa is in the specific combination of three natural factors: therapeutic thermal waters, peloids and carbon dioxide having a purity of about 98%. During pelotherapy, mud exhibits three effects: mechanical, thermal, and pharmacological. Peloids can be used raw or after passing maturation process, but also as a mixture of mud and paraffin and for preparation of cosmetics (<http://bujanovackabanja.org/>).

Experimental

This paper focused on: i) detailed physical-chemical and elemental analysis of salty geothermal water and virgin geomaterial used for peloid maturation process; ii) content of toxic heavy metals, radionuclides, and microorganisms in matured peloid, and iii) processes that took place in a highly heterogeneous and microheterogeneous system solid-water. To date, the latter aspect was very little studied and/or considered in detail.

Virgin clay (native clayey geomaterial for peloid preparation) and thermo-mineral water were the basic ingredients used for the peloid preparation through “maturation” treatment. It was clayey mineral-rich geomaterial of volcanic origin, which was mixed in open air with salty thermo-mineral water, undergoing a maturation process. Already prepared peloid and thermo-mineral water were analyzed without further modifications. All used chemicals were of analytical grade.

Bearing in mind the subject and purpose of this work, program and research methodology included the following:

- ◆ Physical and physical-chemical properties of geothermal mineral water (pH, electrical conductivity, free CO₂, alkalinity, metal cations, anions, *etc.*) were analyzed by the accredited laboratories using the standard methods. These important parameters and factors influenced the ratio of ionic and colloidal states of different ingredients. Details regarding the used analytical methods were provided in Table 1. These analyses were courteously performed at the Institute of Public Health of Serbia “Dr Milan Jovanović Batut”, Belgrade, using adequate analytical methods.

- ◆ Determination of the chemical composition of mineral water for the dumping of peloids, the content of fluoride, chloride, nitrite and nitrate, phosphate, sulfate, Na, K, Mg, Ca, Fe, Mn, Cu, Zn, Pb, Cr, Cd, Co, Ba, Si, Ni, As, Hg, Se, Sb, Al and Sn;
- ◆ Content of the weak electrolyte metasilicic acid (H_2SiO_3) and metaboric (HBO_2) acid.
- ◆ Determining the content of radionuclides in appropriate samples.
- ◆ EDXRF (Energy Dispersive X-ray Fluorescence) spectrometry technique using radioisotopes ^{241}Am and ^{109}Cd as the excitation sources was employed for determination of chemical compositions of two different samples (184/9V and 183/8V), including macro- and microelements, in salty thermo-mineral water and the virgin clay for peloid preparation. The EDXRF spectra were collected using a modified method EPA 6200. These analyses were courteously performed at the “Vinča” Institute of Nuclear Sciences, Belgrade.
- ◆ Macro- and microelements in the virgin clay were determined following the microwave digestion with HNO_3 and H_2O_2 . Heavy metals in the samples of the matured peloid were analyzed after their extraction by boiling in the 0.1 M HCl during 15 min (method: AEL M01-05).
- ◆ Content of relevant radionuclides in the samples was determined using high-resolution gamma-ray spectroscopy with HPGe detector, according to ISO 10703:1997 and ASTM C1402-98.
- ◆ These analyses were courteously performed at the Institute of Chemistry, Technology and Metallurgy – ICTM using adequate analytical methods.
- ◆ All samples for testing, indicated by numbers, were taken in accordance with the standards and were taken on the spot by expert of accredited laboratory, therefore, under objective conditions.

Results and Discussion

The results of EDXRF spectrometry with the use of radioactive isotopes ^{109}Cd and ^{241}Am , for samples 184 / 9V and sample 183 / 8V

The qualitative analysis of thermo-mineral water (sample 184 / 9V) by non-destructive EDXRF spectrometry (Figure 1) showed the presence of the following elements: S, Cl, K, Ca, Fe, Ni, Cu, Pb, Br, Rb, Sr, Ag, Sn, Sb, Cs and Ba. The size of the peaks indicated that K and

Ca were macroelements, and, besides them, the most common were S and Cl. Other detected elements were present in a smaller proportion, or in trace quantities. Marked small peak, observed in Figure 1a, energetically corresponded to Hg (L line 9.9 keV) or germanium (K line 9.87 keV). Hence, in the absence of other/additional lines, it could not be unambiguously specified which one occurred in water. Moreover, there was a possibility that both of them were simultaneously present or the peak could be the result of some other weaker peaks summation.

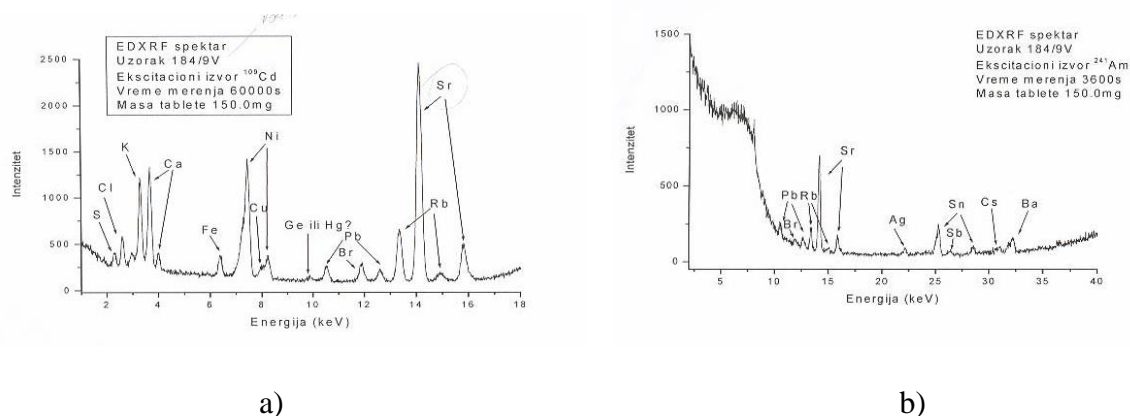
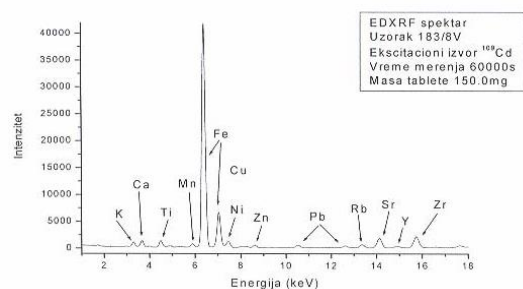
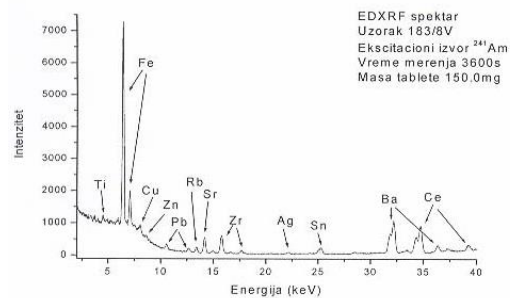


Figure 1. EDXRF spectra of salty geothermal water acquired by using a) ^{109}Cd and b) ^{241}Am as the excitation sources.

As Figure 2 revealed, the elements detected in the EDXRF spectra of virgin clay (sample 183 / 8V) were as follows: Si, K, Ca, Ti, Mn, Fe, Ni, Zn, Pb, Rb, Sr, Y, Zr, Ag, Sn, Ba and Ce. Moreover, by considering the size of peaks in the spectra, it could be concluded that the most common elements were Si, K, Ca and Fe, while other elements were present in smaller proportion, or in trace amounts. On the other hand, the peaks of Fe, Ni, and Pb (for ^{109}Cd) and Ag, Pb, Sn, and Ba (for ^{241}Am) could be aroused as a result of the influence of background radiation. Therefore, on the basis of EDXRF results, the possible presence of these elements in the sample could not be excluded.



a)



b)

Figure 2. EDXRF spectra of virgin clayey geomaterial acquired by using a) ^{109}Cd and b) ^{241}Am as the excitation sources.

The results of sensory, physical, and physical-chemical analysis of water for the sinking of the curative mud, for samples with the identification mark 184 / 9V and sample 183 / 8V

Physical-chemical parameters and quantitative analysis of cations and anions of thermomineral water and virgin clay were summarized in Tables 1 and 2, respectively.

Table 1. Physical and physical-chemical analysis of thermomineral water (sample 184/9V).

N ^o	Analyzed parameter	Unit	Result	Analytical method
1.	Smell	-	no	/
2.	pH	-	7.55	SRPS H.Z1.111.:1987
3.	Electrical conductivity	$\mu\text{S/cm}$	4500	EPA 120.1:1982
4.	Dry residue at 105°C	mg/dm^3	3180	Handbook ¹⁾ P-IV-7
5.	Hydrogen sulphide (H_2S)	mg/dm^3	-	/
6.	Free CO_2	mg/dm^3	55.3	/
7.	KMnO_4 consumption	mg/dm^3	0.69	SRPS EN ISO 8467:2007
8.	Alkalinity (p-alkalinity)	meq/dm^3	0	SRPS EN ISO 9963-1:2007
9.	Alkalinity (m-alkalinity)	meq/dm^3	50.2	SRPS EN ISO 9963-1:2007
10.	Fluoride (F^-)	mg/dm^3	< 1.0	EN ISO 10304-1:1995

11.	Chloride (Cl ⁻)	mg/dm ³	55.2	SRPS-ISO 9297:1997 SRPS-ISO 9297:2007
12.	Nitrite (NO ₂ ⁻)	mg/dm ³	0.016	APHA-Method 4500-NO ₂ ⁻
13.	Nitrate (NO ₃ ⁻)	mg/dm ³	5.8	EN ISO 10304-1:1995
14.	Phosphate (PO ₄ ³⁻)	mg/dm ³	0.046	Handbook ¹⁾ P-V-16/A
15.	Sulphate (SO ₄ ²⁻)	mg/dm ³	200	EN ISO 10304-1:1995
16.	Sodium (Na ⁺)	mg/dm ³	726	APHA-Method 3111-B, 1999
17.	Potassium (K ⁺)	mg/dm ³	49	APHA-Method 3111-B, 1999
18.	Magnesium (Mg ²⁺)	mg/dm ³	8.02	SRPS H.Z1.181:1985
19.	Calcium (Ca ²⁺)	mg/dm ³	41.6	SRPS H.Z1.181:1985
20.	Strontium	mg/dm ³	1.5	/
21.	Total hardness as CaCO ₃	mg/dm ³	156	AEL M02-01
22.	Iron (Fe)	mg/dm ³	0.36	APHA-Method 311-B, 1999
23.	Manganese (Mn)	mg/dm ³	0.05	APHA-Method 311-B, 1999
24.	Copper (Cu)	mg/dm ³	< 0.03	APHA-Method 311-B, 1999
25.	Zinc (Zn)	mg/dm ³	0.018	APHA-Method 311-B, 1999
26.	Lead (Pb)	mg/dm ³	< 0.19	APHA-Method 311-B, 1999
27.	Chromium (Cr)	mg/dm ³	< 0.13	EPA-Method 218.1, 1978
28.	Cadmium (Cd)	mg/dm ³	< 0.014	APHA-Method 311-B, 1999
29.	Cobalt (Co)	mg/dm ³	< 0.05	APHA-Method 311-B, 1999
30.	Barium (Ba)	mg/dm ³	< 1.0	EPA-Method 208.1, 1974
31.	Nickel (Ni)	mg/dm ³	< 0.06	APHA-Method 311-B, 1999
32.	Silicon (Si)	mg/dm ³	57.5	Handbook P-V-40/A
33.	Arsenic (As)	µg/dm ³	72	SRPS ISO 11969:2002

34.	Mercury (Hg)	$\mu\text{g}/\text{dm}^3$	< 1.0	BS EN 1483:2007
35.	Selenium (Se)	$\mu\text{g}/\text{dm}^3$	< 0.3	APHA-Method 3114-B, 1999
36.	Antimony (Sb)	$\mu\text{g}/\text{dm}^3$	2.5	AEL M-02
37.	Aluminum (Al)	mg/dm^3	< 1.5	/
38.	Tin (Sn)	$\mu\text{g}/\text{dm}^3$	< 0.5	AEL M02-03
30.	Metasilicic acid	mg/dm^3	118.00	/
31.	Metaboric acid	mg/dm^3	17.00	/
32.	Total dissolved solids	mg/dm^3	4983.60	/

Peloids acted as ionic mediators on human skin. The pathway of incorporation of exchangeable ions and other compounds existing in peloids in the human body, applied for therapeutic and cosmetic purposes, was the absorption through skin (dermal absorption). For this reason, concentration of toxic heavy metals and other harmful components in peloids should be at the level that does not cause damage to human health (Gerencsér et al., 2010; Vreca and Dolenc, 2005). To date, only the maximum acceptable concentrations established for soils and cosmetics could be used as guidelines for healing mud and peloids. For example, in December 2008, Health Canada released Draft Guidance on Heavy Metal Impurities in Cosmetics, which outlined recommended impurity limits in cosmetic products for lead (10 ppm), arsenic (3 ppm), cadmium (3 ppm), mercury (3 ppm), and antimony (5 ppm) (<https://www.canada.ca/en/health-canada/consumer-product-safety/reports-productions/industry-professionals/guidance-heavy-metal-impurities-cosmetics.html>).

In Europe there was no specific legislation and regulation regarding maximum acceptable concentrations of potential toxic elements in peloids. The European Cosmetics Directive (76/768) and the new Cosmetics Products Regulation (1223/2009) allowed "the non-intended presence of small quantities of a prohibited substance, stemming from impurities of natural or synthetic ingredients, the manufacturing process, storage, migration from packaging, which was technically unavoidable in good manufacturing practice, provided that such presence did not cause damage to human health when the product was applied under normal or reasonably foreseeable conditions of use" (European Union, 2009).

Table 2. Chemical analysis of raw/virgin clayey geomaterial for peloid formulation (sample 183/8V).

Nº	Analyzed parameter	Unit	Result	Guideline value ¹
Microwave digestion with HNO ₃ and H ₂ O ₂				
1	Lead, Pb	mg/kg	69.1	< 30.0
2	Cadmium, Cd	mg/kg	2.20	< 5.0
3	Chromium, Cr	mg/kg	49.8	< 50.0
4	Arsenic, As	mg/kg	9.2	< 5.0
5	Mercury, Hg	mg/kg	2.98	< 10.0
6	Nickel, Ni	mg/kg	42.5	< 50.0
7	Manganese, Mn	mg/kg	562	-
8	Cobalt, Co	mg/kg	13.7	-
9	Zinc, Zn	mg/kg	184.5	-
10	Sodium, Na	mg/kg	22900	-
11	Potassium, K	mg/kg	2770	-
12	Magnesium, Mg	mg/kg	4500	-
13	Calcium, Ca	mg/kg	347.5	-
14	Iron, Fe	mg/kg	2100	-
15	Copper, Cu	mg/kg	59.2	-
16	Tin, Sn	mg/kg	< 0.02	-
17	Selenium, Se	mg/kg	< 0.02	-
18	Antimony, Sb	mg/kg	1.35	-

¹) Mark * refers to the non-accredited method

As Tables 1 and 2 described the amount of heavy metal cations in the matured peloid mud was lower with respect to virgin. When geothermal water was mixed with the virgin clayey geomaterial, content of heavy metals decreased due to ion exchange, hydrolysis, partial dissolution of minerals and other phenomena that will be discussed in detail. The importance of ion exchange mainly refers to major elements, such as alkaline or alkaline earth metal cations (Ca^{2+} , Mg^{2+} , K^+ and Na^+), between geothermal water and the clay. Due to their high concentrations in geothermal water, major elements could replace potentially toxic cations in virgin geomaterial, resulting in the final peloid with significantly lower content of heavy metals.

The results of chemical analysis of thermal mineral water, referring to the characteristic cations, anions, and weak electrolytes

The water temperature at the source was 42 °C, its pH was 7.2, specific mass 1.002, and belongs to category of sodium hydrocarbonate water, fluoride, sulfide and carbonic acid hyperthermia. Dry residue at 180°C was 3.2, and the total mineralization 4.996 g/dm³ in its composition was given in Table 3.

Table 3. The results of chemical analysis of thermal mineral water, referring to the characteristic cations, anions and weak electrolytes.

Cations	Content (mg/dm³)
Sodium	1132.00
Potassium	66.00
Calcium	42.00
Magnesium	11.00
Strontium	1.50
Iron	0.70

Anions	
Hydrocarbonate	3355.00
Chloride	56.00
Fluoride	0.70
Sulphate	183.70
Weak electrolytes	
Metasilicic acid	118.00
Metaboric acid	17.00
The sum of all soluble ingredients	4983.60

The results of radiological tests

Radioactive phases could produce ionising radiations that could be dangerous when exceeding certain levels. Results of radiological study of thermomineral water, virgin clay and peloid samples were comparatively shown in Table 4. The content of radionuclides in the samples was below the limits of radioactive contamination, established for medicinal and cosmetics products based on natural raw materials.

Table 4. The results of radiological examination of mineral water.

Sample	⁴⁰ K (Bq/kg)	²³² Th (Bq/kg)	²²⁶ Ra (Bq/kg)	¹³⁷ Cs (Bq/kg)	²³⁸ U (Bq/kg)	²³⁵ U (Bq/kg)
Mineral water	1.4±0.1	< 0.2	< 1.1	< 0.1	< 0.8	< 0.4
Virgin geomate rial	276±8	22±1	20±2	< 0.1	12±4	< 0.6
Peloid	388±11	29±1	27±2	< 0.1	18±4	< 0.9

Diagnostic criteria established on the basis of the analysis of obtained results

By the analysis of the research results, and bearing in mind the review of literature and theoretical knowledge in the field of colloids and colloidal state, as an important prerequisite for the necessary physical-chemical and medicinal properties of the curative mud, the following diagnostic criteria were achieved:

- ◆ Medicinal waters, by definition, belonged to the category of sodium hydrocarbonate, fluoride, sulfate and carbonic acid hypothermia, with a temperature of 42°C;
- ◆ Thermomineral waters had a very high value of dry residue of 3.2 g/dm³, at 180°C and high mineralization value in an amount of 4.983 g/dm³;
- ◆ According to the content of cations, anions and weak electrolytes (Table 3) and total chemical composition of mineral water for peloid sinking (Table 1), it could be seen that water contained predominantly sodium and potassium, followed by calcium and magnesium, as macrocomponents;
- ◆ Concerning the anions present, the water was rich with HCO₃⁻ ions (3355 mg/dm³), which was mainly related to the alkali and alkaline earth metals;
- ◆ The presence of Cl⁻ and SO₄²⁻ ions was noted, and F⁻ ion in very small quantities of 70 g/dm³;
- ◆ Metasilicic and metaboric acid were found in high quantity, far above the solubility limit;
- ◆ Thermal water contained very small quantities of aluminum (Al) 1500 mg/dm³, arsenic (As) 72 mg/dm³ and silicon (Si) 57.5 mg/dm³;
- ◆ Wet mud contained a number of heavy metals and others; some in traces (Cd, As, Hg, Ni, Sn, and Se), others in microquantities (Pb, Cr, Mn, Co, Sb, and Zn), as well as macrocomponents (Na, K, Mg, Ca and Fe);
- ◆ EDXRF spectra of geothermal water for the peloid preparation (Figure 1) revealed the following elements: S, Cl, K, Ca, Fe, Ni, Cu, Pb, Br, Rb, Sr, Ag, Sn, Sb, Cs and Ba;
- ◆ Based on the size of the peaks of EDXRF spectra for geothermal water, it was concluded that the most common elements were K, Ca, Ni, Cu, Sr, Cl and S, while the other detected elements were present in a smaller share or trace;
- ◆ In EDXRF spectrum of geothermal water a small peak was detected, which corresponded to the Hg (L line 9.9 keV) or germanium (K line 9.87 keV), which in

this case, due to the lack of other lines, could not be determined with certainty (Figure 1);

- ◆ In the EDXRF spectra related to crude mud, which did not undergo the process of ripening, the following elements were detected: Si, K, Ca, Ti, Mn, Fe, Ni, Zn, Pb, Rb, Sr, Y, Zr, Ag, Sn, Ba and Ce (Figure 2);
- ◆ Due to the size of the peaks on EDXRF spectra for raw peloid, it could be concluded that in this sample the most frequent elements were Si, K, Ca and Fe, while the other elements were present in a smaller proportion, *i.e.*, in traces, as microelements;
- ◆ On the other hand, peaks Ni, Pb, Ag, Sn and Ba in the spectra of raw peloid occurred because of the influence of background from the instrument, so the possible presence of these elements in the sample could not be ruled out.

Discussion of possible chemical interactions and processes in heterogeneous systems of peloid

Previous research on peloids primarily focused on their curative and ion-exchange characteristics, paying no attention to other physical-chemical processes and colloidal phenomena in the peloid, and even ignoring a number of microcomponents which had considerable influence on the consistency of peloids. Physico-chemical processes that most likely occurred in peloid during the maturation process were as follows:

- ◆ Water retention, *i.e.*, retention on the external surface of solid particles and within the interlayer space of swelling clay minerals as well as hydration and dehydration of the surface groups on solid surfaces;
- ◆ Adsorption and absorption of ions and molecules on solid surfaces and within pores;
- ◆ Coagulation - flocculation processes;
- ◆ Ion exchange process between mineral water and aluminosilicates;
- ◆ Reactions between adsorbates and adsorbents in which surface complexes were formed;
- ◆ Polymerization of silica acid monomers;
- ◆ Biochemical decomposition of organic phase and its mineralization;
- ◆ Generation of metabolites of some colonizing organisms;
- ◆ Creating inorganic and organic sols and gels;
- ◆ Processes of mass exchange;
- ◆ Formation of crystallization centers and solid phases of new deposits;

◆ Oxido-reduction processes.

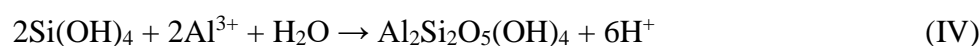
The peloid was extremely macro and micro heterogeneous solid-water system which contained soluble inorganic and organic components in the form of colloids, suspended particles, ions and molecules. Dominant constituents of the peloid were clay minerals, coagulated inorganic and organic sols, complexes of heavy metals with organic ligands, chelates, aqua complexes, hydroxide gels and various metal species (Al, Mg, Ca, Fe); a number of suspended solid particles of silicates, carbonates, sulphates and silica; soluble ions of many cations and anions; chemical compounds in the form of inorganic and organic molecules and polymeric forms of silica. The structures of the most probable colloidal micelles in peloid could be shown as follows.



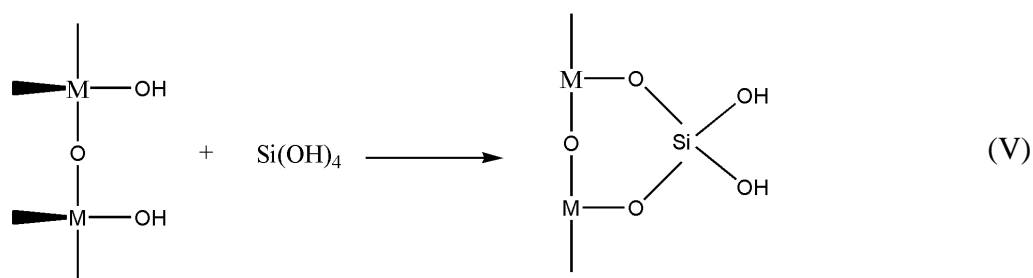
where $\text{M}^{\text{P}+}$ was general symbol for the cations (*e.g.*, Fe^{3+} , Al^{3+} , Ca^{2+} , Mg^{2+} , *etc.*). Cations adsorbed on the surface of colloidal silica species acted as cristalization centers for carbonates, sulphates of calcium and other deposits that could be formed in water.

This complex system, with dominant interfacial mass exchange, was out of equilibrium and unstable. For this reason, colloids tended to be destabilized through coagulation-floculation process, forming precipitate or gelatinous state. Due to low maximum solubility of silica, there were a number of processes in which coagulated and flocculated particles were created, especially in the presence of metal cations (*e.g.*, Fe^{3+} and Al^{3+}) and colloidal hydroxides which noticeably reduced the solubility of silica. Research in this work focused precisely on the impact of colloidal silica on a number of phenomena and processes in peloids. Depending on the crystallographic modification of crystalline SiO_2 , solubility in water was in the range of from 70 to 120 mg/dm³. Thus, for example, at extremely low concentrations of Fe and Al, the solubility of silica was drastically reduced.

For instance, the addition of Fe^{3+} ions in a solution of $\text{Si}(\text{OH})_4$ significantly delayed the polymerization process.



Within the peloid, interaction of monomer $\text{Si}(\text{OH})_4$ with metal hydroxides or oxides could not be avoided. This interaction may be depicted by the following equation:



Deposition of colloidal silica was influenced by flocculating ions and it was significantly diminished if metal cations were previously complexed with the chelate ligands.

The presence of Cl^- ions in geothermal water could significantly stabilize colloidal state, acting as an anticoagulant. On the other hand, the F^- ion had a major impact on the creation and structure of numerous suspended particles and easily transformed orthosilicic acid into H_2SiF_6 in accordance with the following mechanism:



Since it was not possible to avoid the presence of the organic phase in the structure of peloids, and this was not desirable, its presence ensured the creation of molecular solution and organic sols, and in interactions with other micro and macro components chelate a number of organic complexes could be formed, as well as silica-organic compounds.

Water used in the preparation of peloid had a high concentration of sodium, which was available not only for the above reaction, but also for the formation of new phases, such as trona ($\text{Na}_3\text{H}(\text{CO}_3)_2 \cdot 2\text{H}_2\text{O}$), seen in Figure 3. Previous processes which lead to formation of solid deposits caused a considerable change in the chemical composition of geothermal water (a liquid phase in peloid).

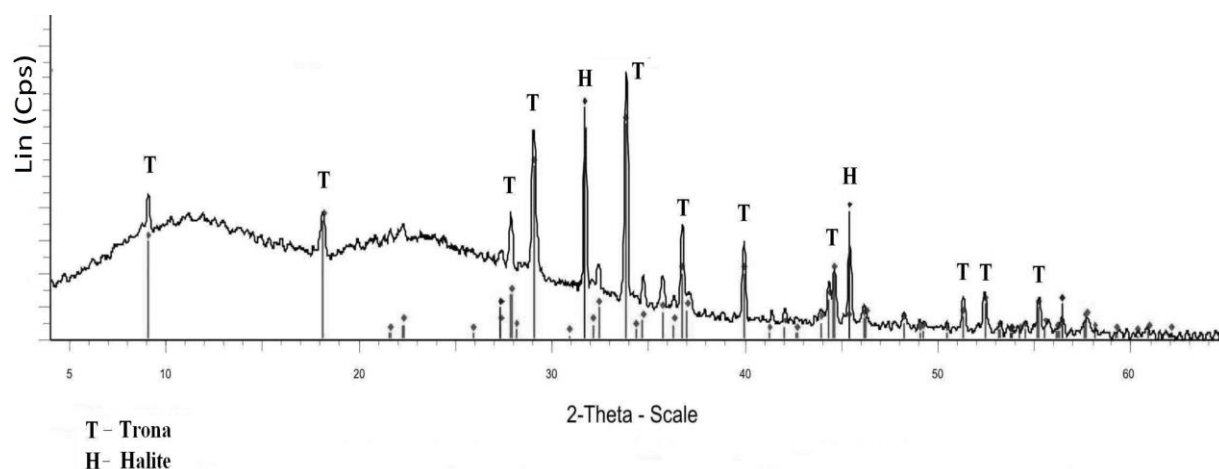


Figure 3. XRD pattern of salty geothermal water.

The main clay minerals in peloid were smectites and minerals based on metal oxides and hydroxides. Smectite was a very good absorber of water, whereby it swelled ensuring high water retention capacity (Cara et al., 2001). Noteworthy, smectite possessed high content of variable exchangeable cations, which could largely vary in hydration degree (Sparks, 2002), thus influencing moisture and water diffusion. A multicomponent mixture in the form of pulp, saturated with H₂S from geothermal waters, upon the occurrence of redox processes of ripening (biochemical processes), could create peloid of strongly mineralized structure, which had good healing and plastic qualities, important for its implementation.

Conclusion

Peloids were considered as highly complex and heterogeneous systems, composed of minerals, amorphous inorganic materials, and organic matter. Therapeutic and curative characteristics of peloid were realized through thermal effects and ion exchange properties in contact with human skin. Due to the potential human toxicity or radiation risks during pelotherapy, this study has involved detailed physical-chemical and radiological analysis of mineral water, virgin geomaterial and final peloid from Bujanovačka Spa. All tested parameters have fulfilled the requirements, according to Serbian regulations.

High mineralized water was extraordinarily suitable for the preparation of peloids. Presence of silicic acid, as well as Al³⁺, Fe³⁺, F⁻ and trace elements, were reflected in the extraordinary process within the peloid at phase boundaries solid-water. Moreover, clay minerals and silicic acid had a key role in processes of hydration and dehydration. Polymer form of silicic acid significantly affected the formation of solid phase and deposits in the form of layers or clusters within the peloids and mediated mass exchange processes between human body and peloids.

The presence of metal cations and hydroxides, anions, clayey material, and organics in ionic, molecular, or colloidal state gave rise to many processes and interactions between all mentioned constituents, forming chelates, organosols, organic complexes with metal cations and polymeric forms of various inorganic and organic compounds.

Peloids should be active, but stable colloidal systems, so, in that sense, a harmonious correlation between the added macro and micro elements and the process of creating peloids was established in this paper.

Acknowledgement

This research is a part of investigations performed within the scope of the project 451-03-9/2021-14/200132. The authors gratefully acknowledge the financial support of Serbian Ministry of Education, Science and Technological Development.

Conflict-of-Interest Statement

None.

References

- Cara, S., Carcangiu, G., Padalino, G., Palomba, M., & Tamanini, M. (2000). The bentonites in pelotherapy: Thermal properties of clay pastes from Sardinia (Italy). *Applied Clay Science*, 16, 125–132.
- Carretero, M. I., Gomes, C. S. F., & Tateo, F. (2006). Clays and human health. In F. Bergaya, B. K. G. Theng, & G. Lagaly, (Eds.), *The Handbook of Clay Science, Developments in Clay Science*, (vol. 1, pp. 717-741). Amsterdam: Elsevier.
- Carretero, M. I., Pozo, M., Martín-Rubí, J. A., Pozo, E., & Maraver, F. (2010). Mobility of elements in interaction between artificial sweat and peloids used in Spanish spas. *Applied Clay Science*, 48, 506–515.
- Cosmetics Products Regulation (1223/2009): Official Journal of the European Union Regulation (EC) No 1223/2009 of the European parliament and of the council of 30 November 2009 on cosmetic products (recast) (Text with EEA relevance).
- Gámiz, E., Martín-García, J. M., Fernández-González, M. V., Delgado, G., & Delgado, R. (2009). Influence of water type and maturation time on the properties of kaolinite-saponite peloids. *Applied Clay Science*, 46, 117–123.
- Gerencsér, G., Murányi, E., Szendi, K., & Varga, C. (2010). Ecotoxicological studies on Hungarian peloids (medicinal muds). *Applied Clay Science*, 50, 47–50.
- <http://bujanovackabanja.org/>
- http://www.hc-sc.gc.ca/cps-spc/pubs/indust/heavy_metals-metaux_lourds/index-eng.php
- Sanchez, C. J., Parras, J., & Carretero, M. I. (2002). The effect of maturation upon the mineralogical and physicochemical properties of illitic-smectitic clays for pelotherapy. *Clay Minerals*, 37, 457–463.

Sparks, D. (2002). *Environmental soil chemistry*. (2nd ed.). Academic Press.

Suárez, M., González, P., Dominguez, R., Bravo, A., Melián, C., Pérez, M., Herrera, I., Blanco, D., Hernández, R., & Fagundo, J. R. (2011). Identification of organic compounds in San Diego de los Banos Peloid (Pinar del rio, Cuba). *The Journal of Alternative and Complementary Medicine*, 17(2), 155-165.

Summa, V., & Tateo, F. (1998). The use of pelitic raw materials in thermal centres: Mineralogy, geochemistry, grain size and leaching tests. Examples from the Lucania area (southern Italy). *Applied Clay Science*, 12, 403–417.

Veniale, F., Barberis, E., Carcangiu, G., Morandi, N., Setti, M., Tamanini M., & Tessier D. (2004). Formulation of muds for pelotherapy: effects of “maturation” by different mineral waters. *Applied Clay Science*, 25, 135– 148.

Veniale, F., Bettero, A., Jobstraibizer, P. G., & Setti, M. (2007). Thermal muds: Perspectives of innovations. *Applied Clay Science*, 36, 141–147.

Vreca, P., & Dolenc, T. (2005). Geochemical estimation of copper contamination in the healing mud from Makirina Bay, central Adriatic. *Environment International*, 31, 53– 61.

Uticaj metalnih mikroelemenata, koloida i organske faze na fizičko-hemijska svojstva i procese u peloidima

Jelena M. Purenović^{1*}, Milovan M. Purenović², Marjan S. Randelović²

1- Univerzitet u Kragujevcu, Fakultet tehničkih nauka, Svetog Save 65, Čačak, Srbija

2- Univerzitet u Nišu, Prirodno-matematički fakultet, Odeljenje za hemiju, Višegradaska 33, Niš, Srbija

SAŽETAK

Glavni akcenat u ovom proučavanju bio je na modifikovanju peloidnih karakteristika kroz procese sazrevanja, fizičko-hemijskoj analizi slane geotermalne vode i netaknutog geomaterijala, kao i na sadržaju toksičnih teških metala, radionukleida i mikroorganizama u zrelim peloidima i fizičko-hemijskim procesima koji se javljaju u visoko heterogenom i mikroheterogenom sistemu čvrsto-voda. Smatra se da su glavni procesi: prenos mase, koloidni procesi, adsorpcija i usložavanje površine makro i mikro elementima iz slane mineralne vode sa površinskim grupama izvornog geomaterijala. Ova proučavanja su pokazala da neorganske i organske komponente peloida mogu biti u obliku koloida, suspendovanih makro i mikro čestica, jona i molekula. Koloidni silicijum-dioksid imao je poseban značaj u peloidima. Zbog niske maksimalne rastvorljivosti silicijum-dioksida, postoji više procesa u kojima su tokom zrenja nastale koagulisane i flokulisane čestice, posebno u prisustvu metalnih katjona (npr. Fe^{3+} i Al^{3+}) i koloidnih hidrokoksida metala koji su приметно smanjili rastvorljivost silicijum-dioksida. Jednoelektrisani katjoni alkalnih metala prouzrokovali su koagulaciju koloidnog silicijum-dioksida zauzimajući mostne položaje između negativno naelektrisanih koloidnih čestica. Koloidni silicijum dioksid u peloidima zajedno sa drugim mikro i makro fazama, a uz pomoć brojnih mikroelemenata, stupa u interakcije, gradeći složena površinska i okludovana jedinjenja. U višefaznom sistemu stvaraju se veoma složena jedinjenja organskog i neorganskog porekla, koja imaju značaj u terapeutske svrhe.

Ključne reči: Peloid, makro/mikro elementi, termomineralna voda, koloidne čestice

L'influence des microéléments métalliques, des colloïdes et de la phase organique sur les propriétés et les processus physico-chimiques des péloïdes

Jelena M. Purenović^{1*}, Milovan M. Purenović², Marjan S. Randelović²

1- Université de Kragujevac, Faculté des sciences techniques, Svetog Save 65, Čačak, Serbie

2- Université de Niš, Faculté des sciences naturelles et des mathématiques, Département de chimie, Višegradska 33, Niš, Serbie

RÉSUMÉ

Dans cette étude, l'accent principal était sur la modification des caractéristiques péloïdes à travers les processus de maturation, sur l'analyse physico-chimique de l'eau géothermique salée et du géomatériau intact, sur la teneur en métaux lourds toxiques, radionucléides et microorganismes dans les péloïdes mûris, ainsi que sur les processus physico-chimiques qui se produisent dans un système solide-eau hautement hétérogène et microhétérogène. Les processus qui sont considérés comme principaux sont les suivants : le transfert de la masse, les processus colloïdaux, l'adsorption et la composition en surface par des macro et micronutriments à partir d'eau minérale salée avec des groupes de surface du géomatériau intact. Cette recherche a montré que les composants inorganiques et organiques du péloïde peuvent apparaître sous forme de colloïdes, de macro et microparticules en suspension, d'ions et de molécules. La silice colloïdale avait une importance particulière dans les péloïdes. En raison de la faible solubilité maximale de la silice, il existe plusieurs processus dans lesquels ont été créées des particules coagulées et floculées durant la maturation, en particulier en présence des cations métalliques (p. ex. Fe^{3+} et Al^{3+}) et des hydroxydes métalliques colloïdaux qui ont sensiblement réduit la solubilité de la silice. Des cations de métaux alcalins à charge unique ont provoqué la coagulation de la silice colloïdale en occupant des positions de pontage entre les particules colloïdales chargées négativement. Dans les péloïdes, la silice colloïdale entre en interaction avec d'autres micro et macrophases à l'aide de nombreux microéléments en créant ainsi une surface complexe et des composés occlus. Au sein du système multiphasique, se forment des composés organiques et inorganiques très complexes, qui sont importants à des fins thérapeutiques.

Mots-clés : péloïde, macro/microéléments, eau thermominérale, particules colloïdales.

Влияние металлических микроэлементов, коллоидов и органической фазы на физико-химические свойства и процессы в пелоидах

Елена М. Пуренович^{1*}, Милован М. Пуренович², Марьян С. Ранжелович²

1- Университет в Крагуевце, Факультет технических наук, Светог Саве 65, Чачак, Сербия

2- Университет в Нише, Естественно-математический факультет, Кафедра химии, Вишеградска 33, 18000 Ниш, Сербия

АННОТАЦИЯ

Основное внимание в этом исследовании уделялось модификации характеристик пелоидов посредством процессов созревания, физико-химическому анализу соленой геотермальной воды и неповрежденного геоматериала, содержанию токсичных тяжелых металлов, радионуклидов и микроорганизмов в зрелых пелоидах, а также физико-химическим процессам, которые происходят в сильно неоднородной и микрогетерогенной системе твердое тело-вода. Основными процессами считались массоперенос, коллоидные процессы, адсорбция и компаундирование поверхности макро- и микроэлементами из соленой минеральной воды с поверхностными группами неповрежденного геоматериала. Это исследование показало, что неорганические и органические компоненты пелоида могут быть в форме коллоидов, взвешенных макро- и микрочастиц, ионов и молекул. Коллоидный кремнезем имел особое значение в пелоидах. Из-за низкой максимальной растворимости кремнезема был ряд процессов, в которых во время созревания образовывались коагулированные и флокулированные частицы, особенно в присутствии катионов металлов (например, Fe^{3+} и Al^{3+}) и коллоидных гидроксидов металлов, которые заметно снижали растворимость кремнезема. Однозарядные катионы щелочных металлов вызывали коагуляцию коллоидного кремнезема, занимающего мостиковые позиции между отрицательно заряженными коллоидными частицами. Коллоидный кремнезем в пелоиде вместе с другими микро- и макрофазами и с помощью многочисленных микроэлементов вступает во взаимодействие, создавая сложную поверхность и поглощая соединения. В многофазной системе образуются очень сложные органические и неорганические соединения, которые важны для терапевтических целей.

Ключевые слова: пелоид, макро / микроэлементы, термоминеральная вода, коллоидные частицы.

Der Einfluss von metallischen Mikroelementen, Kolloiden und der organischen Phase auf physikalisch-chemische Eigenschaften und Prozesse in Peloiden

Jelena M. Purenović^{1*}, Milovan M. Purenović², Marjan S. Randelović²

1- Universität in Kragujevac, Fakultät für Technische Wissenschaften, Svetog Save 65, Čačak, Serbien

2- Universität in Niš, Fakultät für Naturwissenschaften und Mathematik, Lehrstuhl für Chemie, Višegradska 33, Niš, Serbien

ABSTRACT

Der Schwerpunkt dieser Studie lag auf der Veränderung der Eigenschaften der Peloiden durch Reifungsprozesse, auf der physikalisch-chemischen Analyse des geothermischen Salzwassers und des intakten Geomaterials, auf dem Gehalt an toxischen Schwermetallen, Radionukliden und Mikroorganismen im gereiften Peloid, sowie auf auftretenden physikalisch-chemischen Prozessen in einem sehr heterogenen und mikroheterogenen Fest-Wasser-System. Als Hauptprozesse werden Massentransfer, kolloidale Prozesse, Adsorption und zunehmende Oberflächenkomplexität durch Makro- und Mikroelemente aus Salzmineralwasser mit Oberflächengruppen des intakten Geomaterials angesehen. Diese Studie zeigte, dass anorganische und organische Bestandteile des Peloids in Form von Kolloiden, suspendierten Makro- und Mikropartikeln, Ionen und Molekülen vorliegen können. Eine besondere Bedeutung hatte kolloidales Siliziumdioxid bei Peloiden. Aufgrund der geringen maximalen Löslichkeit des Siliziumdioxids gab es eine Reihe von Prozessen, bei denen koagulierte und ausgeflockte Partikel während der Reifung entstanden, insbesondere in Anwesenheit von Metallkationen (z. B. Fe^{3+} und Al^{3+}) und kolloidalen Metallhydroxiden, die die Löslichkeit des Siliziumdioxids merklich verringerten. Einfach geladene Alkalimetallkationen verursachten die Koagulation des kolloidalen Siliziumdioxids, die Brückenpositionen zwischen den negativ geladenen kolloidalen Partikeln besetzten. Kolloidales Siliziumdioxid im Peloid kommt in Wechselwirkung mit anderen Mikro- und Makrophasen, und mittels zahlreicher Mikroelemente, und bildet komplexe Oberflächen- und okkludierte Verbindungen. Im Mehrphasensystem entstehen sehr komplexe organische und anorganische Verbindungen, die für therapeutische Zwecke wichtig sind.

Schlüsselwörter: Peloid, Makro-/Mikroelemente, Thermomineralwasser, kolloidale Partikel.

Development and application of kinetic-spectrophotometric method for analysis of diflubenzuron in soil samples using SPE followed by HPLC method

Emilija Pecev-Marinković^{1*}, Ana Miletić¹, Aleksandra Pavlović¹, Vidoslav Dekić²

1-Faculty of Sciences and Mathematics, Department of Chemistry, Višegradska 33, 18000 Niš, Republic of Serbia

2-Faculty of Sciences and Mathematics, Department of Chemistry, Ivo Lole Ribara 29, Kosovska Mitrovica, Republic of Serbia

ABSTRACT

The purpose of this paper is to present a new sensitive and simple kinetic-spectrophotometric method for the determination of the insecticide diflubenzuron (DFB). The kinetic method is based on the inhibition effect of DFB on the oxidation of sulfanilic acid (SA) by potassium periodate in acetate buffer in the presence of Fe(III) ion as a catalyst and 1,10-phenantroline. The reaction was monitored spectrophotometrically by measuring the increase in absorbance with time of the reaction product at 368 nm. Diflubenzuron was determined with linear calibration graph in the interval from 0.0374 to 0.374 $\mu\text{g}/\text{cm}^3$ and from 0.374 to 26.18 $\mu\text{g}/\text{cm}^3$. The detection limit and quantification limit of the method with 3σ criteria were 0.0039 $\mu\text{g}/\text{cm}^3$ and 0.0131 $\mu\text{g}/\text{cm}^3$, respectively. The relative standard deviations for five replicate determinations of 0.0374, 0.188 and 0.374 $\mu\text{g}/\text{cm}^3$ DFB were 2.24, 2.11 and 1.10%, respectively. The method was successfully applied to determine DFB residues in soil samples. Solid-phase extraction (SPE) was used for extraction of DFB from soil and samples with Chromabond® (Macherey-Nagel) C18 cartridges. The HPLC method was used as a comparative method to verify the results. The results obtained by two different methods showed good agreement.

Keywords: Diflubenzuron, Kinetic method, HPLC method, Solid-phase extraction, Soil samples

Emilija Pecev-Marinković: emilija.pecev@pmf.edu.rs

Ana Miletić: ana.nis.86@hotmail.com

Aleksandra Pavlović: aleksandra.pavlovic@pmf.edu.rs

Vidoslav Dekić: vidoslav.dekic@pr.ac.rs

Introduction

The term pesticide means a various number of compounds like insecticides, germicides, fungicides, herbicides, rodenticides, molluscicides, nematocides, plant growth regulators and acaricides. Several hundred compounds are available for use as pesticides. Pesticides are intensively used in modern agriculture and represent an efficient and economical way to improve the quality and quantity of yields, thus ensuring food safety for a constantly growing population around the world.

Diflubenzuron (Figure 1) is a halogenated benzoylphenylurea pesticide; also, it is an insect growth regulator. It is an effective stomach and contact insecticide acting by inhibition of chitin synthesis and so interfering with the formation of the cuticle. It inhibits chitin synthesis which results in a disruption of the molting process of target pests (Yang et al.,2016; Wang et al., 2018).

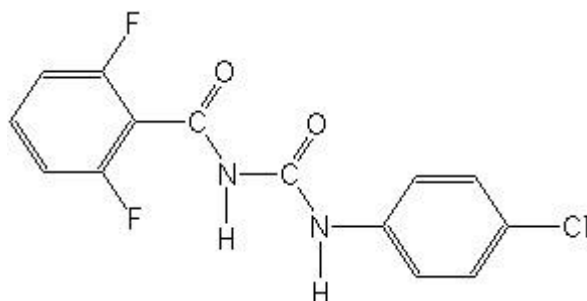


Figure 1. Chemical structure of diflubenzuron

It has been widely used against forest insect pests, and to control dipteran, heteropteran and lepidopteran pests (De Clercq et al., 1995; Erler et al., 2011; Willrich & Boethel, 2001;). Diflubenzuron has shown significant potential in the control of sciarid species (Du et al., 2013). DFB is used in public health applications against mosquitos and noxious fly larvae. It is specified for use as a vector control agent in drinking-water. Specific formulations for control of vectors are specified by WHO/FAO (2020). Difubenzuron was the prototype of all benzoylureas which was firstly discovered in the early 1970's, and in the following 40 years of developing more benzoylureas were prepared and commercialized (Matsmura, 2010; Sun et al., 2015). It is a

direct acting insecticide normally applied directly to plants or water. It is rapidly adsorbed in soil and particles and is immobile in soil. It also rapidly adsorbs to sediments and the sides of vessels and pipes, but it may also partition into the surface film because of its low water solubility. Pesticide analysis is very important because of widespread human exposure to these chemicals. However, with widespread use and accumulation of pesticides over time, the residues of benzoylureas can contaminate water, soil, and food. The pesticides can cause damage effects on human health, such as carcinogenic and allergies, because of long-term toxicity and chronic exposure to these compounds (Olsvik et al., 2013; Wang et al., 2016). The benzoylurea pesticides are not very toxic for numerous marine species such as fish and algae, but due to their specific mode of action they are likely to have adverse effects on non-target species such as the crustaceans and amphipods in the marine environment (Klima, 2011; Macken et al., 2015). Because of these reasons it is important to develop a simple, fast, and sensitive technique for the determination of DFB in different samples.

Numerous analytical methods have been reported for the determination of DFB in various matrices. Many papers reported determination of DFB by HPLC using different detectors (Ambike and Argekar, 2017; Amelin et al., 2013; Huang et al., 2011; Kim et al., 2013; Ouyang et al., 2015; Tfouni et al., 2013; Yang et al., 2015). GC-MS method is frequently used technique for the analysis and the determination of a different group of pesticides in water samples and in river waters (Chen, 2014; Łozowicka, 2017; Shi et al., 2014; Tian, 2020; Zhang et al., 2014). Some authors reported an ultra-performance liquid chromatography coupled with tandem mass spectrometry (UPLC-MS/MS) for the determination of DFB (Carneiro et al., 2013; Chen et al., 2013; Pengqiang, 2013; Wang et al., 2013; Wang et al., 2014). DFB was determined previously using ultra high-performance liquid chromatography coupled to triple quadrupole tandem mass spectrometry (UHPLC-QqQ-MS/MS) (Martínez-Domínguez et al., 2015). There are various studies on the determination of DFB using Liquid Chromatography-Tandem Mass Spectrometry (LC-MS/MS) (Choi et al., 2015; Irungu et al., 2016; Kim et al., 2015; Lee et al., 2011; Macken et al., 2015; Tran et al., 2012; Zainudin et al., 2015).

Authors from Senegal and France reported a Direct Laser-Photo-Induced Fluorescence (DL-PIF) method for the determination of DFB in river and sea water (Diaw et al., 2013).

Sample preparation plays an important role in the pesticide residues analysis. To date, a large number of methods have been developed and reported for the analysis of benzoylureas in different samples (water, juice, fruit, food, soil samples) such as dispersive liquid–liquid microextraction (Wang et al., 2017), solid-phase extraction (SPE) (Huang et al., 2011), solid-phase microextraction (SPME) (Mei et al., 2015), dispersive solid-phase extraction (DSPE) (Martin Pozo et al., 2019) and magnetic dispersive solid-phase extraction (MDSPE) (Huang et al., 2019a). QuEChERS methods are considered to be a quick, easy, cheap, effective, robust, and safe sample preparation methods. These methods have been used for sample preparation of benzoylurea before LC-MS method (Guimarães de Oliveira et al., 2019; Huang et al., 2019b) or HPLC-MS/MS method (Garcia Melo et al., 2020). Some authors developed multiple monolithic fiber-solid-phase microextraction (MMF-SPME) of samples followed by high performance liquid chromatography with diode array detection (Mei et al., 2014).

The aim of this study was to develop a simple, fast, and sensitive kinetic-spectrophotometric method for the determination of pesticide DFB. Finally, it was proposed the method for the determination of DFB in soil samples after their preparation based on SPE. Kinetic methods of chemical analysis are popular methods for rapid determination of organic species. These methods have some advantages like high sensitivity, low detection limit, good selectivity, rapid analysis and using of inexpensive instrument such as spectrophotometer. In the previous work our laboratory developed and validated two kinetic methods for DFB determination. The first work reported DFB determination in the range 0.31 – 3.10 $\mu\text{g}/\text{cm}^3$ and the application in mushroom samples (Grahovac et al., 2010). The second kinetic method reported DFB determination in the interval from 0.102 to 3.40 $\mu\text{g}/\text{cm}^3$. This method was applied for the determination of DFB in water and baby food samples (Pecev-Marinković et al., 2018).

In this study we reported a kinetic - spectrophotometric method for DFB determination based on its inhibitory effect on the oxidation of sulfanilic acid by potassium periodate in acetate buffer in the presence of Fe(III) ion as a catalyst and 1,10-phenantroline, which was monitored at 368 nm. The method is simple, sensitive, rapid, precise, and accurate. The limit of detection (LOD) is 0.0039 $\mu\text{g}/\text{cm}^3$.

Experimental

Reagents and chemicals

All chemicals used were analytical reagent grade. Pesticide standard diflubenzuron DFB with a certified purity of 99% was obtained from Dr. Ehrenstorfer (Augsburg, Germany). Standard stock solutions containing $100 \mu\text{g}/\text{cm}^3$ of DFB were prepared by dissolving the required amounts of the standards in methanol: water (50/50, v/v). They were stored in a refrigerator at 4°C .

A Sulfanilic Acid (SA) solution ($4 \times 10^{-2} \text{ mol}/\text{dm}^3$) was prepared by dissolving a 0.3463 g of SA (Merck) in water in the volumetric flask (50 cm^3).

The initial $1.5 \times 10^{-2} \text{ mol}/\text{dm}^3$ solution of potassium periodate was prepared by dissolving 0.075 g KIO_4 (Merck) in 50 cm^3 of water.

A solution of Fe (III) $1.0 \times 10^{-3} \text{ mol}/\text{dm}^3$ was prepared by dissolving $\text{FeCl}_3 \times 6\text{H}_2\text{O}$ (Merck) in $0.1 \text{ mol}/\text{dm}^3$ HCl.

A solution of 1,10-phenantroline was prepared by dissolving exact amounts in water.

The acetate buffer pH 4.7 was obtained by mixing solutions of CH_3COOH ($1 \text{ mol}/\text{dm}^3$) and NaOH ($1 \text{ mol}/\text{dm}^3$). Analytical-reagent grade solvents, methanol (MeOH), acetone ($(\text{CH}_3)_2\text{CO}$), dichloromethane (DCM) and cyclohexane (CHX) were obtained from J. T. Baker (UK). High purity distilled water obtained from Micro Med water purification system TKA Wasseraufbereitungssysteme GmbH was used for solutions preparation.

Soil samples were collected in the period April-May 2011 from different locations (Knez Selo (village), Grdelica (village), Svrljig (town), Nis (town)).

Apparatus

A Perkin-Elmer Lambda UV/Vis spectrophotometer with 10-cm quartz cell pairs was used for recording the absorbance at 368 nm. A water bath thermostat (n-BIOTEK, INC, model NB-301) was employed to control the reaction temperature. A stopwatch was used to record the reaction time.

Chromatographic analyses were performed with an Agilent Technologies, Series 1200 liquid chromatograph, equipped with an Agilent photodiode array detector (DAD), Model 1200 with RFID tracking technology for flow cells and a UV lamp, an automatic injector and Chem Station software. The analytical column was an Agilent – Eclipse XDBC-18 C_{18} column ($150 \times 4.6 \text{ mm}$).

A model BÜCHI R-200/205 rotary vacuum evaporator including bath B-490 with a vacuum pump was used to evaporate the extracts.

A solid phase extraction system (J. T. Baker Model SPE-12, UK) with a vacuum pump was used for solid phase extraction of samples. SPE with Chromabond® HR-P cartridges (sorbent mass 200 mg, Macherey Nagel, Germany) were used for extraction of DFB.

Hanna pH-meter instrument was used for checking the pH measurements.

The solutions were thermostated at 25 ± 0.1 C ° before the beginning of the reaction.

In addition, high precision volume micropipettes (Lab Mate⁺) of 50, 500 and 1000 μ L were used for handling or pipetting the solutions.

General procedure

The reaction was performed in a special glass four-compartment reaction vessel-mixer with lapped flap. The reaction was carried out in the following way: in reaction-mixture vessel with four compartments, the solution of SA was placed in one compartment, KIO₄ in the second, buffer solution in the third, Fe (III), *o*-phenantroline and DFB solution were added in the fourth compartment and water was added to the total volume of 10 cm³. The mixer-vessel was kept for 10 min at temperature of 25 ± 0.1 °C.

The solutions were mixed and homogenized by shaking, and then transferred into 10 cm constant temperature cell of spectrophotometer. The absorption at 368 nm was read over a period of 6 min. The rate of the reactions at different concentrations of reactants was obtained by measuring the slope of the linear part of kinetic curve to the absorbance – time plot. The calibration graphs were obtained by tangent method under the optimum conditions.

Soil sample preparation

10 g of soil samples were measured and then prepared by the addition of appropriate amount of standard stock solution DFB (2 μ g/cm³) and solution of methanol was added until the solvent completely covered the soil particles. The prepared samples were stayed for 1 day. After that, the prepared soil sample was transferred to a separatory funnel and mechanically shaken with acetone/water mixture (80:20, v/v), then it was centrifuged 3 times for 10 min at 3000 rpm. The separated supernatant was transferred into the separating funnel and extracted using DCM:CHX (1:1) using 3 portions of 100 cm³ solution for 10 min under mechanical shaking. Extracted

solution was put into SPE cartridge which was firstly conditioned. The solution passed through the cartridge under manual positive pressure at flow rate of 1 ml/min. The sample was eluted with $3 \times 1 \text{ cm}^3$ methanol and then extract was collected and evaporated at $60 \text{ }^\circ\text{C}$ in a rotary vacuum evaporator till dryness. The residue was dissolved with methanol:water (80:20, v/v), transferred into volumetric flask (25 cm^3), and divided into two parts. One part of the solution was filtered through a $0.45\text{-}\mu\text{m}$ microporous nylon membrane (Sigma – Aldrich, USA), then it was transferred into vials for HPLC analysis. For kinetic determination 10 cm^3 of this solution was taken and evaporated at temperature of $60 \text{ }^\circ\text{C}$ till dryness. The residue was dissolved in methanol and made up with water in 10-cm^3 volumetric flask and used for kinetic determination. SPE with Chromabond[®] HR-P cartridge was used for the extraction of DFB. Each sample solution was poured into a Chromabond HR-P C_{18} cartridge which had been conditioned with 3 ml acetone and 2 ml ethanol.

Comparative method

HPLC method was performed with an Agilent Technologies Model 1200 instrument with UV detector, fitted with C_{18} (Zorbax $5 \mu\text{m}$, $250 \text{ mm} \times 4.6 \text{ mm}$) analytical column, operating at $25 \text{ }^\circ\text{C}$. The mobile phase was methanol-water (80:20, v/v), delivered at a flow rate $1 \text{ cm}^3/\text{min}$. The eluate was monitored at wavelength of 254 nm . Injected volume was $10 \mu\text{l}$, and the flow rate of the mobile phase was $1 \text{ cm}^3/\text{min}$.

Kinetic Procedure

To obtain good mechanical and thermal stability, the instruments were run for 10 min before the first measurement. The reaction was carried out in the following way. In reaction-mixture vessel with four compartments, the solution of SA was placed in one compartment, KIO_4 in the second, acetate buffer in the third, Fe(III), *o*-phenantroline and DFB solution were added in the fourth compartment and water was added to the total volume of 10 cm^3 . The vessel was thermostated at $25.0 \pm 0.1 \text{ }^\circ\text{C}$.

The content was mixed well and then immediately transferred to the spectrophotometric cell with a path length of 10 cm. The change in absorbance was recorded at 368 nm as a function of time every 30 s over a period of 6 min. The rate of the reaction at different concentrations of each of the reactants was obtained by measuring the slope of the linear part of the kinetic curves of the

absorbance-time plot (from Beer's law $A=\epsilon lc$, $dA/dt=\epsilon l(dc/dt)$, $slope = dA/dt$, $rate=dc/dt$ $dc/dt=(dA/dt)/\epsilon l$). The calibration graph was constructed by plotting the slope of the linear part of the kinetic curve versus concentration of the DFB (c_{DFB} , $\mu\text{g}/\text{cm}^3$).

Results and Discussion

Kinetic studies

The tangent method was used for processing the kinetic data. The rate of the reaction was obtained by measuring the slope of the linear part of the kinetic curves of the absorbance-time plot ($slope=dA/dt$). In order to determine the lowest possible determinable concentration of DFB, working conditions had to be optimized. Therefore, the dependence of the rate of reactions on the concentration of each of the reactants was determined. In Figure 2 the influence of pH on the initial rate in the presence and absence of DFB is shown. The effect of pH on the rate of both reactions, catalytic and inhibited, was studied in the interval pH from 4.0 to 5.0. Reaction rate is increased with increasing pH from 4.0-4.7 for catalytic reaction, and for inhibited reaction is increased from pH 4.0 to 4.5. For further work a pH of 4.7 was used. Catalytic reaction is -0.75 order in the interval pH 4.0 – 4.70, and the inhibited reaction is -1.2 in the mentioned pH interval.

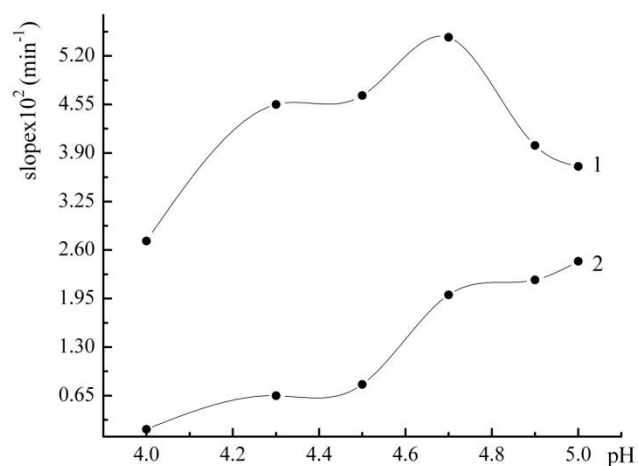


Figure 2. Dependence of the reaction rate on the pH for the catalyzed (1) and inhibited (2) reaction. Initial concentrations: $c(\text{SA}) = 4.0 \times 10^{-3} \text{ mol/dm}^3$; $c(\text{KIO}_4) = 18.0 \times 10^{-4} \text{ mol/dm}^3$; $c(\text{Fe(III)}) = 3.0 \times 10^{-8} \text{ mol/dm}^3$; $c(\text{phen}) = 6.0 \times 10^{-5} \text{ mol/dm}^3$; $c(\text{DFB}) = 26.18 \text{ } \mu\text{g/cm}^3$; $t = 25.0 \pm 0.1^\circ\text{C}$.

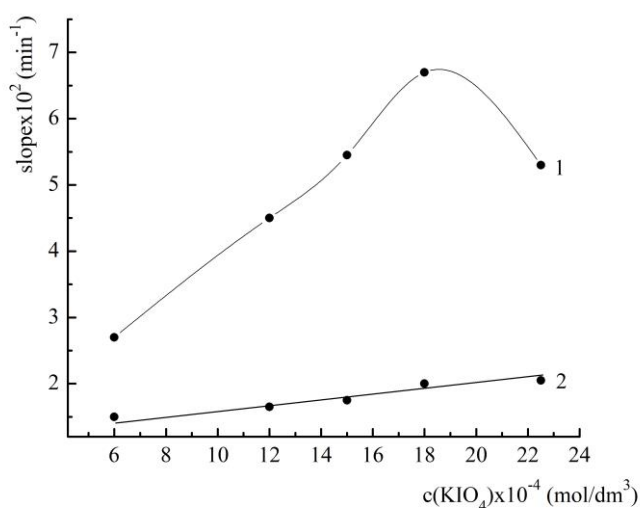


Figure 3. Dependence of the reaction rate on the KIO_4 concentration for the catalyzed (1) and inhibited (2) reaction. Initial concentrations: $\text{pH} = 4.7$; $c(\text{SA}) = 4.0 \times 10^{-3} \text{ mol/dm}^3$; $c(\text{Fe(III)}) = 3.0 \times 10^{-8} \text{ mol/dm}^3$; $c(\text{phen}) = 6.0 \times 10^{-5} \text{ mol/dm}^3$; $c(\text{DFB}) = 26.18 \text{ } \mu\text{g/cm}^3$; $t = 25.0 \pm 0.1^\circ\text{C}$.

The effect of the concentration of KIO_4 on the rates is shown in Figure 3. The influence of KIO_4 was studied in the range $6.0 \times 10^{-4} - 22.5 \times 10^{-4} \text{ mol/dm}^3$. The reaction rate of both reactions is increased with increasing KIO_4 concentration. A KIO_4 concentration of $18.0 \times 10^{-4} \text{ mol/dm}^3$ was selected for the further work. Catalytic reaction is the first order in the interval KIO_4 $6.0 \times 10^{-4} - 18.0 \times 10^{-4} \text{ mol/dm}^3$, and inhibited reaction is the first order through the whole investigated interval.

The effect of the concentration of SA was studied (Figure 4) in the interval of $1.0 \times 10^{-3} - 6.0 \times 10^{-3} \text{ mol/dm}^3$.

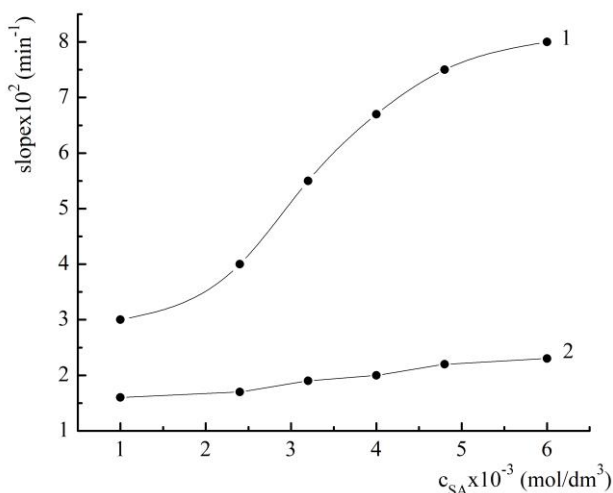


Figure 4. Dependence of the reaction rate on the SA concentration for the catalyzed (1) and inhibited (2) reaction. Initial concentrations: $\text{pH} = 4.7$; $c(\text{KIO}_4) = 18.0 \times 10^{-4} \text{ mol/dm}^3$; $c(\text{Fe (III)}) = 3.0 \times 10^{-8} \text{ mol/dm}^3$; $c(\text{phen}) = 6.0 \times 10^{-5} \text{ mol/dm}^3$; $c(\text{DFB}) = 26.18 \text{ } \mu\text{g/cm}^3$; $t = 25.0 \pm 0.1^\circ\text{C}$.

The rate of the catalyzed and inhibited reaction is increased with increasing SA concentration through the whole investigated interval. For further work a concentration of $4.8 \times 10^{-3} \text{ mol/dm}^3$ was selected. Both reactions are the first order in the whole investigated interval.

Influence of the *o*-phenantroline concentration on reaction rates is shown in Figure 5. It is examined in the interval $2.0 \times 10^{-5} - 8.0 \times 10^{-5} \text{ mol/dm}^3$. The rate of the catalyzed and inhibited reaction was increased with increasing *o*-phenantroline concentration from 2.0×10^{-5} to $6.0 \times 10^{-5} \text{ mol/dm}^3$. For further work a concentration of $6.0 \times 10^{-5} \text{ mol/dm}^3$ was selected.

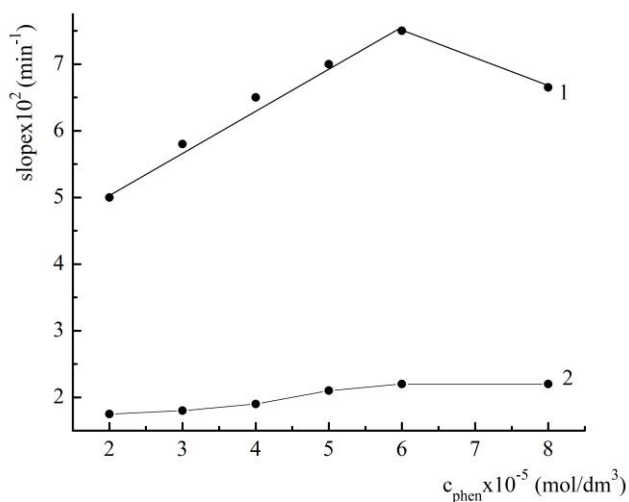


Figure 5. Dependence of the reaction rate on the *o*-phenantroline concentration for the catalyzed (1) and inhibited (2) reaction. Initial concentrations: pH = 4.7; $c(\text{KIO}_4) = 18.0 \times 10^{-4} \text{ mol/dm}^3$; $c(\text{SA}) = 4.8 \times 10^{-3} \text{ mol/dm}^3$; $c(\text{Fe (III)}) = 3.0 \times 10^{-8} \text{ mol/dm}^3$; $c(\text{DFB}) = 26.18 \text{ }\mu\text{g/cm}^3$; $t = 25.0 \pm 0.1^\circ\text{C}$.

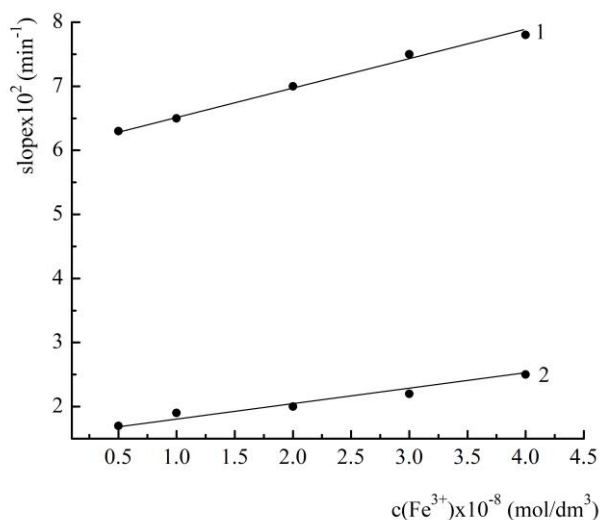


Figure 6. Dependence of the reaction rate on the Fe(III) concentration for the catalyzed (1) and inhibited (2) reaction. Initial concentrations: pH = 4.7; $c(\text{KIO}_4) = 18.0 \times 10^{-4} \text{ mol/dm}^3$; $c(\text{SA}) = 4.8 \times 10^{-3} \text{ mol/dm}^3$; $c(\text{phen}) = 6.0 \times 10^{-5} \text{ mol/dm}^3$; $c(\text{DFB}) = 26.18 \text{ }\mu\text{g/cm}^3$; $t = 25.0 \pm 0.1^\circ\text{C}$.

The correlation between the slope and the Fe (III) concentration is given in Figure 6. The influence of the concentration of Fe (III) ion on the reaction rates of catalyzed and inhibited reactions was examined in the range 0.5×10^{-8} – 4.0×10^{-8} mol/dm³. A concentration of 3.0×10^{-8} mol/dm³ in the final solution was used throughout the experiments.

Under the optimum reaction conditions: pH=4.7; $c(\text{KIO}_4) = 18.0 \times 10^{-4}$ mol/dm³; $c(\text{SA}) = 4.8 \times 10^{-3}$ mol/dm³; $c(o\text{-phenantroline}) = 6.0 \times 10^{-5}$ mol/dm³; $c(\text{Fe(III)}) = 3.0 \times 10^{-8}$ mol/dm³; $t = 25.0 \pm 0.1$ °C, the DFB concentration was varied from 0.374 to 26.18 µg/cm³ and from 0.0374 to 0.374 µg/cm³. Figure 7 shows the calibration curve at the temperature of 25 °C, which can be used for the determination of the DFB concentration in the interval from 0.0374 to 0.374 µg/cm³. The least squares equation ($y = bx + a$, where b and a are the slope and intercept, respectively) for the calibration graphs and correlation coefficient, r (Miller, 1991) for the determination of DFB in the concentration range 0.0374 to 0.374 µg/cm³ and 0.374 – 26.18 µg/cm³ under the optimal reaction conditions, mentioned above, were calculated:

$$\text{Slope} \times 10^2 = -0.1057 \times c_{\text{DFB}} + 7.89 \quad r = -0.9979 \quad (1)$$

$$\text{Slope} \times 10^2 = -0.00066 \times c_{\text{DFB}} + 3.80 \quad r = -0.9927 \quad (2)$$

where *slope* is the slope of the linear part of the kinetic curve of the absorbance-time plot ($\text{Slope} = dA/dt = \epsilon l (dc/dt)$) and c_{DFB} is the DFB concentration expressed in µg/cm³.

The following kinetic equations for the catalyzed and inhibited reaction were deduced based on the obtained graphic correlations:

$$\text{Rate}_I = k_1 \cdot c_{\text{H}^+}^{-0.75} \cdot c_{\text{KIO}_4} \cdot c_{\text{SA}} \cdot c_{\text{phen}} \cdot c_{\text{Fe(III)}} \quad (3)$$

$$\text{Rate}_{II} = k_2 \cdot c_{\text{H}^+}^{-1.2} \cdot c_{\text{KIO}_4} \cdot c_{\text{SA}} \cdot c_{\text{Fe(III)}} \cdot c_{\text{DFB}}^{-1} \quad (4)$$

,where k_1 and k_2 are constant proportional to the rate constant of the catalyzed and inhibited reaction, respectively.

The equations are valid for the following concentrations: acetate buffer pH 4.0 – 4.7 for catalytic reaction and from 4.5 to 5.0 for inhibited reaction; $c(\text{KIO}_4) = 6.0 \times 10^{-4}$ – 18.0×10^{-4} mol/dm³; $c(\text{SA}) = 1.0 \times 10^{-3}$ – 6.0×10^{-3} mol/dm³; $c(o\text{-phen}) = 5.0 \times 10^{-5}$ – 8.0×10^{-5} mol/dm³; $c(\text{Fe(III)}) = 0.5 \times 10^{-8}$ – 4.0×10^{-8} mol/dm³ and $c(\text{DFB}) = 0.0374$ – 26.8 µg/cm³.

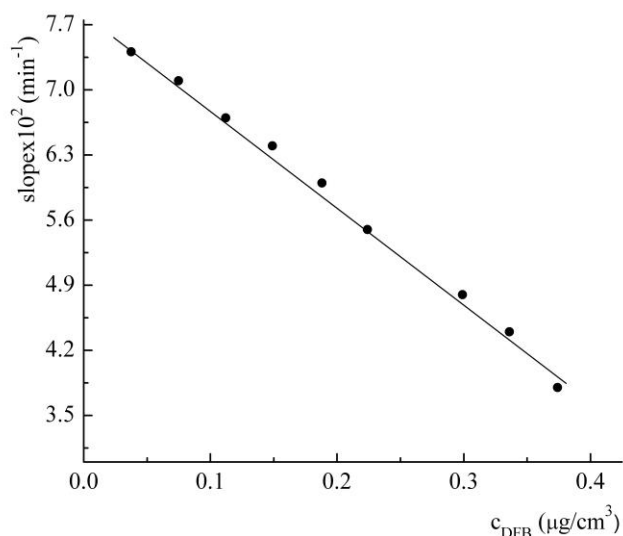


Figure 7. Dependence of the reaction rate on the DFB concentration in the interval 0.0374-0.374 $\mu\text{g}/\text{cm}^3$. Initial concentrations: $\text{pH} = 4.7$; $c(\text{KIO}_4) = 18.0 \times 10^{-4} \text{ mol}/\text{dm}^3$; $c(\text{SA}) = 4.8 \times 10^{-3} \text{ mol}/\text{dm}^3$; $c(o\text{-phen}) = 6.0 \times 10^{-5} \text{ mol}/\text{dm}^3$; $c(\text{Fe (III)}) = 3.0 \times 10^{-8} \text{ mol}/\text{dm}^3$; $t = 25.0 \pm 0.1^\circ\text{C}$.

The Limit of Detection (LOD) and Quantification (LOQ) were evaluated using the following equations (Bendito and Silva, 1988; Motolla, 1988; Prichard and Barwick, 2007): $\text{LOD} = 3.3S_0/b$ and $\text{LOQ} = 10S_0/b$, where S_0 is the standard deviation of the calibration line and b is the slope. They were found to be $0.0039 \mu\text{g}/\text{cm}^3$ and $0.0131 \mu\text{g}/\text{cm}^3$, respectively.

The precision and accuracy of the system were studied by performing the experiment 5 times for different concentration of DFB. The results of accuracy and precision of the recommended procedure are presented in Table 1.

Table 1. Accuracy and precision of DFB determination

Added ($\mu\text{g}/\text{cm}^3$)	Determined ^{a)} $\bar{x} \pm \text{SD}$ ($\mu\text{g}/\text{cm}^3$)	n	RSD (%)	G (%)	$\frac{\bar{x} - \mu}{\mu} \cdot 100$ (%) ^{b)}	Recovery (%)
0.0374	0.0366 ± 0.0008	5	2.22	2.78	-2.14	97.86
0.188	0.193 ± 0.004		2.11	2.63	2.66	102.65
0.374	0.382 ± 0.005		1.30	1.35	2.13	102.10

^{a)} Mean and standard deviation of five determinations at the 95 % confidence level; n- number of replicates; RSD - relative standard deviation; G- relative error; ^{b)} accuracy of the method

Interference studies

To assess the selectivity of the method, the interference due to several cations and anions was studied in detail. Different amounts of ionic species were added to the DFB solution. Table 2 gives the tolerance limits (expressed as v/v ratios), for the species studied in the determination of 3.74 $\mu\text{g}/\text{cm}^3$ of DFB. The maximum tolerated level was taken as that causing a difference in the rate of the inhibited reaction not larger than 5%. It may be seen that Cu^{2+} to DFB interferes with reaction. The other investigated ions have practically no influence on the determination of DFB by this method. And it means that selectivity of the method is good.

Table 2. Effect of the foreign species on the determination of 3.74 $\mu\text{g}/\text{cm}^3$ of DFB

Foreign species	Tolerance level ($C_{\text{Interferent}}/C_{\text{DFB}}$)	
$\text{Li}^+, \text{Na}^+, \text{K}^+, \text{Mg}^{2+}, \text{NH}_4^+, \text{NO}_3^-, \text{F}^-, \text{Cl}^-$	10^3	5-10
$\text{Mg}^{2+}, \text{Ca}^{2+}, \text{SO}_4^{2-}, \text{As}^{3+}, \text{S}_2\text{O}_3^{2-}$	10^2	5-10
$\text{I}^-, \text{NO}_2^-$	10	<5
$\text{Ba}^{2+}, \text{SO}_3^{2-}, \text{CO}_3^{2-}, \text{Mn}^{2+}, \text{Ni}^{2+}, \text{Zn}^{2+}, \text{Al}^{3+}$	1	<5
$\text{Co}^{2+}, \text{Fe}^{2+}$	0.1	5-10
Cu^{2+}		interfere

Applicability of the proposed method

The proposed method was applied to the determination of DFB in soil samples using the direct calibration curve. The results were compared with parallel HPLC method using a point hypothesis test (Hartman et al., 1995; Skoog et al., 1996). Detection of DFB under the optimum conditions (methanol-water (80:20, v/v)) delivered at a flowrate of 1 mL/min, and detection at a constant wavelength of 254 nm gave satisfactory results for the sensitivity of all spiked samples. They were treated as described in the Experimental section. As can be seen from Table 3, the results obtained for this method are in accordance with the parallel HPLC method. Therefore, the proposed method could be used for the determination of DFB in real samples after SPE. Table 3 shows that F and t values at 95% confidence level are less than the theoretical ones, confirming no significant differences between the performance of the proposed and HPLC method.

Table 3. Determination of diflufenzuron in soil samples by kinetic and HPLC method

Soil sample	Added DFB (µg/cm ³)	Found by kinetic method ^a $\bar{x} \pm SD$ (µg/cm ³)	RSD ^a (%)	$\frac{\bar{x} - \mu}{\mu} \cdot 100$	Recovery ^a (%)	Found by HPLC ^a $\bar{x} \pm SD$ (µg/cm ³)	Recovery ^a (%)	F value ^b	t value ^b
S1	0.10	0.093±0.003	3.20	-7.0	93.00	0.094±0.002	94.00	1.12	0.63
S2	0.20	0.195±0.01	5.10	-2.5	97.50	0.193±0.01	96.50	2.56	1.33
S3	0.26	0.249±0.006	2.40	-4.23	95.70	0.25±0.002	96.15	2.45	1.05
S4	0.18	0.17±0.003	1.76	-5.55	94.40	0.178±0.002	98.80	1.86	0.74
S5	0.08	0.085±0.001	1.17	6.25	106.25	0.087±0.001	108.75	1.09	0.25
S6	0.05	0.047±0.007	6.40	-6.0	94.00	0.049±0.001	98.00	1.17	0.74
S7	0.60	0.56±0.02	3.57	-6.66	95.00	0.58±0.03	96.66	2.86	1.25
S8	0.90	0.86±0.05	5.80	-4.44	95.50	0.85±0.05	94.44	2.92	2.14
S9	1.70	1.73±0.03	1.73	1.76	101.00	1.72±0.02	101.17	1.03	0.71
S10	3.60	3.57±0.2	5.60	-0.83	99.16	3.58±0.1	99.45	1.78	0.65
S11	7.00	7.05±0.3	4.25	0.71	100.00	7.02±0.3	100.30	2.59	1.05
S12	10.20	10.13±0.5	4.93	-0.68	99.30	10.19±0.5	99.90	1.37	0.96

^a Data are based on the average obtained from five determinations.

^b Theoretical F-value (v1=4, v2=4) and t-value (v=8) at 95 % confidence level are 6.39 and 2.306, respectively

Conclusion

The new kinetic-spectrophotometric method for the determination of diflubenzuron proposed in this paper is simple, rapid, inexpensive, and thus, it is very appropriate for routine quality control analysis of DFB in real samples. Spectrophotometry is the technique of choice even today due to its inherent simplicity. It is frequently used in the laboratories of the developing countries to overcome a variety of analytical problems. For the most laboratories for kinetic evaluations, spectrophotometer is available, and it is not an expensive apparatus. Advantage of the proposed method is simplicity owing to the elimination of some experimental steps such as extraction, and derivatization prior to absorbance measurements. The simple and not expensive chemicals are used. The procedure is easy to execute and requires less sample handling than some other methods currently described in the literature. Statistical comparison of the results with parallel HPLC method showed good agreement and indicates no significant difference in accuracy and precision. Reliable recovery data were found at various concentrations, after spiking samples, and good limits of quantification were attained. Therefore, the proposed method could be used for the determination of DFB in soil samples after extraction.

Acknowledgment

This research was supported by the Serbian Ministry of Education, Science and Technological Development (Agreement number 451-03-9/2021-14/200124). The authors are grateful for the financial support provided by the Ministry.

Conflict-of-Interest Statement

None.

References

- Amelin, V. G., Lavrukhin, D. K., & Tret'yakov, A. V. (2013). Dispersive liquid-liquid microextraction for the determination of herbicides of urea derivatives family in natural waters by HPLC. *Journal of Analytical Chemistry*, 68, 822-830.
- Ambike, V., & Argekar, A. (2017). Stability indicating HPLC method for the determination of diflubenzuron insecticide. *Science Journal of Energy Engineering*, 5(6), 152-157.
- Bendito, D. P., & Silva, M. (1988.). *Kinetic Methods in Analytical Chemistry*. Ellis Horwood: Chichester.
- Carneiro, R. P., Oliveira, F. A. S., Madureira, F. D., Silva, G., de Souza W. R., & Pereira Lopes, R. (2013). Development and method validation for determination of 128 pesticides in bananas by modified QuEChERS and UHPLC-MS/MS analysis. *Food Control*, 33, 413-423.
- Chen, B., Jin, B., Jiang, R., Xie, L., Lin, Y., Feng, W., & Ouyang, G. (2014). Screening and quantification of 304 pesticides and related organic pollutants in surface water using dispersive Liquid-Liquid Microextraction Coupled with Gas Chromatography-Mass Spectrometry. *Analytical Methods*, 6, 1743-1752.
- Chen, X., Zhao, K., Ge, B., & Chen, Q. (2013). Simultaneous determination of 44 pesticides in tobacco by UPLC/MS/MS and a modified QuEChERS procedure. *Journal of AOAC International*, 96, 422-431.
- Choi, S., Kim, S., Shin, J.Y., Kim, M., & Kim, J.-H. (2015). Development and verification for analysis of pesticides in eggs and egg products using QuEChERS and LC-MS/MS. *Food Chemistry*, 173, 1236-1242.
- Diaw, P. A., Maroto, A., Mbaye, O. M. A., Gaye-Seye, M. D., Stephan, L., Coly, A., Deschamps, L., Tine, A., Aaron, J. J., & Giamarchi, P. (2013). Determination of phenylurea pesticides by direct laser photo-induced fluorescence. *Talanta*, 116, 569-574.
- De Clercq, P., De Cock, A., Tirry, L., Viñuela, E., & Degheele, D. (1995). Toxicity of diflubenzuron and pyriproxyfen to the predatory bug *Podisus maculiventris*. *Entomologia Experimentalis et Applicata*, 74, 17-22.
- Du, P., Liu, X., Gu, X., Dong, F., Xu, J., Kong, Z., Wu, Y., Zhu, Y., Li, Y., & Zheng, Y. (2013). Rapid residue analysis of pyriproxyfen, avermectins and diflubenzuron in mushrooms by ultra-

performance liquid chromatography coupled with tandem mass spectrometry. *Analytical Methods*, 5, 6741-6747.

Erler, F., Polat, E., Demir, H., Catal, M., & Tuna, G. (2011). Control of mushroom sciarid fly *Lycoriella ingenua* populations with insect growth regulators applied by soil drench. *Journal of Economic Entomology*, 104(3), 839-844.

Graça Melo, M., Carqueijo, A., Freitas, A., Barbosa, J., & Sanches Silva, A. (2019). Modified QuEChERS extraction and HPLC-MS/MS for simultaneous determination of 155 pesticide residues in rice (*Oryza sativa* L.). *Foods* 9, 18. doi:10.3390/foods9010018.

Grahovac, Z. M., Mitić, S. S., Pecev, E. T., & Pavlović, A. N. (2010). Determination of the insecticide diflubenzuron in mushrooms by kinetic method and high-performance liquid chromatographic method. *Journal of Environmental Science and Health, Part B: Pesticides, Food Contaminants, and Agricultural Wastes*, 45, 783-789.

Guimarães de Oliveira, L., Ramkumar, A., Moloney, M., Scherer Kurz, M. H., Ferreira Gonçalves, F., Prestes, O. D., & Danaher, M. (2019). Vibrational extraction QuEChERS for analysis of antiparasitic agents in fish by liquid chromatography coupled with tandem mass spectrometry. *Analytical and Bioanalytical Chemistry*, 411, 6913-6929.

Huang, X., Qiao, K., Li, L., Liu, G., Xu, X., Lu, R., Gao, H., & Xu, D. (2019a). Preparation of a magnetic graphene/polydopamine nanocomposite for magnetic dispersive solid-phase extraction of benzoylurea insecticides in environmental water samples. *Scientific Reports*, 9:8919. DOI: 10.1038/s41598-019-45186-z

Huang, Y., Zhou, Q., Xie, G., Liu, H., & Lin, H. (2011). Titanium dioxide nanotubes for solid phase extraction of benzoylurea insecticides in environmental water samples, and determination by high performance liquid chromatography with UV detection. *Microchimica Acta*, 172, 109–115.

Hartmann, C., Smeyers-Verbeke, J., Penninckx, W., Vander Heyden, Y., Vankeerberghen, P., & Massart, D. L. (1995). Reappraisal of hypothesis testing the method validation: detection of systematic error by comparing the means of two methods or of two laboratories. *Analytical Chemistry*, 67, 4491-4499.

Huang, Y., Shi, T., Luo, X., Xiong, H., Min, F., Chen, Y., Nie, S., & Xie, M. (2019b). Determination of multi-pesticide residues in green tea with a modified QuEChERS protocol coupled to HPLC-MS/MS. *Food Chemistry*, 275, 255-264.

Irungu, J., Raina, S., & Torto, B. (2016). Determination of pesticide residues in honey: a preliminary study from two of Africa's largest honey producers. *International Journal of Food Contamination*, 3, 1-14.

Choi, S., Kim, S., Shin, J. Y., Kim, M., & Kim, J.-H. (2015). Development and verification for analysis of pesticides in eggs and egg products using QuEChERS and LC-MS/MS. *Food Chemistry*, 173, 1236–1242.

Kim, J.-H., Seo, J.-S., Moon, J.-K., & Kim, J.-H. (2013). Multi-residue method development of 8 benzoylurea insecticides in mandarin and apple using high performance liquid chromatography and liquid chromatography-tandem mass spectrometry. *Journal of the Korean Society for Applied Biological Chemistry*, 56, 47-54.

Klima of Forensnings Direktoratet (Klif). (2011). Environmental screening of veterinary medicines used in aquaculture – diflubenzuron and teflubenzuron. TA 2773. Utført av NIVA (Norwegian Institute for Water Research).

Łozowicka, B., Rutkowska, E., & Jankowska, M. (2017). Influence of QuEChERS modifications on recovery and matrix effect during the multi-residue pesticide analysis in soil by GC/MS/MS and GC/ECD/NPD. *Environmental Science and Pollution Research*, 24, 7124–7138.

Lee, S. W., Choi, J.-H., Cho, S.-K., Yu, H.-A., Abd El-Aty, A.M., & Shim, J.-H. (2011). Development of a new QuEChERS method based on dry ice for the determination of 168 pesticides in paprika using tandem mass spectrometry. *Journal of Chromatography A*, 1218, 4366–4377.

Matsumura, F. (2010). Studies on the action mechanism of benzoylurea insecticides to inhibit the process of chitin synthesis in insects: A review on the status of research activities in the past, the present and the future prospects. *Pesticide Biochemistry and Physiology*, 97, 133–139.

Macken, A., Lillicrap, A., & Langford, K. (2015). Benzoylurea pesticides used as veterinary medicines in aquaculture: risks and developmental effects on non-target crustaceans. *Environmental Toxicology and Chemistry*, 34(7), 1533-1542.

- Martínez-Domínguez, G., Nieto-García, A. J., Romero-González, R., & Frenich, A. G. (2015). Application of QuEChERS based method for the determination of pesticides in nutraceutical products (*Camellia sinensis*) by liquid chromatography coupled to triple quadrupole tandem mass spectrometry. *Food Chemistry*, 177, 182–190.
- Martín-Pozo, L., de Alarcón-Gómez, B., Rodríguez-Gómez, R., García-Córcoles, M. T., Çipa, M., & Zafra-Gómez, A. (2019). Analytical methods for the determination of emerging contaminants in sewage sludge samples. A review. *Talanta*, 192, 508-533.
- Mei, M., Huang X., Liao, K., & Yuan, D. (2015). Sensitive monitoring of benzoylurea insecticides in water and juice samples treated with multiple monolithic fiber solid-phase microextraction and liquid chromatographic analysis. *Analytica Chimica Acta*, 860, 29–36.
- Mei, M., Huang, X., & Yuan, D. (2014). Multiple monolithic fiber solid-phase microextraction: A new extraction approach for aqueous samples. *Journal of Chromatography A*, 1345, 29-36.
- Miller, J. N. (1991). Basic statistical methods for analytical chemistry. Part 2. Calibration and regression methods. A review. *Analyst*, 116, 3-14.
- Mottola, H. A. (1988). *Kinetic Aspects of Analytical Chemistry*. Wiley: New York.
- Ouyang, H., He, Y., & Lin, L. (2015). Determination of four kinds of pesticide residues in edible mushrooms by HPLC. *Journal of Southern Agriculture*, 46, 437-440.
- Olsvik, P. A., Samuelsen, O. B., Erdal, A., Holmelid, B., & Lunestad, B. T. (2013). Toxicological assessment of the anti-salmon lice drug diflubenzuron on Atlantic cod *Gadus morhua*. *Diseases of Aquatic Organisms*, 105, 27–43.
- Pecev-Marinković, E. T., Grahovac, Z. M., Pavlović, A. N., Tošić, S. B., Rašić Mišić, I. D., Mitić, M. N., Miletić, A. S., & Sejmanović, D. M. (2018). Development of a kinetic spectrophotometric method for insecticide diflubenzuron determination in water and baby food samples. *Hemijska Industrija*, 72(5), 305–314.
- Prichard, E., & Barwick, V. (2007). *Quality Assurance in Analytical Chemistry*. John Wiley & Sons: Teddington.
- Shi, X., Tang, Z., Sun, A., Zhou, L., Zhao, J., Li, D., Chen, J., & Pan, D. (2014). Simultaneous analysis of polychlorinated biphenyls and organochlorine pesticides in seawater samples by membrane-assisted solvent extraction combined with Gas Chromatography–Electron Capture

Detector and Gas Chromatography–Tandem Mass Spectrometry. *Journal of Chromatography B*, 972, 58–64.

Sun, R., Liu, C., Zhang, H., & Wang, Q. (2015). Benzoylurea chitin synthesis inhibitors. *Journal of Agricultural and Food Chemistry*, 63, 6847–6865.

Skoog, D. A., West, D. M., & Holler, F. J. (1996). *Fundamentals of Analytical Chemistry*. Saunders College Publishing: Philadelphia.

Tian, F., Qiao, C., Luo, J., Guo, L., Pang, T., Pang, R., Li, J., Wang, C., Wang, R., & Xie, H. (2020). Method development and validation of ten pyrethroid insecticides in edible mushrooms by modified QuEChERS and gas chromatography-tandem mass spectrometry. *Scientific Reports*. 10:7042. <https://doi.org/10.1038/s41598-020-64056-7>

Tfouni, S.A.V., Furlani, R.P.Z., Carreiro, L.B, Loredó, I.S.D., Gomes, A.G, Alves, L.A, Mata, R.S.S., Fonseca, A.M.D., & Rocha, R.M.S. (2013). Determination of diflubenzuron residues in milk and cattle tissues. *Arquivo Brasileiro de Medicina Veterinaria e Zootecnia*, 65, 301-307.

Tran, K., Eide, D., Nickols, S. M., Cromer, M. R., Sabaa-Srur, A., & Smith, R. E. (2012). Finding of pesticides in fashionable fruit juices by LC–MS/MS and GC–MS/MS. *Food Chemistry*, 134, 2398–2405.

Wang, J., Jiao, C., Li, M., Wang, X., Wang, C., Wu, Q., & Wang, Z. (2018). Porphyrin based porous organic polymer modified with Fe₃O₄ nanoparticles as an efficient adsorbent for the enrichment of benzoylurea insecticides. *Microchimica Acta*, 185, 36.

Wang, X., Yang, C., Huang, M., Wang, M., Zha, Y., Lin, L., & Zeng, S. (2014). Determination of diflubenzuron residues in vegetables by UPLC-MS/MS. *Advanced Materials Research*, 852, 266-269.

Willrich, M. M., & Boethel, D. J. (2001). Effects of diflubenzuron on *Pseudoplusia includens* (Lepidoptera: Noctuidae) and its parasitoid *Copidosoma floridanum* (Hymenoptera: Encyrtidae). *Environmental Entomology*, 30, 794-797.

WHO/FAO (2020). *Fao specifications and evaluations for agricultural pesticides*, Food and Agriculture Organisation of the United Nations.

Wang, H., Hu, L., Li, W., Lu, R., Zhang, S., Zhou, W., & Gao, H. (2016). A rapid and simple pretreatment method for benzoylurea insecticides in honey samples using in-syringe dispersive

liquid–liquid microextraction based on the direct solidification of ionic liquids. *Journal of Chromatography A*, 1471, 60–67.

Wang, H., Hu, L., Li, W., Yang, X., Lu, R., Zhang, S., Zhou, W., Gao, H., & Li, J. (2017). In-syringe dispersive liquid-liquid microextraction based on the solidification of ionic liquids for the determination of benzoylurea insecticides in water and tea beverage samples. *Talanta*, 162, 625–633.

Wang, S., Zhang, S., Dong, C., Wang, G., Guo, J., & Sun, W. (2013). Simultaneous determination of four herbicide and pesticide residues in Chinese green tea using QuEChERS purification procedure and UPLC-MS/MS analysis. *Advanced Materials Research*, 634-638, 1586-1590.

Yang, X., Qiao, K., Ye, Y., Yang, M., Li, J., Gao, H., Zhang, S., Zhou, W., & Lu, R. (2016). Facile synthesis of multifunctional attapulgite/Fe₃O₄/polyaniline nanocomposites for magnetic dispersive solid phase extraction of benzoylurea insecticides in environmental water samples. *Analytica Chimica Acta*, 934, 114–121.

Yang, M., Xi, X., Yang, X., Bai, L., Lu, R., Zhou, W., Zhang, S. & Gao, H. (2015). Determination of benzoylurea insecticides in environmental water and honey samples using ionic-liquid-mingled air-assisted liquid–liquid microextraction based on solidification of floating organic droplets. *RCS Advances*, 32(5), 25572-25580.

Zhang, Z., Lefebvre, T., Kerr, C., & Osprey, M. (2014). Simultaneous extraction and determination of various pesticides in environmental waters. *Journal of Separation Science*, 37, 3699–3705.

Zainudin, B. H., Salleh, S., Mohamed, R., Choy Yap, K., & Muhamad, H. (2015). Development, validation, and determination of multiclass pesticide residues in cocoa beans using gas chromatography and liquid chromatography tandem mass spectrometry. *Food Chemistry*, 172, 585–595.

Razvoj i primena kinetičko-spektrofotometrijske metode za analizu diflubenzurona u uzorcima zemljišta primenom SPE praćene HPLC metodom

Emilija Pecev-Marinković^{1*}, Ana Miletić¹, Aleksandra Pavlović¹, Vidoslav Dekić²

1- Univerzitet u Nišu, Prirodno-matematički fakultet, Departman za hemiju, Višegradska 33, 18000 Niš, Republika Srbija

2- Univerzitet u Prištini, Prirodno-matematički fakultet, Departman za hemiju, Ivo Lole Ribara 29, Kosovska Mitrovica, Republika Srbija

SAŽETAK

U radu je predstavljena nova osetljiva i jednostavna kinetičko-spektrofotometrijska metoda za određivanje insekticida diflubenzurona (DFB). Kinetička metoda je bazirana na inhibitornom efektu DFB na oksidaciju sulfanilne kiseline (engl. SA) kalijum-perjodatom u prisustvu Fe(III) jona kao katalizatora i 1,10-fenantrolina. Reakcija je praćena spektrofotometrijski merenjem apsorbance proizvoda reakcije sa vremenom na 368 nm. Diflubenzuron je određen pomoću linearnog kalibracionog grafika u intervalu od 0,0374 do 0,374 $\mu\text{g}/\text{cm}^3$ i od 0,374 do 26,18 $\mu\text{g}/\text{cm}^3$. Limit detekcije i limit kvantifikacije metode sa 3σ -kriterijumima su bili 0,0039 $\mu\text{g}/\text{cm}^3$ i 0,0131 $\mu\text{g}/\text{cm}^3$, redom. Relativne standardne devijacije za pet replikatnih određivanja od 0,0374, 0,188 i 0,374 $\mu\text{g}/\text{cm}^3$ DFB su bile 2,24, 2,11 i 1,10%, redom. Metoda je uspešno primenjena za određivanje DFB ostataka u uzorcima zemljišta. Tvrdofazna ekstrakcija (engl. SPE) je korišćena za ekstrakciju DFB iz zemljišta sa Chromabond® (Macherey-Nagel) C18-kertridžima. HPLC metoda korišćena je kao komparativna metoda za verifikaciju rezultata. Rezultati dobijeni korišćenjem dve različite metode pokazali su dobro slaganje.

Ključne reči: diflubenzuron, kinetička metoda, HPLC metoda, čvrsto-fazna ekstrakcija, uzorci zemljišta

Développement et application d'une méthode cinétique-spectrophotométrique pour l'analyse du diflubenzuron dans des échantillons de sol à l'aide de la SPE suivie de la méthode HPLC

Emilija Pecev-Marinković^{1*}, Ana Miletić¹, Aleksandra Pavlović¹, Vidoslav Dekić²

1- Université de Niš, Faculté des sciences naturelles et des mathématiques, Département de chimie, Višegradska 33, 18000 Niš, République de Serbie

2- Université de Priština, Faculté des sciences naturelles et des mathématiques, Département de chimie, Ivo Lole Ribara 29, Kosovska Mitrovica, République de Serbie

RÉSUMÉ

Le but de cet article est de présenter une nouvelle méthode cinétique-spectrophotométrique sensible et simple pour la détermination de l'insecticide diflubenzuron (DFB). La méthode cinétique est basée sur l'effet inhibiteur du DFB sur l'oxydation de l'acide sulfanilique (en anglais SA) par le periodate de potassium dans un tampon acétate en présence de l'ion Fe(III) comme catalyseur et du 1,10-phénantroline. La réaction a été contrôlée par spectrophotométrie en mesurant l'augmentation de l'absorbance du produit de la réaction avec le temps à 368 nm. Le diflubenzuron a été déterminé au moyen du graphique d'étalonnage linéaire dans l'intervalle de 0,0374 à 0,374 $\mu\text{g}/\text{cm}^3$ et de 0,374 à 26,18 $\mu\text{g}/\text{cm}^3$. La limite de la détection et la limite de la quantification de la méthode avec les critères 3σ étaient respectivement de 0,0039 $\mu\text{g}/\text{cm}^3$ et 0,0131 $\mu\text{g}/\text{cm}^3$. Les écarts relatifs standard pour les cinq déterminations répétées de 0,0374, 0,188 et 0,374 $\mu\text{g}/\text{cm}^3$ de DFB étaient de 2,24, 2,11 et 1,10%, respectivement. La méthode a été appliquée avec succès pour déterminer les résidus du DFB dans des échantillons de sol. L'extraction en phase solide (en anglais SPE) a été utilisée pour l'extraction du DFB du sol et des échantillons avec des cartouches Chromabond® (Macherey-Nagel) C18. La méthode HPLC a été utilisée en tant que méthode comparative pour la vérification des résultats. Les résultats obtenus à l'aide des deux méthodes différentes ont montré une bonne concordance.

Mots-clés: diflubenzuron, méthode cinétique, méthode HPLC, extraction en phase solide, échantillons de sol.

Разработка и применение кинетико-спектрофотометрического метода анализа дифлубензулона в образцах почвы с использованием ТФЭ с последующей ВЭЖХ.

Эмилия Пецев-Маринкович^{1*}, Ана Милетич¹, Александра Павлович¹, Видослав Декич²

1- Университет в Нише, Естественно-математический факультет, Кафедра химии, Вишеградска 33, 18000 Ниш, Сербия

2- Университет в Приштине, Естественно-математический факультет, Кафедра химии, Иво Лоле Рибара 29, Косовска Митровица, Республика Сербия

АННОТАЦИЯ

Цель данной статьи - представить новый чувствительный и простой кинетико-спектрофотометрический метод определения инсектицида дифлубензулона (ДФБ). Кинетический метод основан на ингибирующем действии ДФБ на окисление сульфаниловой кислоты (СК) периодатом калия в ацетатном буфере в присутствии иона Fe(III) в качестве катализатора и 1,10-фенантролина. За реакцией следили спектрофотометрические измеряя увеличение поглощения продукта реакции при длине волны 368 nm с течением времени. Дифлубензурон определяли по линейному градуировочному графику в интервале от 0,0374 до 0,374 $\mu\text{g}/\text{cm}^3$ и от 0,374 до 26,18 $\mu\text{g}/\text{cm}^3$. Предел обнаружения и предел количественной оценки метода с критерием 3σ составили 0,0039 $\mu\text{g}/\text{cm}^3$ и 0,0131 $\mu\text{g}/\text{cm}^3$ соответственно. Относительные стандартные отклонения для пяти повторных определений 0,0374, 0,188 и 0,374 $\mu\text{g}/\text{cm}^3$ ДФБ составили 2,24, 2,11 и 1,10% соответственно. Метод успешно применен для определения остатков ДФБ в образцах почвы. Твердофазную экстракцию (ТФЭ) использовали для экстракции ДФБ из почвы и образцов с картриджами Chromabond® (Macherey-Nagel) C18. Метод ВЭЖХ использовался в качестве сравнительного метода для проверки результатов. Результаты, полученные двумя разными методами, показали хорошее согласие.

Ключевые слова: дифлубензурон, кинетический метод, метод ВЭЖХ, твердофазная экстракция, образцы почвы.

Entwicklung und Anwendung einer kinetisch-spektrophotometrischen Methode zur Analyse von Diflubenzuron in Bodenproben mittels SPE gefolgt von HPLC-Methode

Emilija Pecev-Marinković^{1*}, Ana Miletić¹, Aleksandra Pavlović¹, Vidoslav Dekić²

1- Universität in Niš, Fakultät für Naturwissenschaften und Mathematik, Lehrstuhl für Chemie, Višegradska 33, 18000 Niš, Republik Serbien

2- Universität in Priština, Fakultät für Naturwissenschaften und Mathematik, Lehrstuhl für Chemie, Ivo Lole Ribara 29, Kosovska Mitrovica, Republik Serbien

ABSTRACT

Ziel dieser Arbeit ist es, eine neue empfindliche und einfache kinetisch-spektrophotometrische Methode zur Bestimmung des Insektizids Diflubenzuron (DFB) vorzustellen. Die kinetische Methode basiert auf hemmender Wirkung von DFB auf die Oxidation von Sulfanilsäure (eng. SA) durch Kaliumperiodat in Acetatpuffer in Gegenwart von Fe(III)-Ionen als Katalysator und 1,10-Phenanthrolin. Die Reaktion wurde spektrophotometrisch überwacht, indem die Absorption des Reaktionsprodukts mit der Zeit bei 368 nm gemessen wurde. Diflubenzuron wurde mit linearer Kalibrierungsgrafik im Intervall von 0,0374 bis 0,374 $\mu\text{g}/\text{cm}^3$ und von 0,374 bis 26,18 $\mu\text{g}/\text{cm}^3$ bestimmt. Die Nachweis- und Bestimmungsgrenze der Methode mit 3σ -Kriterien betrug 0,0039 $\mu\text{g}/\text{cm}^3$ bzw. 0,0131 $\mu\text{g}/\text{cm}^3$, nacheinander. Die relativen Standardabweichungen für fünf Wiederholungsbestimmungen von 0,0374, 0,188 und 0,374 $\mu\text{g}/\text{cm}^3$ DFB betrugen 2,24, 2,11 bzw. 1,10 %, nacheinander. Die Methode wurde erfolgreich zur Bestimmung von DFB-Rückständen in Bodenproben angewendet. Die Festphasenextraktion (eng. SPE) wurde zur Extraktion von DFB aus Boden mit Chromabond® (Macherey-Nagel) C18-Kartuschen verwendet. Als Vergleichsmethode wurde die HPLC-Methode zur Überprüfung der Ergebnisse verwendet. Die mit zwei verschiedenen Methoden erhaltenen Ergebnisse zeigten eine gute Übereinstimmung.

Schlüsselwörter: Diflubenzuron, Kinetische Methode, HPLC-Methode, Festphasenextraktion, Bodenproben

Synthesis, characterization, and antimicrobial activity of novel 2-ferrocenyl-1,3-thiazolidin-4-thiones

Todosijević Anka^{1*}, Jančić Minić Aleksandra², Mihailović Vladimir³, Srećković Nikola³

1- University of Niš, Faculty of Agriculture, Kosančićeva 4, 37000 Kruševac, Serbia

2- University of Priština, Faculty of Technical Sciences, Knjaza Miloša 7, 38220 Kosovska Mitrovica, Serbia

3- University of Kragujevac, Faculty of Science Department of Chemistry, Radoja Domanovića 12, 34000 Kragujevac, Serbia

ABSTRACT

Synthesis of five novel 2-ferrocenyl-1,3-thiazolidin-4-thiones has been achieved in good to excellent yields through the treatment of 2-ferrocenyl-1,3-thiazolidin-4-ones with Lawesson's reagent. The reaction was performed by refluxing the reactants mixture in toluene overnight. All prepared compounds were characterized by the IR and NMR spectral data. Further, the obtained products were evaluated for their antibacterial and antifungal activity.

Keywords: Ferrocene, 2-Ferrocenyl-1,3-thiazolidin-4-thiones, 2-Ferrocenyl-1,3-thiazolidin-4-ones, Characterization, Antimicrobial activity.

Todosijević Anka*: anka.pejovic@gmail.com

Minić Aleksandra: aleksandra.minic.989@gmail.com and aleksandra.minic@pr.ac.rs

Mihailović Vladimir: vladimir.mihailovic@pmf.kg.ac.rs

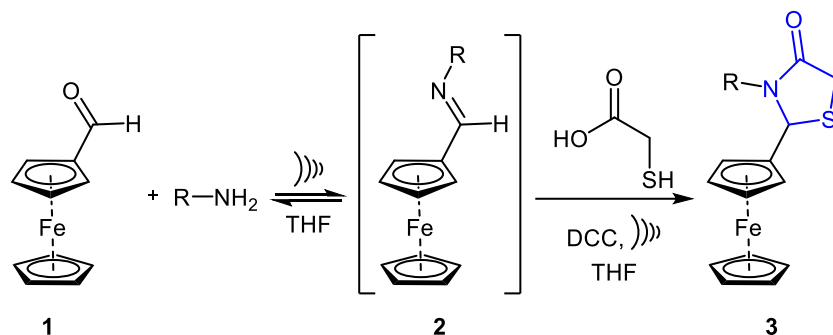
Srećković Nikola: nikola.sreckovic@pmf.kg.ac.rs

Introduction

Since the middle of the last century, antimicrobial agents have been efficiently used in health care. However, recent success in the application of antibiotics in infections treatment has been eroded by the increased resistance of bacteria. Therefore, there is a permanent interest in the development of novel compounds that exhibit antimicrobial activity (Hawkey, 2008; Cantón, 2009). Ferrocene derivatives have been demonstrated to possess a broad spectrum of biological activity, including antibacterial (Damljanović et al., 2009; Li et al., 2013), antifungal (Rubbiani, 2016), anti-inflammatory (Shinde et al., 2018), antitumor (Staveren and Metzler-Nolte, 2004; Fouda, 2007; Hillard, 2010; Biot, 2000) and anti-HIV (Kondapi et al., 2006) activity. In addition, due to the favorable electronic properties of ferrocene and its easy functionalization, these substances have been found many applications in materials science, including sensors (Labande and Astruc, 2000; Labande et al., 2002; Daniel et al., 2003, Astruc et al., 2004, Armada et al., 2006; Ornelas, 2007; Astruc, 2008; Ornelas et al., 2009; Djeda, 2010), catalysts (Astruc, 2008; Wei et al. 2002, Zhang et al., 2002; Ornelas et al., 2007; Diallo et al., 2007; Ornelas et al., 2008), electroactive materials (Daniel et al., 2006, Astruc et al., 2008; Ornelas et al., 2008; Wang et al., 2009; Astruc et al., 2009; Megiatto et al., 2010) and aerospace materials (Ansari et al., 2018; Neuenfeldt et al., 2011).

On the other hand, the chemistry of thiazolidinone ring is of substantial interest as it represents is a core structure in numerous synthetic medicaments displaying a wide variety of biological activities (Makwana and Malani, 2017). The thiazolidinone scaffold is also found in various natural products, especially thiamines, molecules possessing cardiac and glycemic benefits such as troglitazone (Ghazzi et al., 1997) and many metabolic products of fungi and primitive marine animals, including 2-(aminoalkyl)-4-carboxylic acids (Schmidt et al., 1987). A number of thiazolidinone derivatives have displayed various biological activities such are antidiabetic (Verma and Thareja, 2016), anticancer (Szychowski et al., 2017), anticonvulsant (Mishchenko et al., 2020), antimicrobial (Viswajanani et al., 2005), anti-HIV (Rawal et al., 2005), PAF antagonist (Tanabe et al., 1991), COX inhibitory (Ottana et al., 2002), tumor necrosis factor- α antagonist (Voss et al., 2003) and antioxidant (Shih and Ke, 2004). Besides, thiazolidinone derivatives are of interest in a wide range of pharmaceutical, agrochemical,

coordination, medicinal, and organic chemistry applications (Chaves et al., 2014; Corrêa et al., 2016; Deng et al., 2011).



Scheme 1. Synthesis of *N*-substituted 2-ferrocenyl-1,3-thiazolidin-4-ones **3** (Pejović et al., 2014).

Several years ago, our team reported an easy and efficient method for the synthesis of the novel thiazolidinone derivatives - 2-ferrocenyl-1,3-thiazolidin-4-ones **3** (Scheme 1) (Pejović et al., 2014). These heterocycles that showed strong anxiolytic activity also demonstrated great initial results in the synthesis of another ferrocene containing thiazolidinones (Pejović et al., 2018). Bearing all previously mentioned in mind, we planned to synthesize 2-ferrocenyl-1,3-thiazolidin-4-thiones using 2-ferrocenyl-1,3-thiazolidin-4-ones **3** as starting material. Thus, in this research, we put emphasis on the synthesis, assignment of 1H and ^{13}C NMR spectral data of novel 2-ferrocenyl-1,3-thiazolidin-4-thiones as well as examination of their antimicrobial activity.

Experimental

Reagents and chemicals

All chemicals were commercially available and used as received, except the solvents, which were purified by distillation. Chromatographic separations were carried out using silica gel 60 (Merck, 230–400 mesh ASTM), whereas silica gel 60 on Al plates, layer thickness 0.2 mm (Merck) was used for TLC. Melting points (uncorrected) were determined on a Mel-Temp capillary melting points apparatus, model 1001. The 1H and ^{13}C NMR spectra of the samples in $CDCl_3$ were recorded on a Varian Gemini (200 MHz) (1H at 200 MHz, ^{13}C at 50 MHz) NMR

spectrometer. Chemical shifts are expressed in δ (ppm), relative to residual solvent protons as the internal standard (CDCl_3 : 7.26 ppm for ^1H and 77 ppm for ^{13}C). IR measurements were carried out with a Perkin–Elmer FTIR 31725-X spectrophotometer.

2-Ferrocenyl-1,3-thiazolidin-4-ones (3a-e)

2-Ferrocenyl-1,3-thiazolidin-4-ones (**3a-e**) were synthesized according to the previously described procedure (Pejović et al., 2014).

General procedure for the synthesis of 2-ferrocenyl-1,3-thiazolidin-4-thiones (5a-e)

A toluene solution of the suitable 2-ferrocenyl-1,3-thiazolidin-4-one (1 mmol), obtained according to a previously reported procedure (Pejović et al., 2014), was heated under stirring with Lawesson's reagent (1 mmol) overnight. The solvent was then evaporated, and the residue extracted with dichloromethane (three 20 mL portions). After drying overnight (anhydrous Na_2SO_4), the solvent was evaporated and the crude product purified by column chromatography (SiO_2 , hexane/ethyl acetate = 8: 2).

3-Butyl-2-ferrocenyl-1,3-thiazolidin-4-thione (**5a**). Orange solid. Yield 88%; m.p. = 119 °C; IR (neat): ν_{max} = 2952, 1181 cm^{-1} ; ^1H NMR (200 MHz, CDCl_3 , ppm): δ 5.88 (br t, 1H), 4.50 – 4.44 (m, 1H), 4.37 – 4.17 (m, 5H), 4.25 (s, 5H), 3.94 – 3.74 (m, 1H), 3.35 – 3.13 (m, 1H), 1.68 – 1.12 (m, 4H), 0.85 (t, J = 7.0 Hz, 3H); ^{13}C NMR (50 MHz, CDCl_3 , ppm): δ 195.3, 83.6, 71.5, 70.1, 70.0, 69.3, 68.9, 68.1, 47.5, 45.2, 27.7, 20.1, 13.7.

2-Ferrocenyl-3-hexyl-1,3-thiazolidin-4-thione (**5b**). Orange solid. Yield 90%; m.p. = 92 °C; IR (neat): ν_{max} = 2928, 1176 cm^{-1} ; ^1H NMR (200 MHz, CDCl_3 , ppm): δ 5.88 (br t, 1H), 4.51 – 4.41 (m, 1H), 4.36 – 4.05 (m, 6H), 4.24 (s, 5H), 3.90 – 3.70 (m, 1H), 3.35 – 3.15 (m, 1H), 1.65 – 1.07 (m, 8H), 0.84 (t, J = 6.5 Hz, 3H).; ^{13}C NMR (50 MHz, CDCl_3 , ppm): δ 195.1, 83.5, 71.4, 70.1, 70.0, 69.2, 68.8, 68.0, 47.7, 45.2, 31.1, 26.4, 25.5, 22.4, 13.9.

2-Ferrocenyl-3-octyl-1,3-thiazolidin-4-thione (**5c**). Orange solid. Yield 88%; m.p. = 78 °C; IR (neat): ν_{max} = 2920, 1203 cm^{-1} ; ^1H NMR (200 MHz, CDCl_3 , ppm): δ 5.87 (br t, 1H), 4.49 – 4.31 (m, 1H), 4.35 – 4.14 (m, 6H), 4.25 (s, 5H), 3.92 – 3.66 (m, 1H), 3.37 – 3.13 (m, 1H), 1.74 – 1.04

(m, 12H), 0.87 (t, $J = 6.5$ Hz, 3H); ^{13}C NMR (50 MHz, CDCl_3 , ppm): δ 195.3, 83.6, 71.5, 70.1, 70.0, 69.3, 68.8, 68.1, 47.8, 45.2, 31.7, 29.0, 26.8, 25.6, 22.6, 14.1.

2-Ferrocenyl-3-(*m*-tolyl)-1,3-thiazolidin-4-thione (**5d**). Orange solid. Yield 65%; m.p. = 78 °C; IR (neat): $\nu_{\text{max}} = 2956, 1165 \text{ cm}^{-1}$; ^1H NMR (200 MHz, CDCl_3 , ppm): δ 7.35 – 7.29 (m, 2H), 6.93 – 6.83 (m, 2H), 6.16 (br s, 1H), 4.36 – 4.07 (m, 4H), 4.25 (s, 5H), 3.86 (d, $J = 10.3$ Hz, 1H), 3.45 (d, $J = 10.3$ Hz, 1H), 2.29 (s, 3H); ^{13}C NMR (50 MHz, CDCl_3 , ppm): δ 198.4, 139.6, 129.2, 128.6, 127.9, 83.3, 74.5, 70.7, 69.7, 69.1, 68.7, 67.5, 45.7.

2-Ferrocenyl-3-(*p*-tolyl)-1,3-thiazolidin-4-thione (**5e**). Yield 60%, brown oil; IR (neat): $\nu_{\text{max}} = 2917, 1168 \text{ cm}^{-1}$; ^1H NMR (200 MHz, CDCl_3 , ppm): δ 7.09 – 6.93 (m, 2H), 6.90 – 6.68 (m, 2H), 6.10 (br s, 1H), 4.55 – 4.36 (m, 4H), 4.23 (s, 5H), 3.84 (d, $J = 10.3$ Hz, 1H), 3.55 (d, $J = 10.3$ Hz, 1H), 2.77 (s, 3H); ^{13}C NMR (50 MHz, CDCl_3 , ppm): δ 195.24, 158.18, 130.07, 129.59, 113.86, 83.38, 71.96, 70.23, 70.19, 69.25, 68.91, 68.11, 49.70, 30.9.

Antimicrobial activity determination

The antimicrobial activity of newly synthesized compounds was tested on four bacterial (*Enterococcus faecalis* ATCC 29212, *Escherichia coli* ATCC 25922, *Staphylococcus aureus* ATCC 25923, and *Salmonella enteritidis* ATCC 13076) and four fungal strains (*Candida albicans* ATCC 10231, *Fusarium oxysporum* FSB 91, *Aspergillus brasiliensis* ATCC 16404, and *Penicillium canescens* FSB 24). The microorganisms were obtained from the Institute of Public Health, Kragujevac, Serbia. For the determination of the antimicrobial activity of synthesized compounds, bacterial strains were grown on nutrient agar 24 h before the experiment, *C. albicans* was grown on sabouraud dextrose agar for 48 h, while molds were grown on potato glucose agar for 3–7 days before testing.

The minimal inhibitory concentrations (MICs) of tested compounds, standard antibiotic chloramphenicol, and antimycotic nystatin against selected bacterial and fungal strains were determined by the microdilution method in the sterile 96-well microtiter plates (A. Pejović et al., 2017). The different concentrations of compounds for antimicrobial testing were made in the sterile 96-well microtiter plates using Mueller–Hinton broth for bacterial strains and sabouraud dextrose broth for fungal growth. The evaluation of antibacterial and antifungal activities was

performed according to the CLSI recommendations (Clinical and Laboratory Standards Institute, 2012; Clinical and Laboratory Standards Institute, 2008a; Clinical and Laboratory Standards Institute, 2008b). Indicator resazurin was used for the detection of bacterial growth in microtiter plates, while the growth of fungi was monitored visually. The lowest concentration (in mg per mL) of tested compounds that inhibit visible bacterial or fungal growth was considered as minimal inhibitory concentration (MIC) value.

Results and Discussion

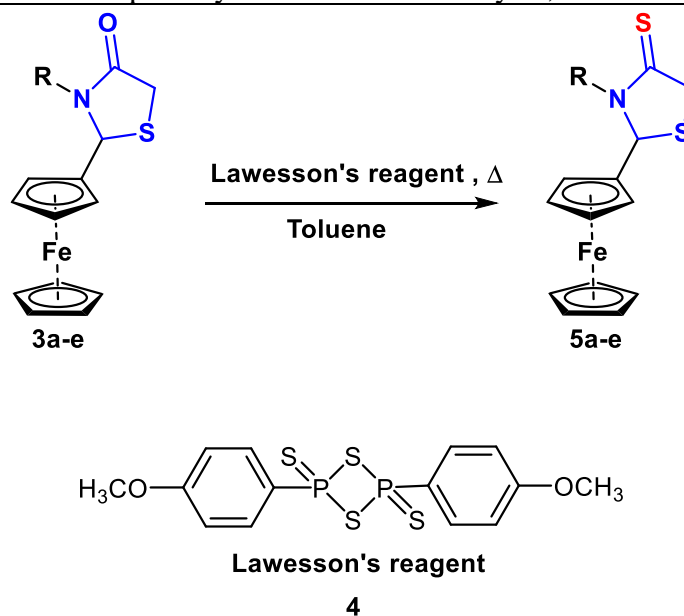
General synthesis of 2-ferrocenyl-1,3-thiazolidin-4-thiones **5a-e**

The obtaining of target compounds was conceived as the functionalization of the 2-ferrocenyl-1,3-thiazolidin-4-ones (Table 1, **3a-e**). It should comprise their thionation to afford the series of appropriate 2-ferrocenyl-1,3-thiazolidin-4-thiones. The thionation reaction of the thiazolidinone derivatives is commonly carried out in one of two reagents, phosphorus pentasulfide (P_4S_{10}) or Lawesson's reagent (LR) (Ozturk et al., 2008). In the last few years, scientists are claimed that Lawesson's reagent has advantages over P_4S_{10} in terms of requirements for excess P_4S_{10} , longer reaction time and higher temperature (Ozturk et al., 2008). Therefore, we considered synthesizing a series of novel ferrocene-containing thiazolidinthiones using Lawesson's reagent, and all in order to evaluate antimicrobial potential of the desired products.

The realization of this synthetic plan began with the preparation of the ferrocene-containing thiazolidinones, 2-ferrocenyl-1,3-thiazolidin-4-ones (Table 1, **3a-e**). A few years ago, we designed and optimized reaction conditions for their synthesis in high yields. The protocol involved a 25 min ultrasonic irradiation of the reaction mixture consisting of an amine, ferrocenecarboxaldehyde and thioglycolic acid in the ratio of 1/1/2. Thus, we synthesized the starting material by using this protocol. After the preparation of starting material, in the test experiment, the reaction between **3a** and Lawesson's reagent **4** was investigated. This reaction mixture was refluxed in the toluene during the night. After usual workup and column chromatography (SiO_2 /hexane = 8:2, v/v), the desired thiazolidinthione **5a** was obtained in great

yield (88%, Table 1, entry 1). These results did not require additional screenings, so we accepted them as the optimal ones.

Table 1. The substrate scope of synthesis of 2-ferrocenyl-1,3-thiazolidin-4-thiones **5a-e**



Entry	R	Product	Yields* (%)
1	n-Butyl	5a	88
2	n-Hexyl	5b	90
3	n-Octyl	5c	88
4	<i>m</i> -Tolyl	5d	65
5	<i>p</i> -Tolyl	5e	60

*Isolated yield after column chromatography.

The scope of the reaction was investigated on five known ferrocene-containing thiazolidinones. The desired products **5a-e** have been obtained in moderate to excellent yields (up to 90%) after the purification by means of column chromatography. Structural characterization has been confirmed by spectroscopic methods (NMR, IR) for all prepared compounds.

We have observed that electronic properties, as well as steric hindrance of the substituents on the *N*-atom, have an influence on reaction outcomes (See Table 1). Regarding that, the products with the aliphatic group bonded to the *N*-atom were obtained in excellent yields (up to 90%). The hexyl derivatives were isolated in the highest yield (90%, Table 1, entry

2), while the butyl derivative was obtained in a slightly low yield (88%, Table 1, entry 1). These results can be explained by electron-donating effect of these groups. The octyl derivative deviates a little bit from this rule (88%, entry 3, Table 1). We believe that the volume of the octyl group influenced the reaction outcome. In addition, the electronic properties also have an influence on the reaction outcome since the thiazolidinones with a methyl group on the phenyl ring leads to moderate yields (60 and 65%, Table 1, entries 5 and 4).

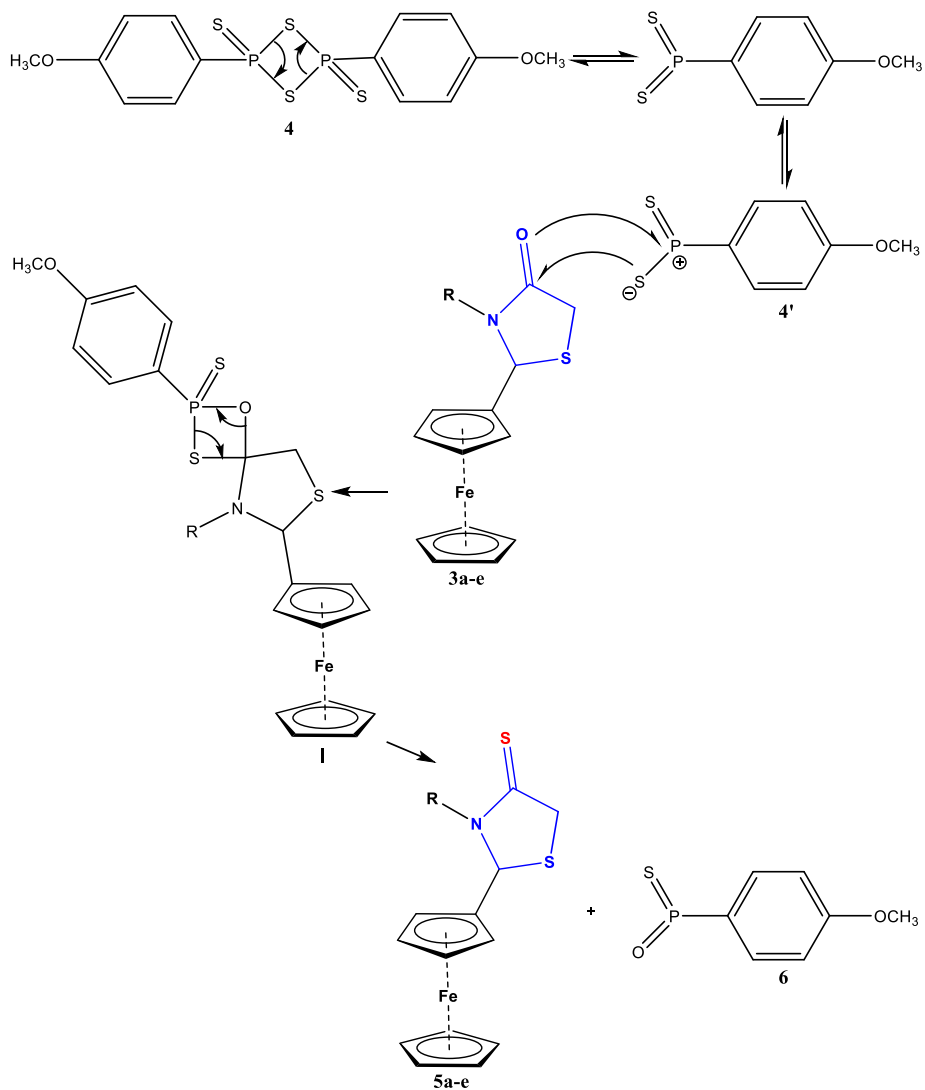
Several research groups investigated a mechanism of the thionation reaction of carbonyl compounds with Lawesson's reagent (Ozturk et al., 2008). Thus, a plausible reaction mechanism of thionation of ferrocene-containing thiazolidinone **3a** with Lawesson's reagent **4** is illustrated in Scheme 2. The first step of the mechanism of the reaction involves dissociation of Lawesson's reagent **4**. After dissociation, the reaction takes place through a two-step mechanism involving (i) a concerted cycloaddition between dithiophosphine ylide **4'** and the thiazolidinone compound **3a** to form a four-membered intermediate thioxaphosphetane **I** and (ii) a cycloreversion leading to the thiocarbonyl derivative **5a** and phenyl(thio)phosphine oxide **6**.

Spectral characterization

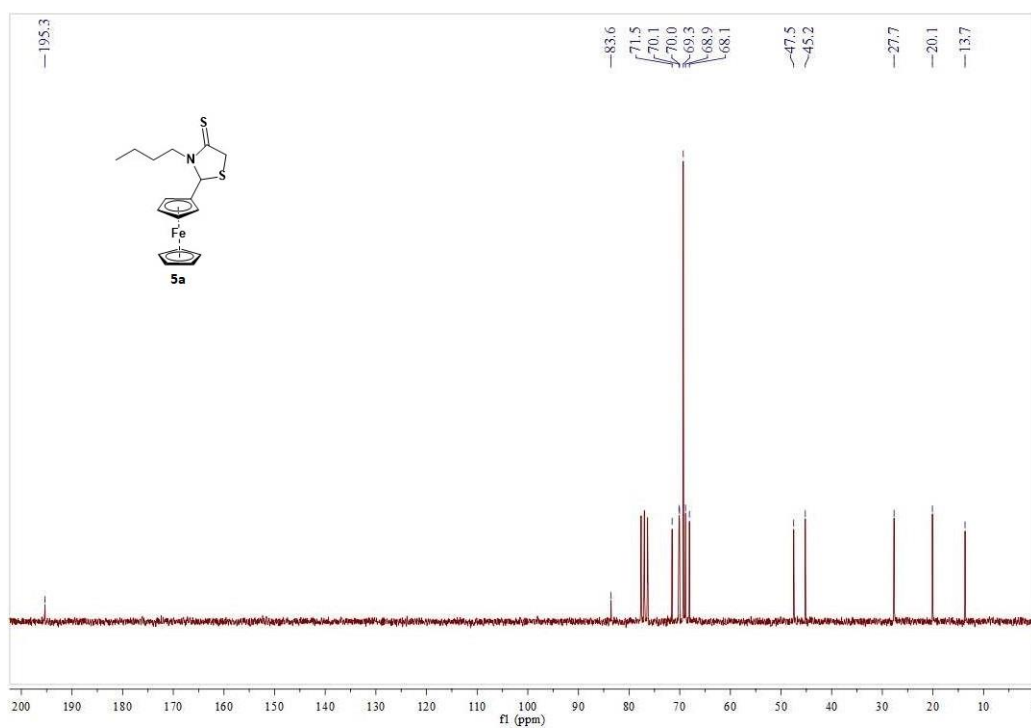
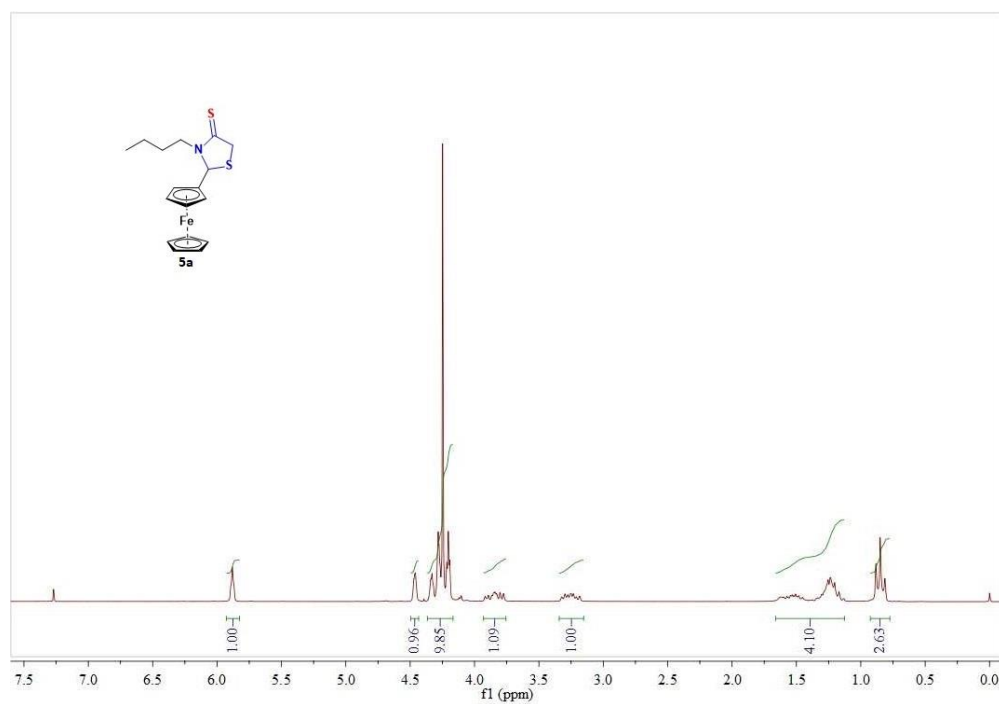
All synthesized ferrocene-containing thiazolidin-4-thiones **5a-e** were characterized by standard spectroscopic techniques (IR, ^1H -, and ^{13}C NMR). The collected data were in complete agreement with the proposed structures.

The main common feature of the IR spectra of five new thiazolidin-4-thiones **5a-e** is a strong band in range $1203\text{-}1165\text{ cm}^{-1}$, which is attributed to the C=S stretching vibrations. NMR spectra utterly confirm the structures of synthesized compounds. Thus, in the ^1H NMR spectra of all thiazolidin-4-thiones **5a-e** signals of the cyclopentadienyl rings, protons appear at similar positions in the spectra (4.25-4.23 ppm for the unsubstituted, and 4.55 - 4.05 ppm for the substituted rings). The ^1H NMR spectra of **5a-e** also contain characteristic signals for aliphatic and aromatic protons. They are located in the expected regions of ^1H NMR spectra. In addition, in ^1H NMR spectra of **5a-e**, one signal appears at about 6.16-5.87 ppm, which corresponds to the methine protons of thiazolidinthione moiety. On the other hand, their ^{13}C NMR spectra lack the carbonyl carbon from the thiazolidinone ring resonances, thus distinguishing themselves from

the corresponding precursors **3a-e**. The ^1H -, and ^{13}C NMR spectra of **5a** are presented in Figure 1 and Figure 2.



Scheme 2. The plausible schematic mechanism for the synthesis of titled compounds **5**



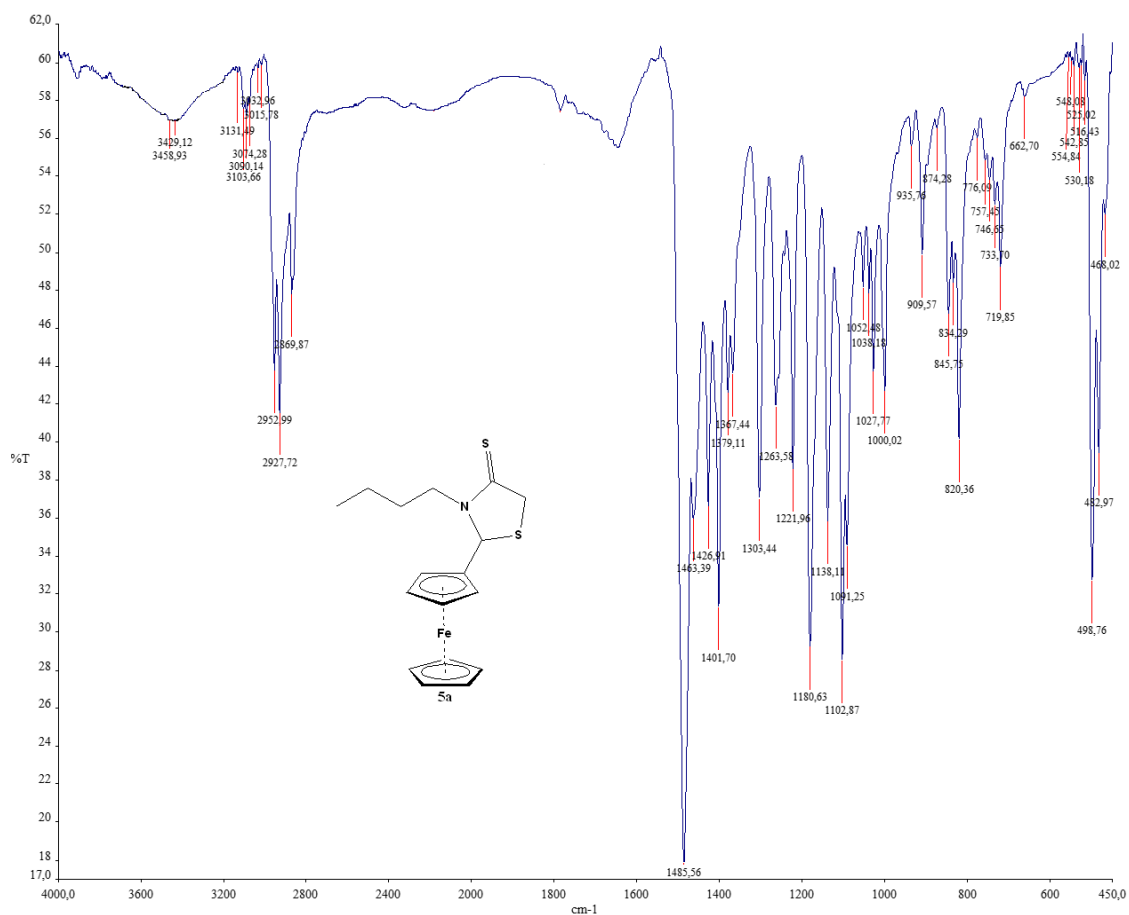


Figure 3. FTIR spectrum of **5a**

Antimicrobial activity

All types of synthesized compounds showed a low to moderate antimicrobial activity against most of the tested bacterial and fungal species. The most active compounds against *E. faecalis* (0.5 mg/mL) were **5a** and **5d**, while the MIC values for other bacteria were ranged from 1 to 2 mg/mL for all tested compounds, as presented in **Table 2**. However, **5e** did not show antibacterial activity against *S. aureus* in applied concentration. The antifungal activity of synthesized compounds was slightly better than their antibacterial activity according to obtained MIC values in tests with bacteria and fungi. The most of synthesized compounds inhibited the growth of tested molds and *C. albicans* in a concentration of 1 mg/mL. The only exception was *A. brasiliensis*, as the most resistant fungi on tested compounds with MIC values of 2 mg/mL for all compounds. MIC values of synthesized compounds were compared with the well-known

antibiotic (chloramphenicol) and antimycotic (nystatin), whereby results indicated much higher antibacterial and antifungal activities than synthesized compounds.

Table 2. Antibacterial and antifungal activities of synthesized compounds

Bacteria		MIC ^a (mg/mL)					MIC (µg/mL)
		5a	5b	5c	5d	5e	Chloramphenicol
<i>E. faecalis</i>	ATCC 29212	0.5	1	2	0.5	2	0.625
<i>E. coli</i>	ATCC 25922	2	2	1	2	2	0.625
<i>S. aureus</i>	ATCC 25923	2	2	2	2	>2	5
<i>S. enteritidis</i>	ATCC 13076	2	2	2	2	2	2.5
Fungi							Nystatin
<i>C. albicans</i>	ATCC 10259	1	1	1	2	1	2.5
<i>F. oxysporum</i>	FSB 91	1	1	1	1	2	1.25
<i>A. brasiliensis</i>	ATCC 16404	2	2	2	2	2	1.25
<i>P. canescens</i>	FSB 24	1	2	1	1	1	2.5

^aMIC- minimum inhibitory concentration.

Conclusion

Five novel 2-ferrocenyl-1,3-thiazolidin-4-thiones were prepared in moderate to excellent yields (up to 90%) using the standard synthetic protocol. The structures of all the obtained products were confirmed by the usage of standard spectroscopic methods.

The prepared heterocycles were tested against four bacterial (*Enterococcus faecalis*, *Escherichia coli*, *Staphylococcus aureus*, and *Salmonella enteritidis*) and four fungal strains (*Candida albicans*, *Fusarium oxysporum*, *Aspergillus brasiliensis*, and *Penicillium canescens*) using the microdilution method. The results of the experiment indicated that synthesized heterocycles showed moderate to weak antibacterial activity against less number of examined microorganisms. Besides, it was found that *N*-butyl and *N*-*m*-tolyl derivatives are the most active compounds against *E. faecalis*. Furthermore, antifungal activity of the synthesized ferrocene

derivatives tested on the human pathogen yeasts *C. albicans*, *F. oxysporom*, and *P. canescens*, showed that the obtained compounds have more pronounced antifungal potential.

Acknowledgment

This work was supported by the Ministry of Education, Science and Technological Development of the Republic of Serbia (Agreement No. 451-03-68/2020-14/200122).

Conflict-of-Interest Statement

None.

References

- Ansari, M. F., Idrees, D., Hassan, Md. I., Ahmad, K., AVECILLA, F., Azam, A. (2018). Design, synthesis and biological evaluation of novel pyridine-thiazolidinone derivatives as anticancer agents: Targeting human carbonic anhydrase IX. *European Journal of Medicinal Chemistry*, 144, 544–556.
- Armada, M. P. G., Losada, J., Zamora, M., Alonso, B., Cuadrado, I., Casado, C. M. (2006). Electrocatalytical properties of polymethylferrocenyl dendrimers and their applications in biosensing. *Bioelectrochemistry*, 69, 65–73.
- Astruc, D., Daniel, M. C., Ruiz, J. (2004). Dendrimers and gold nanoparticles as exo-receptors sensing biologically important anions. *Chemical Communication*, 2637–2649.
- Astruc, D., Ornelas, C., Aranzaes, J. R. (2008). Ferrocenyl-terminated dendrimers: Design for applications in molecular electronics, molecular recognition and catalysis. *Journal of Inorganic Organometallic Polymers and Materials*, 18, 4–17.
- Astruc, D., Ornelas, C., Ruiz, J. (2008). Metallocenyl dendrimers and their applications in molecular electronics, sensing, and catalysis. *Accounts of Chemical Research*, 41, 841–856.
- Astruc, D., Ornelas, C., Ruiz, J. (2009). Dendritic molecular electrochromic batteries based on redox-robust metallocenes. *Chemistry A European Journal*, 15, 8936–8944.

Biot, C., François, N., Maciejewski, L., Brocard, J., Poulain, D. (2000). Synthesis and antifungal activity of a ferrocene–fluconazole analogue. *Bioorganic & Medicinal Chemistry Letters*, 10, 839–841.

Cantón, R. (2009). Antibiotic resistance genes from the environment: a perspective through newly identified antibiotic resistance mechanisms in the clinical setting. *Clinical Microbiology and Infection*, 15, 20–25.

Chaves, J. D. S., Neumann, F. T., Francisco, T. M., Corrêa, C. C., Lopes, M. T. P., Silva, H., Fontes, A. P. S., Almeida, M. V. (2014). Synthesis and cytotoxic activity of gold(I) complexes containing phosphines and 3-benzyl-1,3-thiazolidine-2-thione or 5-phenyl-1,3,4-oxadiazole-2-thione as ligands. *Inorganica Chimica Acta*, 414, 85–90.

Clinical and Laboratory Standards Institute (2008a). Reference method for broth dilution antifungal susceptibility testing of yeasts (approved standard. document M27-A3). (3rd ed.). Wayne, PA.

Clinical and Laboratory Standards Institute (2008b). Reference method for broth dilution antifungal susceptibility testing of filamentous fungi (approved standard. document M38-A2.). (2nd ed.). Wayne, PA.

Clinical and Laboratory Standards Institute (2012). Methods for dilution antimicrobial susceptibility tests for bacteria that grow aerobically (approved standard. document M07-A9). (9th ed.). Wayne, PA.

Corrêa, R. S., Silva, M. M., Graminha, A. E., Meira, C. S., Santos, J. A. F., Moreira, D. R. M., Soares, M. B. P., Poelhsitz, G. V., Castellano, E. E., Bloch, C., Cominetti, M. R., Batista, A. A. (2016). Ruthenium(II) complexes of 1,3-thiazolidine-2-thione: Cytotoxicity against tumor cells and anti-*Trypanosoma cruzi* activity enhanced upon combination with benznidazole. *Journal of Inorganic Biochemistry*, 156, 153–163.

Daniel, M. C., Ruiz, J., Astruc, D. (2003). Supramolecular H-bonded assemblies of redox-active metallodendrimers and positive and unusual dendritic effects on the recognition of H_2PO_4^- . *Journal of the American Chemical Society*, 125, 1150–1151.

Daniel, M. C., Sakamoto, A., Ruiz, J., Astruc, D., Nishihara, H. (2006). Photoisomerization-induced Change in the Size of Ferrocenylazobenzene-attached Dendrimers. *Chemistry Letters*, 35, 38–39.

Damljanović, I., Vukićević, M., Radulović, N., Palić, R., Ellmerer, E., Ratković, Z., Joksović, M. D., Vukićević, R. D. (2009). Synthesis and antimicrobial activity of some new pyrazole derivatives containing a ferrocene unit. *Bioorganic & Medicinal Chemistry Letters*, 19, 1093–1096.

Deng, X., Chen, N., Wang, Z., Li, X., Hu, H., Xu, J. (2011). A convenient synthesis of thiazolidin-2-ones from thiazolidine-2-thiones: Antibiotic activity and revisiting the mechanism. *Phosphorus, Sulfur, Silicon Related Elements*, 186, 1563–1571.

Diallo, A. K., Ornelas, C., Salmon, L., Aranzaes, J. R., Astruc, D. (2007). "Homeopathic" catalytic activity and atom-leaching mechanism in Miyaura–Suzuki reactions under ambient conditions with precise dendrimer-stabilized Pd nanoparticles. *Angewandte Chemie International Edition*, 46, 8644–8648.

Djeda, R., Rapakousiou, A., Liang, L., Guidolin, N., Ruiz, J., Astruc, D. (2010). Click syntheses of 1,2,3-triazolylbiferrocenyl dendrimers and the selective roles of the inner and outer ferrocenyl groups in the redox recognition of ATP^{2-} and Pd^{2+} . *Angewandte Chemie International Edition*, 49, 8152–8156.

Fouda, M. F. R., Abd-Elzaher, M. M., Abdelsamaia, R. A., Labib, A. A. (2007). On the medicinal chemistry of ferrocene. *Applied Organometallic Chemistry*, 21, 613–625.

Hawkey, P. M. (2008). The growing burden of antimicrobial resistance. *Journal of Antimicrobial Chemotherapy*, 62, 1–9.

Hillard, E. A., Vessières A., Jaouen, G. (2010). Ferrocene functionalized endocrine modulators as anticancer agents. *Topics in Organometallic Chemistry*, 32, 81–117.

Kondapi, A. K., Satyanarayana, N., Saikrishna, A. D. (2006). A study of the topoisomerase II activity in HIV-1 replication using the ferrocene derivatives as probes. *Archives of Biochemistry and Biophysics*, 450, 123–132.

Labande, A., Astruc, D. (2000). Colloids as redox sensors: recognition of $H_2PO_4^-$ and HSO_4^- by amidoferrocenylalkylthiol–gold nanoparticles. *Chemical Communications*, 1007–1008.

- Labande, A., Ruiz, J., Astruc, D. (2002). Supramolecular gold nanoparticles for the redox recognition of oxoanions: Syntheses, titrations, stereoelectronic effects, and selectivity. *Journal of the American Chemical Society*, 124, 1782–1789.
- Li, S., Wang, Z., Wei, Y., Wu, C., Gao, S., Jiang, H., Zhao, X., Yan, H., Wang, X. (2013). Antimicrobial activity of a ferrocene-substituted carborane derivative targeting multidrug-resistant infection. *Biomaterials*, 34, 902–911.
- Makwana, H. R., Malani, A. H. (2017). A brief review article: thiazolidines derivatives and their pharmacological activities *Journal of Applied Chemistry*, 10, 76–84.
- Megiatto, J. D., Li, K., Schuster, D. I., Palkar, A., Herranz, M. A., Echegoyen, L., Abwandner, S., Miguel, G., Guldi, D. M. (2010). Convergent synthesis and photoinduced processes in multi-chromophoric rotaxanes. *The Journal of Physical Chemistry B*, 114, 14408–14419.
- Mishchenko, M., Shtrygol, S., Kaminsky, D., Lesyk, R. (2020). Thiazole-bearing 4-thiazolidinones as new anticonvulsant agents. *Scientia Pharmaceutica*, 88, 16.
- Neuenfeldt, P. D., Drawanz, B. B., Aguiar, A. C. C., Figueiredo, Jr. F., Krettli, A. U., Cunico, W. (2011). Multicomponent synthesis of new primaquine thiazolidinone derivatives. *Synthesis*, 23, 3866–3870.
- Ornelas, C., Aranzaes, J. R., Cloutet, E., Alves, S., Astruc, D. (2007). Click assembly of 1,2,3-triazole-linked dendrimers, including ferrocenyl dendrimers, which sense both oxo anions and metal cations. *Angewandte Chemie International Edition*, 46, 872–877.
- Ornelas, C., Aranzaes, J. R., Salmon, L., Astruc, D. (2008). "Click" dendrimers: Synthesis, redox sensing of Pd(OAc)₂, and remarkable catalytic hydrogenation activity of precise Pd nanoparticles stabilized by 1,2,3-triazole-containing dendrimers. *Chemistry– A European Journal*, 14, 50–64.
- Ornelas, C., Ruiz, J., Astruc, D. (2009). Dendritic and ion-pairing effects in oxo-anion recognition by giant alkylferrocenyl dendrimers. *Organometallics*, 28, 4431–4437.
- Ornelas, C., Ruiz, J., Belin, C., Astruc, D. (2009). Giant dendritic molecular electrochromic batteries with ferrocenyl and pentamethylferrocenyl termini. *Journal of the American Chemical Society*, 131, 590–601.

Ornelas, C., Salmon, L., Aranzaes, J. R., Astruc, D. (2007). Catalytically efficient palladium nanoparticles stabilized by "click" ferrocenyl dendrimers. *Chemical Communications*, 46, 4946–4948.

Ottana, R., Mazzon, E., Dugo, L., Monforte, F., Maccari, R., Sautebin, L., De Luca, G., Vigorita, M. G., Alcaro, S., Ortuso, F., Caputi, A. P., Cuzzocrea, S. (2002). Modeling and biological evaluation of 3,3'-(1,2-ethanediyl)bis[2-(4-methoxyphenyl)-thiazolidin-4-one], a new synthetic cyclooxygenase-2 inhibitor. *European Journal of Pharmacology*, 448, 71–80.

Ozturk, T., Ertas, E., Mert, O. (2007). Use of Lawesson's reagent in organic syntheses. *Chemical Reviews*, 107, 5210–5278.

Pejović, A., Denić, M. S., Stevanović, D., Damljanović, I., Vukićević, M., Kostova, K., Tavlinova-Kirilova, M., Randjelović, P., Stojanović, N. M., Bogdanović, G. A., Blagojević, P., D'hooghe, M., Radulović, N. S., Vukićević, R. D. (2014). Discovery of anxiolytic 2-ferrocenyl-1,3-thiazolidin-4-ones exerting GABA_A receptor interaction *via* the benzodiazepine-binding site. *European Journal of Medicinal Chemistry*, 83, 57–73.

Pejović, A., Damljanović, I., Stevanović, D., Minić, A., Jovanović, J., Mihailović, V., Katanić, J., Bogdanović, G. A. (2017). Synthesis, characterization and antimicrobial activity of novel ferrocene containing quinolines: 2-ferrocenyl-4-methoxyquinolines, 1-benzyl-2-ferrocenyl-2,3-dihydroquinolin-4(1*H*)-ones and 1-benzyl-2-ferrocenylquinolin-4(1*H*)-ones. *Journal of Organometallic Chemistry*, 846, 6–17.

Pejović, A., Minić, A., Jovanović, J., Pešić, M., Ilić Komatina, D., Damljanović, I., Stevanović, D., Mihailović, V., Katanić, J., Bogdanović, G. A. (2018). Synthesis, characterization, antioxidant and antimicrobial activity of novel 5-arylidene-2-ferrocenyl-1,3-thiazolidin-4-ones. *Journal of Organometallic Chemistry*, 869, 1–10.

Rawal, R. K., Prabhakar, Y. S., Katti, S. B., Clercq, E. D. (2005). 2-(Aryl)-3-furan-2-ylmethyl-thiazolidin-4-ones as selective HIV-RT inhibitors. *Bioorganic Medicinal Chemistry*, 13, 6771–6776.

Rubbiani, R., Blacque, O., Gasser, G. (2016). Sedaxicenes: potential new antifungal ferrocene-based agents? *Dalton Transactions*, 45, 6619–6626.

Scmidt, U., Utz, R., Lieberknecht, A., Griesser, H., Potzulli, B., Bahr, J., Wagner, K., Fischer, P. (1987). Amino acids and peptides; Synthesis of biologically active cyclopeptides; Synthesis of 16 isomers of dolastatin 3; Synthesis of the 2-(1-aminoalkyl)-thiazole-4-carboxylic acids. *Synthesis*, 233–236.

Shih, M. H., Ke, F. Y. (2004). Syntheses and evaluation of antioxidant activity of sydnonyl substituted thiazolidinone and thiazoline derivatives. *Bioorganic & Medicinal Chemistry*, 12, 4633–4643.

Shinde, D. N., Trivedi, R., Krishna, N. V., Giribabu, L., Sridhar, B., Rathod, B. B., Prakasham, R. S. (2018). Facile synthesis, characterisation and anti-inflammatory activities of ferrocenyl ester derivatives of 4-arylidene-5-imidazolinones. *Applied Organometallic Chemistry*, 32, e4021.

Staveren, D. R., Metzler-Nolte, N. (2004). Bioorganometallic chemistry of ferrocene. *Chemical Reviews*, 104, 5931–5986.

Szychowski, K. A., Leja, M. L., Kaminsky, D. V., Binduga, U. E., Pinyazhko, O. R., Lesyk, R. B., Gmiński, J. (2017). Study of novel anticancer 4-thiazolidinone derivatives. *Chemico-Biological Interactions*, 262, 46–56.

Tanabe, Y., Suzukamo, G., Komuro, Y., Imanishi, N., Morooka, S., Enomoto, M., Kojima, A., Sanemitsu, Y., Mizutani, M. (1991). Structure-activity relationship of optically active 2-(3-pyridyl)thiazolidin-4-ones as a PAF antagonists. *Tetrahedron Letters*, 32, 379–382.

Verma, S. K., Thareja, S. (2016). Molecular docking assisted 3D-QSAR study of benzylidene-2,4-thiazolidinedione derivatives as PTP-1B inhibitors for the management of type-2 diabetes mellitus. *RSC Advances*, 6, 33857–33867.

Viswajanani, J. S., Ajay, S., Smita, S., Seema, K., Manisha, P., Pragya, B., Tarun, M., Ashok, R., Mohan, K. J., Anitha, M. (2005). Synthesis and antimicrobial activity of novel thiazolidinones. *ARKIVOC*, 46–59.

Voss, M. E., Carter, P. H., Tebben, A. J., Scherle, P. A., Brown, G. D., Thompson, L. A., Xu, M., Lo, Y. C., Yang, G., Liu, R. Q., Strzemenski, P., Everlof, J. G., Trzaskos, J. M., Decicco, C. P. (2003). Both 5-arylidene-2-thioxodihydropyrimidine-4,6(1*H*,5*H*)-diones and 3-thioxo-2,3-dihydro-1*H*-imidazo[1,5-*a*]indol-1-ones are light-dependent tumor necrosis factor- α antagonists. *Bioorganic & Medicinal Chemistry Letters*, 13, 533–538.

Wang, A., Ornelas, C., Astruc, D., Hapiot, P. (2009). Electronic communication between immobilized ferrocenyl-terminated dendrimers. *Journal of the American Chemical Society*, 131, 6652–6653.

Wei, B., Vajtai, R., Choi, Y. Y., Ajayan, P. M., Zhu, H., Xu, C., Wu, D. (2002). Structural characterizations of long single-walled carbon nanotube strands. *Nano Letters*, 2, 1105–1107.

Zhang, X., Cao, A., Wei, B., Li, Y., Wei, J., Xu, C., Wu, D. (2002). Rapid growth of well-aligned carbon nanotube arrays. *Chemical Physics Letters*, 362, 285–290.

Sinteza, karakterizacija i antimikrobna aktivnost novih 2-ferocetil-1,3-tiazolidin-4-tiona

Todosijević Anka¹, Minić Aleksandra², Mihailović Vladimir³, Srećković Nikola³

1- Univerzitet u Nišu, Poljoprivredni fakultet, Kosančićeva 4, 37000 Kruševac, Srbija

2- Univerzitet u Prištini, Fakultet tehničkih nauka, Knjaza Miloša 7, 38220 Kosovska Mitrovica, Srbija

3- Prirodno-matematički fakultet, Univerzitet u Kragujevcu, Institut za hemiju, Radoja Domanovića 12, 34000 Kragujevac, Srbija

SAŽETAK

Serijski novih derivata 3-ferocetil-1,3-tiazolidin-4-tiona sintetisani su polazeći od odgovarajućih 3-ferocetil-1,3-tiazolidin-4-ona. Sintetisani jedinjenja su u potpunosti okarakterisani spektroskopskim metodama analize (¹H i ¹³C NMR, IR).

U narednom koraku biološka aktivnost novosintetisanih molekula testirana je protiv četiri soja bakterija (*Enterococcus faecalis*, *Escherichia coli*, *Staphylococcus aureus*, i *Salmonella enteritidis*) i četiri soja gljivica (*Candida albicans*, *Fusarium oxysporum*, *Aspergillus brasiliensis*, i *Penicillium canescens*). Na osnovu rezultata dobijenih ovim eksperimentom može se zaključiti da su sintetisani heterocikli pokazali umerenu do slabu antibakterijsku aktivnost protiv testiranih sojeva bakterija. Najveću antibakterijsku aktivnost ispoljila su dva ferocenska derivata, N-butil- i N-tolil-tiazolidintioni, protiv *E. faecalis*. Osim toga, rezultati antimikrobne aktivnosti ukazuju da novosintetisani ferocenski derivati imaju veći antifungalni potencijal.

Ključne reči: ferocetil, 2-ferocetil-1,3-tiazolidin-4-tioni, 2-ferocetil-1,3-tiazolidin-4-oni, karakterizacija, antimikrobna aktivnost.

Synthèse, caractérisation et activité antimicrobienne de nouvelles 2-ferrocényl-1,3-thiazolidine-4-thiones

Todosijević Anka¹, Minić Aleksandra², Mihailović Vladimir³, Srećković Nikola³

1- Université de Niš, Faculté d'agriculture, Kosančićeva 4, 37000 Kruševac, Serbie

2- Université de Priština, Faculté des sciences techniques, Knjaza Miloša 7, 38220 Kosovska Mitrovica, Serbie

3- Université de Kragujevac, Faculté des sciences, Département de chimie, Radoja Domanovića 12, 34000 Kragujevac, Serbie

RÉSUMÉ

La synthèse des cinq nouvelles 2-ferrocényl-1,3-thiazolidine-4-thiones a été réalisée avec des rendements bons à excellents grâce au traitement des 2-ferrocényl-1,3-thiazolidine-4-ones avec le réactif de Lawesson. La réaction a été effectuée en chauffant au reflux le mélange de réactifs dans du toluène pendant une nuit. Tous les composés préparés ont été caractérisés par les données spectrales IR et RMN. De plus, les produits obtenus ont été évalués pour leurs activités antibactérienne et antifongique.

Mots-clés : ferrocène, 2-ferrocényl-1,3-thiazolidin-4-thiones, 2-ferrocényl-1,3-thiazolidin-4-ones, caractérisation, activité antimicrobienne.

Синтез, характеристика и антимикробная активность новых 2-ферроценил-1,3-тиазолидин-4-тионов

Тодосиевич Анка^{1*}, Минич Александра², Михайлович Владимир³, Сречкович Никола³

1- Университет в Нише, Факультет сельского хозяйства, Косанчичева 4, 37000 Крушевац, Сербия

2- Университет в Приштине, Факультет технических наук, Княза Милоша 7, 38220 Косовска Митровица, Сербия

3- Университет в Крагуевце, Естественно-математический факультет, Кафедра химии, Радоя Домановича 12, 34000 Крагуевац, Сербия

АННОТАЦИЯ

Синтез пяти новых 2-ферроценил-1,3-тиазолидин-4-тионов был достигнут с выходами от хороших до отличных за счет обработки 2-ферроценил-1,3-тиазолидин-4-онов реактивом Лавессона. Реакцию проводили путем кипячения смеси реагентов в толуоле в течение ночи. Все полученные соединения охарактеризованы данными ИК- и ЯМР-спектров. Далее полученные продукты оценивали на их антибактериальную и противогрибковую активность.

Ключевые слова: ферроцен, 2-ферроценил-1,3-тиазолидин-4-тионы, 2-ферроценил-1,3-тиазолидин-4-оны, характеристика, антимикробная активность.

Synthese, Charakterisierung und antimikrobielle Aktivität von neuartigen 2-Ferrocenyl-1,3-Thiazolidin-4-thionen

Todosijević Anka¹, Minić Aleksandra², Mihailović Vladimir³, Srećković Nikola³

1- Universität in Niš, Landwirtschaftliche Fakultät, Kosančićeva 4, 37000 Kruševac, Serbien

2- Universität in Priština, Fakultät für Technische Wissenschaften, Knjaza Miloša 7, 38220 Kosovska Mitrovica, Serbien

3- Universität in Kragujevac, Mathematisch-Naturwissenschaftliche Fakultät, Lehrstuhl für Chemie, Radoja Domanovića 12, 34000 Kragujevac, Serbien

ABSTRACT

Ausgehend von entsprechenden 3-Ferrocenyl-1,3-Thiazolidin-4-on wurde eine Reihe neuer 3-Ferrocenyl-1,3-Thiazolidin-4-thion-Derivate synthetisiert. Die synthetisierten Verbindungen wurden durch spektroskopische Analysemethoden (¹H und ¹³C-NMR, IR) vollständig charakterisiert. Im nächsten Schritt wurde die biologische Aktivität der neu synthetisierten Moleküle gegen vier Bakterienstämme (*Enterococcus faecalis*, *Escherichia coli*, *Staphylococcus aureus* und *Salmonella enteritidis*) und vier Pilzstämme (*Candida albicans*, *Fusarium oxysporum*, *Aspergillus brasiliensis* und *Penicillium canescens*) getestet. Basierend auf den Ergebnissen dieses Versuchs wurde festgestellt, dass die synthetisierten Heterocyclen eine mäßige bis schwache antibakterielle Aktivität gegen die getesteten Bakterienstämme aufwiesen. Die höchste antibakterielle Aktivität zeigten zwei Ferrocen-Derivate, N-Butyl- und N-Tolyl-Thiazolidintione, gegen *E. faecalis*. Darüber hinaus weisen die Ergebnisse der antimikrobiellen Aktivität darauf hin, dass neu synthetisierte Ferrocenderivate ein höheres antimykotisches Potential aufweisen.

Schlüsselwörter: Ferrocen, 2-Ferrocenyl-1,3-Thiazolidin-4-thione, 2-Ferrocenyl-1,3-Thiazolidin-4, Charakterisierung, antimikrobielle Aktivität.

Investigation of Electrochemical Behavior of Mordant Dye (C.I. 17135) at Glassy Carbon and Silver Electrodes

Necati Menek^{1*}, Serpil Zeyrekl¹ and Yeliz Karaman²

1- Ondokuz Mayıs University, Sciences and Arts Faculty, Department of Chemistry, 55139, Kurupelit-Samsun, Turkey

2- Sinop University, Sciences and Arts Faculty, Department of Chemistry, 57000, Sinop, Turkey

ABSTRACT

In this study, the electrochemical behaviour of Mordant dye (C.I. 17135) was investigated in Britton-Robinson (BR) buffer (pH 2.0-12.0) media by using different voltammetric techniques: square wave voltammetry (SWV), cyclic voltammetry (CV), differential pulse voltammetry (DPV) and direct current voltammetry (DCV). The electrochemical behavior of the dye has been investigated by using a glassy carbon electrode (GCE) and silver electrode (SE). The broad peak of the azo dye occurred at SW and DP voltammograms, is due to its adsorption on the glassy carbon and silver electrode surfaces. Two reduction peaks were observed at pH < 9.5, and one reduction peak was observed at pH > 9.5 for SWV and DPV techniques at a glassy carbon electrode. From the voltammetric data electrochemical reaction mechanism of the azo dye has been suggested at glassy carbon and silver electrodes.

Keywords: Azo compound, Mordant dyes, Voltammetry, Reaction mechanism.

Necati Menek*: nmenek@omu.edu.tr

Introduction

Azo dyes, which are characterized by the azo functional group (-N=N-), have widespread applications in lots of areas such as textile processing, paper, food, cosmetics, medicine, leather, plastics, varnish, automobiles. The azo dyes are called as monoazo, diazo, triazo, polyazo and azoic dyes, according to the number of azo groups, which is in the same molecule of the dye.

Mordant dyes compose the largest class of synthetic azo dyes, which are extensively employed for the coloration of textile fibers, such as wool, silk, polyester, cotton, and nylon (Yıldız and Boztepe 2002, Pervez et al., 2019). Mordant dyes which contain hydroxyl groups in the ortho position, have capacity to produce metal-dye complexes, by binding the dye molecule to the fibers (Abu-El-Wafa et al., 2005, Ali et al., 2019, Ding and Freeman 2017, Yıldız and Boztepe 2002).

In the literature, there were studies reported about the voltammetric behavior of o-hydroxy azo dyes such as Amaranth and Allura Red AC on silver solid amalgam electrodes and solvent Orange 7 and Eriochrome Black T on glassy carbon electrode and carbon paste electrode, respectively (Chandra et al., 2008, Romanini et al., 2009, Tvorynska et al., 2019).

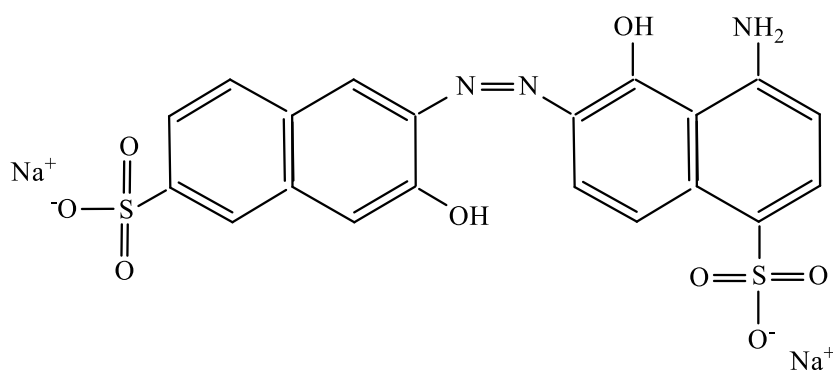
The purpose of this work is to investigate the voltammetric behavior of Mordant dye (C.I. 17135) at a GCE and a SE. The voltammetric techniques employed for the voltammetric analysis of the dye are, SWV, DPV, DCV and CV techniques. At the same time, this present study contributes to previous studies on the voltammetric behavior of azo compounds (Eriksson and Nyholm, 2001, Lucilha et al., 2010, Menek, 1998, Socha et al., 2007). The structure of the Mordant dye (C.I. 17135) is given below (Scheme 1). For Mordant dye (C.I. 17135), no studies have been found so far on glassy carbon and silver electrodes.

Experimental

6-[2-hydroxy-6-sulfonaphthaleneazo]-3-amino-5-hydroxy-1-naphthalene sulfonic acid disodium salt (Mordant dye C.I. 17135) was purchased from Aldrich and employed without further purification. A 10^{-3} M stock solution of Mordant dye was prepared by dissolving weighted mass of solid in deionized water. The BR (0.04 M) buffer solution employed as the supporting electrolyte was prepared by using 0.04 M phosphoric acid, 0.04 M acetic acid and

0.04 M boric acid and fixed to the desired pH with concentrated sodium hydroxide. All chemicals used for buffer preparation were of p.a. purity.

The Metrohm 757 VA Computrace Electrochemical Analyser was used for the voltammetric measurements of Mordant dye at room temperature. A three-electrode system was employed which consisted of a working electrode (GCE and SE), a Ag/AgCl (saturated KCl) reference electrode and a platinum wire auxiliary electrode. Voltammetric experiments were carried out in the voltammetric cell, where nitrogen gas was passed through the solution for five minutes before the experiments. SWV, DPV, DCV and CV techniques were employed for the voltammetric analysis of the dye. The experimental parameters for the SWV, DPV, DCV and CV techniques were pulse amplitude, 50 mV and potential step 4 mV, DPV was recorded at $v = 4$ mV/s and pulse time 1 s. For the SWV technique, frequency was 50 Hz and $v = 200$ mV/s.



Scheme 1. Molecular structure of the Mordant dye (C.I. 17135), (6-[2-hydroxyl-6-sulfonaphthaleneazo]-3-amino-5-hydroxy-1-naphthalene sulfonic acid disodium salt).

Results and discussion

Glassy carbon electrode

SWV and DPV studies

The SW and DP voltammograms of the Mordant dye in BR (pH 2.0-12.0) buffer are presented in Figs. 1 and 3. Two reduction peaks were observed at $\text{pH} < 9.5$, and one reduction peak was observed at $\text{pH} > 9.5$ for SWV and DPV techniques (Fig. 1). The presence of two peaks at $\text{pH} < 9.5$ and a single reduction peak at $\text{pH} > 9.5$, indicated that two-step electrode reaction occurred at $\text{pH} < 9.5$ and one-step electrode reaction occurred at $\text{pH} > 9.5$. The observed shift of the reduction peaks to more negative potentials with increasing pH indicates that protons are involved in the electrode reaction (Fig.2). For SWV and DPV techniques, the current values of the first peak in the acidic media, was much greater than the current values of

the second peak in the acidic media. Especially in voltammograms obtained in the basic media, the current values are quite low for both peaks (Fig. 1). As seen in Fig. 1, the broad peak of the azo dye occurred is due to its adsorption on the electrode surface (Char et al., 2008, Karaman and Menek, 2012, Karaman, 2014, Ma and Song, 2008, Mirceski and Lovri, 2004, Sun et al., 2005). The linear regression equations of azo dye between the peak potentials and pH were given for the SWV and DPV techniques, respectively, in BR buffer media (Table 1). The data given in Figures 1, 2 and Table 1, show that the addition of protons occurs in the reduction reaction.

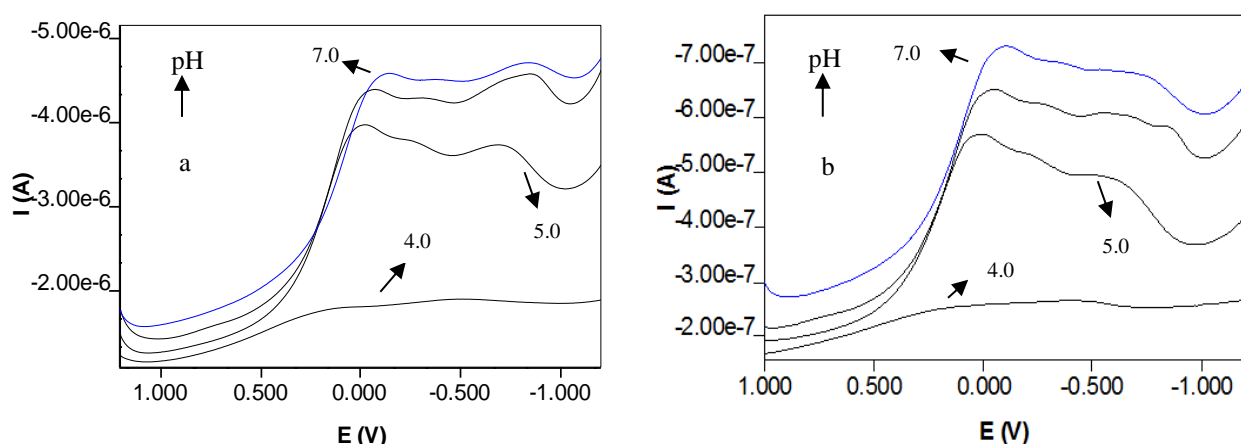


Figure 1. a) SWV b) DP voltammograms of 4.76×10^{-5} M Mordant dye in BR buffer (0.04 M) pH 4.0, 5.0, 6.0 and 7.0, at GCE.

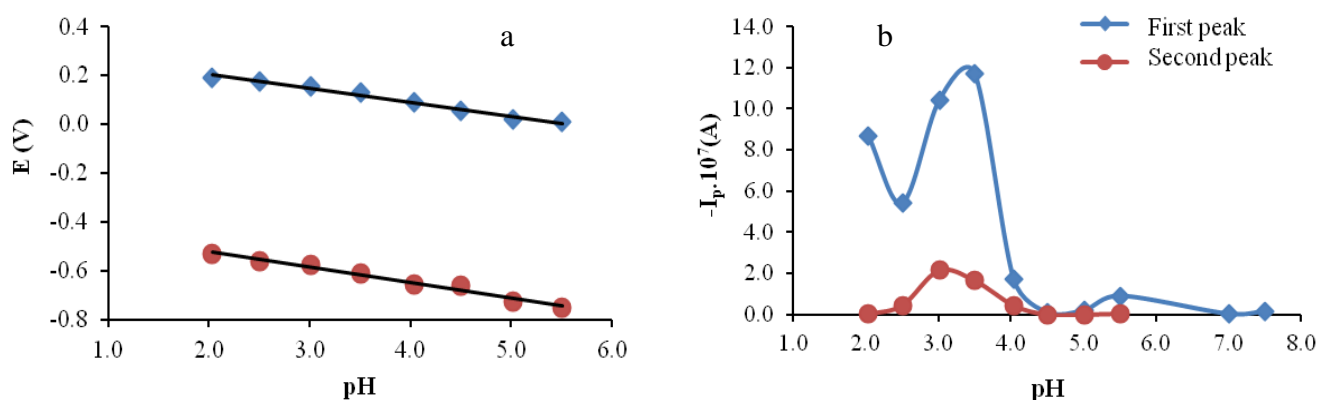


Figure 2. The change in a) cathodic peak potentials and b) cathodic peak currents versus pH in BR buffer obtained for 4.76×10^{-5} M Mordant dye using SWV technique at GCE.

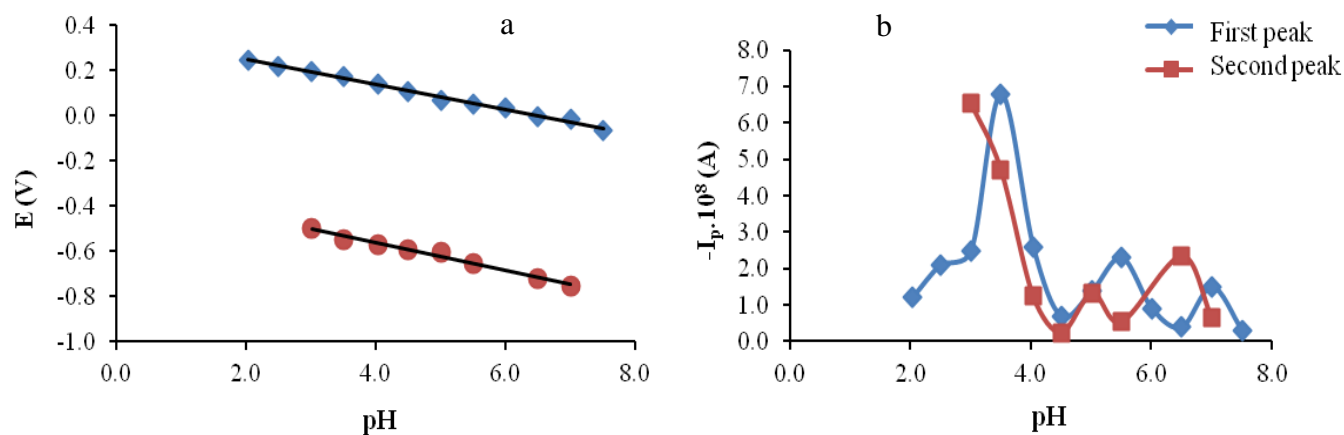


Figure 3. The change in a) cathodic peak potentials and b) cathodic peak currents versus pH in BR buffer obtained for 4.76×10^{-5} M Mordant dye using the DPV technique at GCE.

Table 1. The change in peak potentials with pH.

Medium	Electrode	Peak	Peak equation	r^2 (Regression coefficient)	Technique
BR buffer (pH 2.0-5.5)	GCE	First peak	E_p (V) = $0.317 - 0.0567pH$	0.988	SWV
BR buffer (pH 2.0-5.5)	GCE	Second peak	E_p (V) = $-0.3963 - 0.063pH$	0.981	SWV
BR buffer (pH 2.0-7.5)	GCE	First peak	E_p (V) = $0.3856 - 0.0617pH$	0.989	DPV
BR buffer (pH 2.0-7.0)	GCE	Second peak	E_p (V) = $-0.3182 - 0.0618pH$	0.995	DPV
BR buffer (pH 2.0-12.0)	SE	First wave	$E_{1/2}$ (V) = $-0.0228 - 0.0464pH$	0.983	DCV
BR buffer (pH 3.0-12.0)	SE	Second wave	$E_{1/2}$ (V) = $-0.1454 - 0.0709pH$	0.957	DCV

DCV studies

DC voltammograms of the azo dye in BR buffer media were also studied. One broad reduction wave was observed in the pH range of 2.0 to 12.0. The dependence of the peak potential on pH is given in Table 1. The limiting current is approximately constant in neutral and basic media. Electron transfer coefficient (α) was calculated from the Heyrovsky Ilkovic equation. The change α n versus pH is given in Figure 4. The α n values are below 1.0 at all pH values.

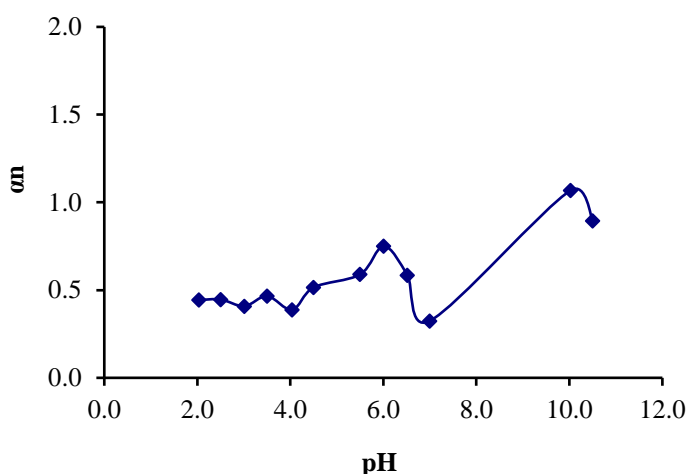


Figure 4. The change in αn with pH for Mordant dye in BR buffer with a GCE.

CV studies

To investigate the electrochemical behavior of the azo dyes, cyclic voltammetry is an important technique that give information about the reversibility or irreversibility of the electrode reactions. For this purpose, the CV voltammograms obtained in BR buffer (pH 2.0-12.0) are given in Fig. 5. During the cathodic potential sweep from 1.2 to -1.2 V, two cathodic peaks (1c, 2c) were seen at 0.097 V and -0.617 V for pH 3.0 in B-R buffer, which were attributed to the reduction of the azo group to amines in acidic media. On the reverse scan from -1.2 to 1.2 V, small corresponding anodic peaks (1a, 2a) were observed at 0.319 and 0.692V for pH 3.0 in BR buffer which were attributed to the oxidation of phenolic hydroxyl groups in the Mordant dye (Fig. 5) (Hattori et al.,2006, Karaman, 2014). As stated in previous studies, amines were produced with the reduction of the azo compounds, which have hydroxyl groups adjacent to an azo group, which was most likely to be reoxidized in the return scan (Yu et al.,

2004). One reduction peak was observed in cathodic scan and one anodic peak was seen in reverse scan in basic media. Peak currents have a sharp increase and decrease in the pH range of 2.0-4.0. After pH 4.0, in the absence of the second peak, the first peak current values increase with increasing pH (Fig. 6).

The peak potential values shifted to more negative values with increasing pH, indicated that protons are involved in the electrode reaction (Fig. 6).

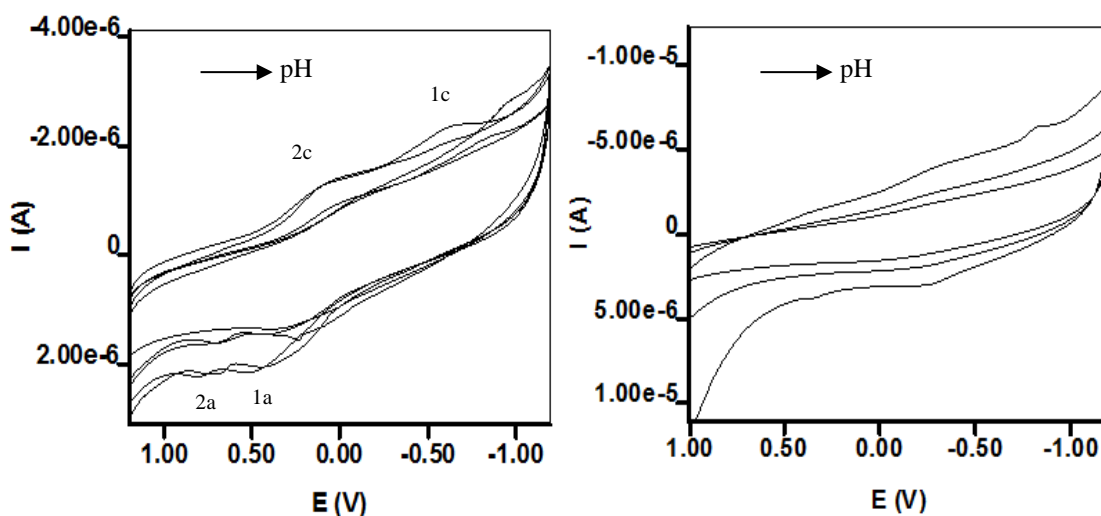


Figure 5. CV voltammograms of 4.76×10^{-5} M Mordant dye in BR (0.04 M) buffer at GCE a) pH 2.0, 3.0, 4.0, 5.0, and 6.0 b) pH 9.5, 10.0 and 10.5.

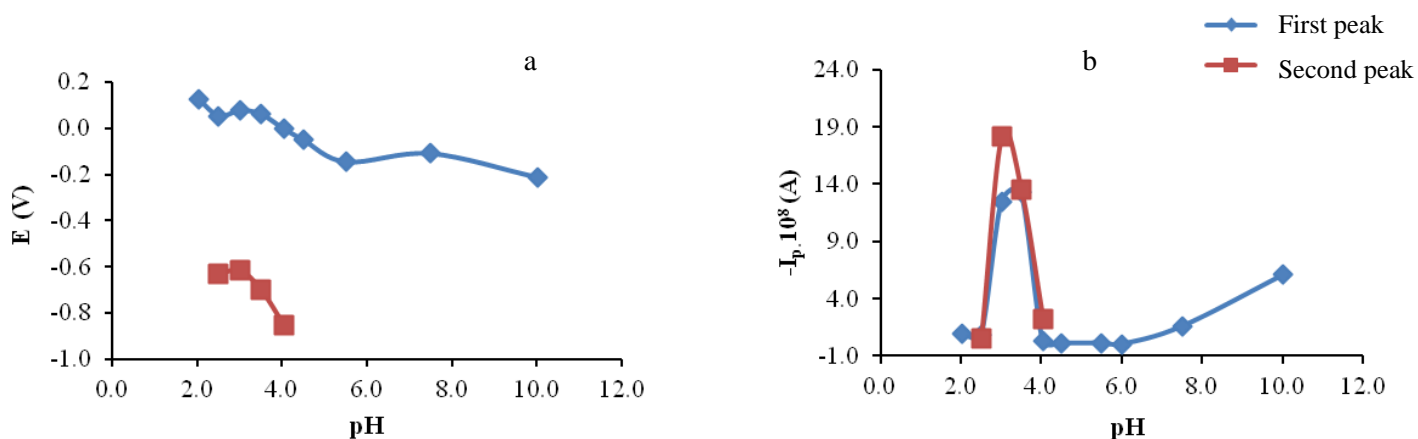


Figure 6. The change in a) cathodic peak potentials and b) cathodic peak currents versus pH in BR buffer obtained for 4.76×10^{-5} M Mordant dye using CV technique at GCE, $\nu = 200$ mV/s.

The effect of square root of scan rate ($\nu = 20\text{-}1000$ mV/s) on the peak current of the dye at a GCE was examined in BR buffer at different pH values (pH 3.0, 4.5, 6.0 and 7.0) (Fig. 7). Two reduction peaks were observed at pH 3.0 and one reduction peak was observed at pH 4.5, 6.0 and 7.0. The I_p versus $\nu^{1/2}$ relation is not linear, and the $I_p/\nu^{1/2}$ slope increases with increasing scan rate. This result confirms that the azo compound has an adsorption controlled reaction on the electrode surface (Char et al., 2008, Guaratini et al., 2001).

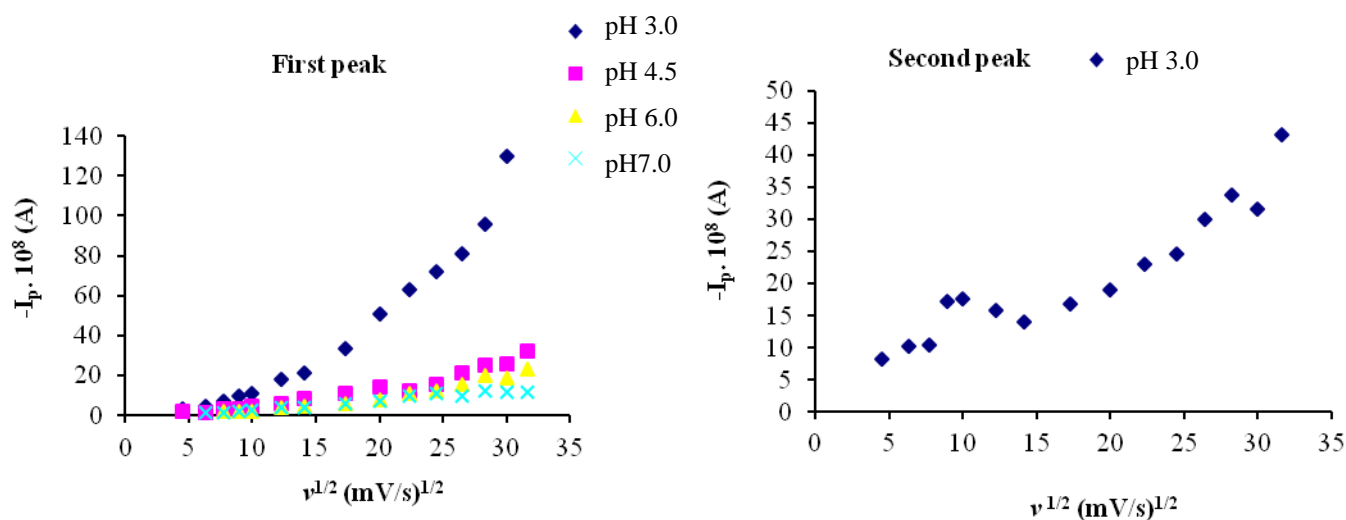


Figure 7. The change in cathodic peak currents with square root of scan rate at different pH values at GCE for 4.76×10^{-5} M Mordant dye in BR buffer, $\nu = 20\text{-}1000$ mV/s.

Small anodic peaks were observed at acidic and neutral pH. However, the exponential dependence of peak current with the square root of scan rate is evidence of the kinetic controlling reaction occurring. This indicates that the reaction mechanism is complex.

Silver Electrode

SWV and DPV studies

The SW and DP voltammograms of the Mordant dye in BR (pH 2.0-12.0) buffer are presented in Figure 8. Two reduction peaks were seen at pH 6.0, 7.0, 9.5 and 11.0 for SWV technique and two reduction peaks were observed at pH 3.0, 4.0, 5.0, 6.0, 7.0, 8.0 and 9.0 for DPV technique (Fig. 8). The presence of two peaks indicated that two-step electrode reaction occurred at the electrode surface. As seen in Fig. 8, the broad peak of the azo dye occurred is

due to its adsorption on the electrode surface (Char et al., 2008, Karaman and Menek, 2012, Ma and Song, 2008, Mirceski and Lovri, 2004, Sun et al., 2005).

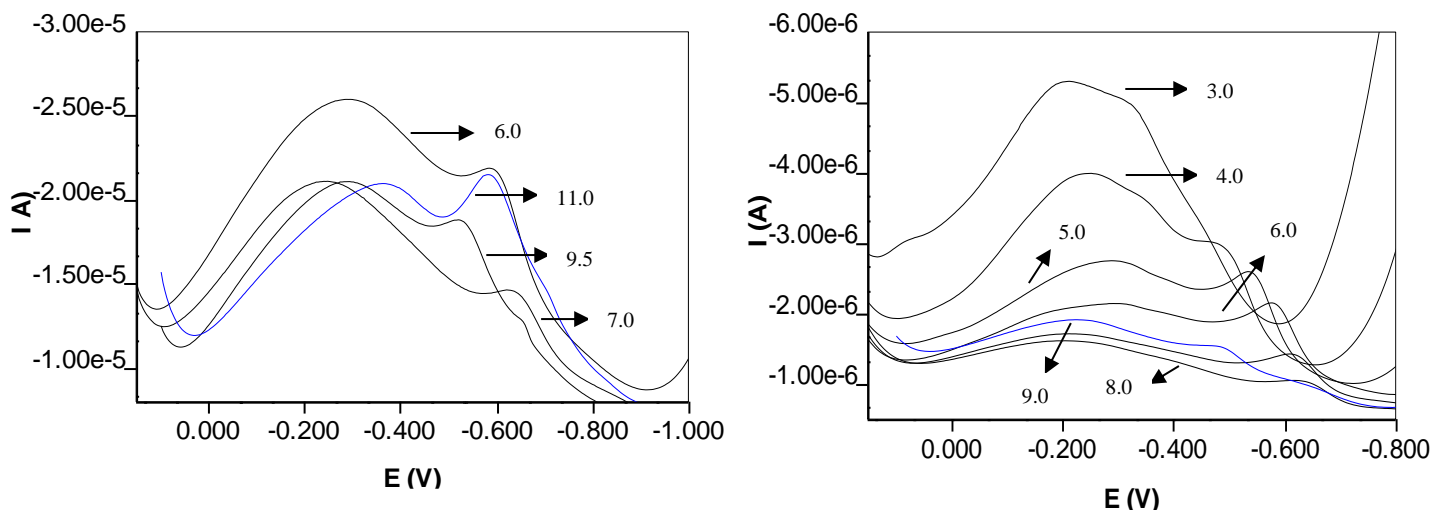


Figure 8. Voltammograms of 4.76×10^{-5} M Mordant dye in BR buffer (0.04 M) at SE a) SWV, (pH 6.0, 7.0, 9.5 and 11.0, $\nu = 200$ mV/s) and b) DPV (pH 3.0, 4.0, 5.0, 6.0, 7.0, 8.0 and 9.0).

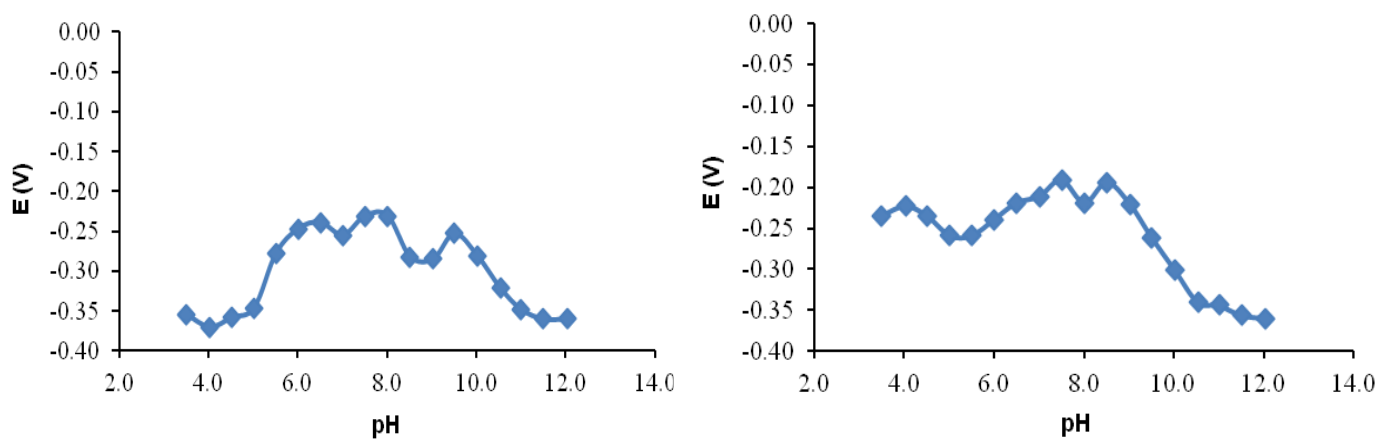


Figure 9. The change in cathodic peak potentials versus pH in BR buffer for Mordant dye at SE a) SWV, b) DPV.

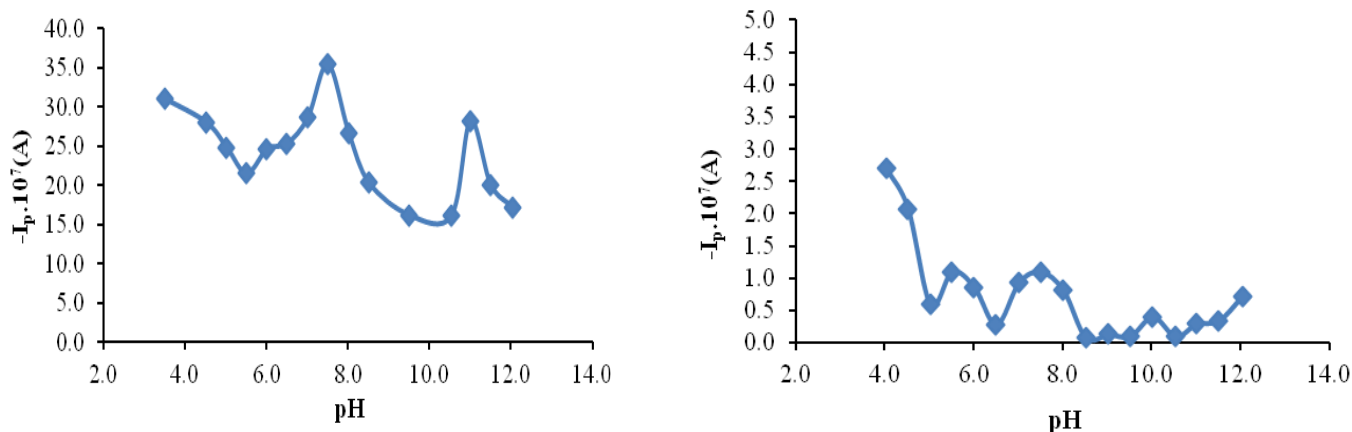


Figure 10. The change in cathodic peak currents versus pH in BR buffer for Mordant dye at SE a) SWV, b) DPV.

The change in peak currents versus pH for the azo dye is approximately constant in the range of pH 6.0-9.0 and decreases after pH 9.5 for the SWV technique. However, in DPV technique, it is seen that the peak potential is almost constant in the range of pH 3.5-9.0 and decreases at higher pH values (Fig. 9). As seen in SW and DP voltammograms (Figs. 9, 10), after pH 3.0, the brode peak was observed at negative potentials. These results indicates that there is a two step reduction reaction occurs on the electrode surface.

DCV studies

DC voltammograms of the azo dye in BR buffer are shown in Fig. 11. Two reduction waves were seen after pH 3.0 and at pH > 9.0, while one reduction wave was observed at pH 7.0-9.0. As seen in Fig. 11, first and second reduction wave potentials of the dye shifted to more negative values with increasing pH, showed that protons are involved in the electrode reaction. The linear regression equations of azo dye between the half wave potentials and pH were given for the DCV technique in BR buffer media (Table 1).

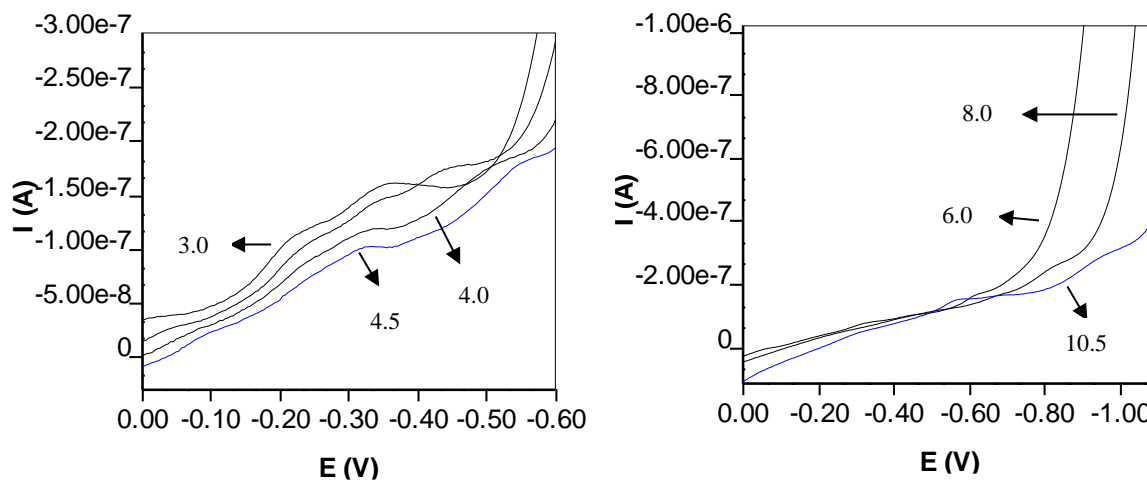


Figure 11. DC voltammograms of 4.76×10^{-5} M Mordant dye in BR (0.04 M) buffer at SE a) pH 3.0, 3.5, 4.0 and 4.5 b) pH 6.0, 8.0 and 10.5

The αn values were calculated from the logarithmic analyses of the reduction waves by using the Heyrovsky-Ilkovic equation in BR buffer (2.0–12.0). (Bard and Faulkner, 1980, Karaman, 2014, Meites, 1965, Zuman and Perin, 1965). The αn values of the second wave in the acidic region (pH 3.0, 3.5 and 4.0) are greater than the αn values of the first wave, although both give similar results in the basic region (pH 10.0, 10.5 and 11.0) (Fig. 12).

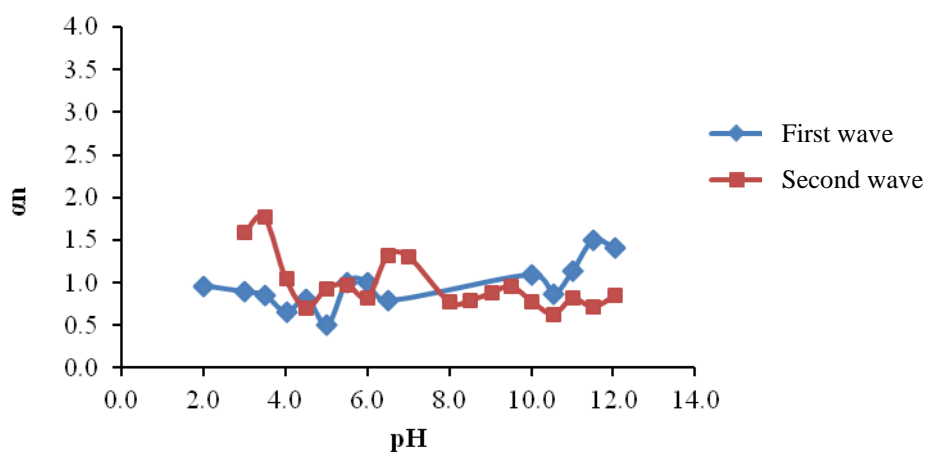


Figure 12. The change in αn with pH for Mordant dye in BR buffer recorded at SE.

CV studies

CV voltammograms recorded in BR buffer (pH 2.0-12.0) are given in Fig. 13. Two reduction peaks were observed in cathodic scan, which was attributed to the reduction of the azo group to amines in acidic media, and two anodic peaks were observed in reverse scan in acidic media. One reduction peak was observed in cathodic scan and one anodic peak was seen in reverse scan in basic media.

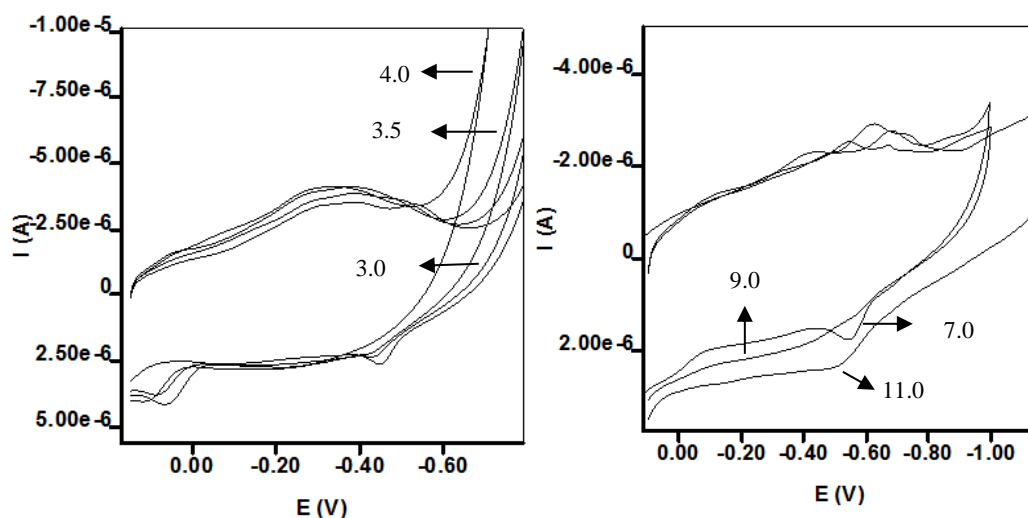


Figure 13. CV voltammograms of 4.76×10^{-5} M Mordant dye in BR (0.04 M) buffer at SE a) pH 2.0, 3.0, 3.5, and 4.0, b) pH 7.0, 9.0 and 11.0 solutions.

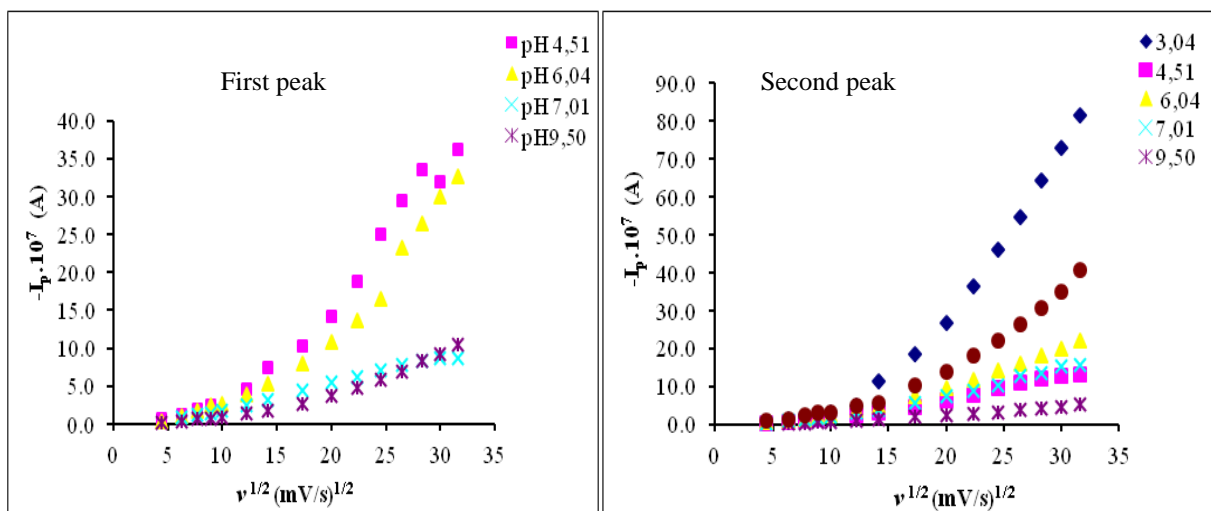
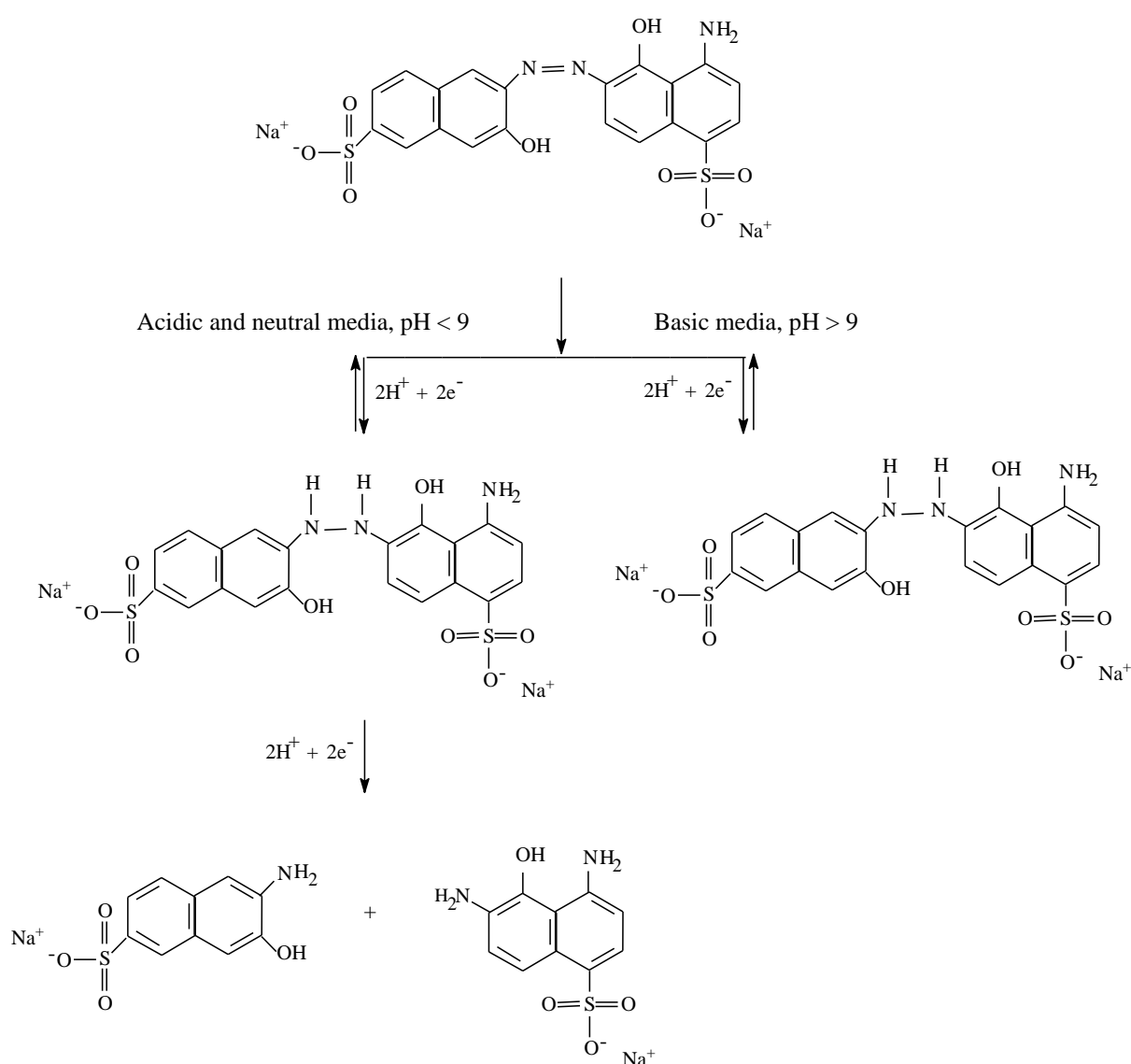


Figure 14. a) The change in cathodic peak currents of Mordant dye with square root of scan rate at different pHs at SE, $v = 20$ -1000 mV/s.

The effect of square root of scan rate ($\nu = 20-1000$ mV/s) on the cathodic peak currents of the dye at a SE was examined in BR buffer at different pH values (Fig. 14). Two reduction peaks were observed at pH 4.5, 6.0, 7.0, 9.5 and 11.0 and one reduction peak was observed at pH 3.0. The linear relation of cathodic peak currents versus ν with increasing scan rate, indicating that the azo compound has an adsorption-controlled reaction on the electrode surface (Char et al., 2008, Guaratini et al., 2001, Yu et al., 2004). The reaction mechanism of Mordant dye at glassy carbon and silver electrodes, has been proposed from the voltammetric data (Scheme 2).



Scheme 2. The proposed reaction mechanism of Mordant dye.

Conclusions

The electrochemical behavior of Mordant dye at a glassy carbon electrode and silver electrode has been studied in BR buffer (pH 2.0-12.0) media by using SWV, DPV, DCV and CV techniques. Two reduction peaks were observed at pH < 9.5, and one reduction peak was observed at pH > 9.5 for SWV and DPV techniques with a glassy carbon electrode and silver electrode. The presence of two peaks at pH < 9.5 and a single reduction peak at pH > 9.5, indicated that two-step electrode reaction occurred at pH < 9.5 and one-step electrode reaction occurred at pH > 9.5. The effect of the scan rate on the peak current studies, indicates that the electrode process of the dye at glassy carbon and silver electrodes is adsorption controlled. It was observed from SWV, DPV, DCV and CV techniques that reduction reaction of the Mordant dye corresponds to the cleavage of the azo bond to give the reductive amines.

Conflict-of-Interest Statement:

None.

References

- Abu-El-Wafa, S. M., El-Wakiel, N. A., Issa, R. M., & Mansour, R. A. (2005). Formation of novel mono- and multi-nuclear complexes of Mn(II), Co(II) and Cu(II) with bis azo-dianils containing the pyrimidine moiety: Thermal, magnetic and spectral studies. *Journal of Coordination Chemistry*, 58, 683-694.
- Ali, Dr. N. F., EL-Khatib, E. M., Saadia, A., & El-Megied A. (2019). Modification of wool and silk fibers by pretreatment with quaternary ammonium salt and dyeing with new metal complex dye. *World Journal of Pharmaceutical and Life Sciences*, 5, 73-79.
- Bard, A. J. & Faulkner, L. R. (1980). *Electrochemical Methods*, JohnWiley & Sons, New York.
- Chandra, U., Gilbert, O., Kumara Swamy, B. E., Bodke, Y. D., & Sherigara, B. S. (2008). Electrochemical studies of Eriochrome Black T at carbon paste electrode and immobilized by SDS surfactant: A cyclic voltammetric study. *International Journal of Electrochemical Science*, 3, 1044-1054.
- Char, M. P., Niranjana, E., Kumara Swamy, B. E., Sherigara, B. S., & Pai, V. (2008). Electrochemical studies of Amaranth at surfactant modified carbon paste electrode: A cyclic voltammetry. *International Journal of Electrochemical Science*, 3, 588-596.

Ding, Y.& Freeman, H. S. (2017). Mordant Dye application on cotton: optimisation and combination with natural dyes. *Coloration Technology*, 133, 369-375.

Eriksson, A.,& Nyholm, L. (2001). Coulometric and spectroscopic investigations of the oxidation and reduction of some azosalicylic acids at glassy carbon electrodes. *Electrochimica Acta*, 496, 1113-1129.

Guaratini, C. C. I., Fogg, A. G., & Zanoni, M. V. B. 2001. Studies of the Voltammetric Behavior and Determination of Diazo Reactive Dyes at Mercury Electrode. *Electroanalysis*, 13, 1535-1543.

Hattori, T., Tsurumi, N., Kato R., & Nakayama M. (2006). Adsorptive voltammetry of 2-(5-bromo-2-pyridyl)azo-5-[N-n-propyl-N-(3-sulfopropyl)amino]phenol on a carbon paste electrode in the presence of organic cations and polycation. *Analytical Science*, 22, 1577-1580.

Karaman, Y., & Menek, N. (2012). Investigation of electrochemical behavior of 2-(5-bromo-2-pyridylazo)-5-[N-propyl-N-(3-sulfopropyl)amino]phenol disodium salt dihydrate. *Journal of the Electrochemical Society*, 159, H805-H810.

Karaman, Y. (2014). Investigation of electrochemical behavior of Calmagite at a glassy carbon electrode. *Dyes and Pigments*, 106, 39-44.

Lucilha, A. C., Bonancêa, C. E., Barretoc, W. J., & Takashima, K. (2010). Adsorption of the Diazo Dye Direct Red 23 onto a zinc oxide surface: A spectroscopic study. *Spectrochimica Acta Part A*, 75, 389-393.

Ma, M. M., & Song, J. F. (2008). Square wave voltammetric label-free determination of the natural protein material silk fibroin. *Chinese Journal of Chemistry*, 26, 2081-2085.

Meites, L. (1965). *Polarographic Techniques*. John Wiley & Sons, New York.

Menek, N. (1998). Polarographic and voltammetric behaviour of 2-hydroxy-3-methoxy-5-(2-propenyl)azobenzene. *Analytical Letters*, 31, 275-282.

Mirceski, V., & Lovri, M. (2004). EC mechanism of an adsorbed redox couple. Volume vs surface chemical reaction. *Journal of Electroanalytical Chemistry*, 565, 191-202.

Pervez, M. N., Telegin, F. Y., Cai, Y., Dongsheng, Xia, D., Zarra, T., & Naddeo, V. (2019). Efficient degradation of Mordant Blue 9 using the fenton-activated persulfate system. *Water*, 11, 2532-2546.

Romanini, D. C., Trindade, M. G. A., & Zanoni, M. V. B. (2009). A simple electroanalytical method for the analysis of the dye solvent orange 7 in fuel ethanol. *Fuel*, 88: 105-109.

Socha, A., Sochocka, E., Podsiadły, R., & Sokolowska, J. (2007). Electrochemical and photoelectrochemical treatment of C.I. Acid Violet 1. *Dyes and Pigments*, 73, 390-393.

Sun, W., Jiang, H., & Jiao, K. (2005). Electrochemical determination of hydrogen peroxide using o-dianisidine as substrate and hemoglobin as catalyst, *Journal of Chemical Science*, 117, 317–322.

Tvorynska, S., Josypcuk, B., Jiri Barek, J., & Liliya Dubenska, L. (2019). Electrochemical behavior and sensitive methods of the voltammetric determination of food azo dyes Amaranth and Allura Red AC on amalgam electrodes. *Food Analytical Methods*, 12, 409-421.

Yıldız, E., & Boztepe, H. (2002). Synthesis of novel acidic mono azo dyes and an investigation of their use in the textile industry. *Turkish Journal of Chemistry*, 26, 897-903.

Yu, J., Jia, J., & Ma, Z. (2004). Comparison of electrochemical behavior of hydroxyl-substituted and nonhydroxyl-substituted azo dyes at a glassy carbon electrode. *Journal of the Chinese Chemical Society*, 51, 1319-1324.

Zuman, P., & Perin, C. L. (1965). *Organic Polarography*. John Wiley & Sons, New York.

Istraživanje elektrohemijskog ponašanja Mordant boje (C.I. 17135) na staklenim ugljeničnim i srebrnim elektrodama

Necati Menek^{1*}, Serpil Zeirekli¹, Jeliz Karaman²

1- Univerzitet Ondokuz Mais, Fakultet nauka i umetnosti, Departman za hemiju, 55139, Kurupelit-Samsun, Turska

2- Sinop Univerzitet, Fakultet nauka i umetnosti, Departman za hemiju, 57000, Sinop, Turska

SAŽETAK

U ovoj studiji je ispitivano elektrohemijsko ponašanje Mordant boje (CI 17135) u puferu Briton-Robinson (BR) (pH 2,0-12,0) različitim voltametrijskim tehnikama: voltametrija kvadratnog talasa (SVV), ciklična voltametrija (CV), diferencijalna impulsna voltametrija (DPV) i voltametrija jednosmerne struje (DCV). Elektrohemijsko ponašanje boje ispitano je upotrebom staklene ugljenične elektrode (GCE) i srebrne elektrode (SE). Široki vrh azo boje nastao je na SV i DP voltamogramima, zbog njegove adsorpcije na staklenim površinama ugljenične i srebrne elektrode. Dva redukciona pika su primećena pri pH <9,5, a jedan redukcioni pik je primećen pri pH > 9,5 za SVV i DPV tehnike na staklenoj ugljeničnoj elektrodi. Prema voltametrijskim podacima, predložen je elektrohemijski mehanizam reakcije azo boje na staklenim ugljeničnim i srebrnim elektrodama.

Ključne reči: Azo jedinjenje, Mordant boje, voltametrija, mehanizam reakcije.

Enquête sur le comportement électrochimique du colorant Mordant (C.I. 17135) aux électrodes de carbone vitreux et d'argent

Necati Menek^{1*}, Serpil Zeyrekli¹, Yeliz Karaman²

1- Université Ondokuz Mayıs, Faculté des sciences et des arts, Département de chimie, 55139, Kurupelit-Samsun, Turquie

2- Sinop Université, Faculté des sciences et des arts, Département de chimie, 57000, Sinop, Turquie

ABSTRACT

Dans cette étude, le comportement électrochimique du colorant Mordant (CI 17135) a été examiné dans un milieu tampon Britton-Robinson (BR) (pH 2,0-12,0) en utilisant les différentes techniques de voltampérométrie : la voltamétrie à onde carrée (SWV), la voltamétrie cyclique (CV), la voltamétrie différentielle à impulsions (DPV) et la voltamétrie à courant continu (DCV). Le comportement électrochimique du colorant a été recherché au moyen de l'électrode de carbone vitreux (GCE) et de l'électrode d'argent (SE). Le pic large du colorant azoïque survenu aux voltamogrammes SW et DP est dû à son adsorption sur les surfaces vitreuses des électrodes en carbone et en argent. Les deux pics de réduction ont été observés à $\text{pH} < 9,5$, tandis qu'un pic de réduction a été observé à $\text{pH} > 9,5$ pour les techniques SWV et DPV sur une électrode en carbone vitreux. Suivant les données voltamétriques, le mécanisme électrochimique de la réaction du colorant azoïque a été suggéré au niveau des électrodes de carbone vitreux et d'argent.

Mots-clés : Composé azoïque, Colorants mordants, Voltamétrie, Mécanisme de réaction.

Исследование электрохимического поведения красителя протравы (С.I. 17135) на стеклоуглеродных и серебряных электродах

Нечати Менек^{1*}, Серпил Зейрекли¹, Елиз Караман²

1-Университет Ондокуз Майис, Факультет наук и искусств, Кафедра химии, 55139, Курупелит-Самсун, Турция

2-Синопский университет, Факультет наук и искусств, Кафедра химии, 57000, Синоп, Турция

АННОТАЦИЯ

В этом исследовании электрохимическое поведение красителя протравы (СI 17135) было исследовано в среде с буфером Бриттона-Робинсона (BR) (рН 2,0-12,0) с использованием различных вольтамперометрических методов: прямоугольной вольтамперометрии (СВВ), циклической вольтамперометрии (ЦВ), дифференциальной импульсной вольтамперометрии (ДПВ) и вольтамперометрией постоянного тока (ДЦВ). Электрохимическое поведение красителя было исследовано с использованием стеклоуглеродного электрода (СУЕ) и серебряного электрода (СЕ). Широкий пик азокрасителя, возникающий на вольтамперограммах СВ и ДП, связан с его адсорбцией на поверхности стеклоуглерода и серебряного электрода. Два пика восстановления наблюдали при рН <9,5, и один пик при рН > 9,5 для методов СВВ и ДПВ на стеклоуглеродном электроде. На основании данных вольтамперометрии был предложен механизм электрохимической реакции азокрасителя на стеклоуглеродных и серебряных электродах.

Ключевые слова: азосоединение, протравы, вольтамперометрия, механизм реакции.

Untersuchung zum elektrochemischen Verhalten von Mordant-Farbstoff (C.I. 17135) an Glaskohlenstoff- und Silberelektroden

Necati Menek^{1*}, Serpil Zeyrekli¹, Yeliz Karaman²

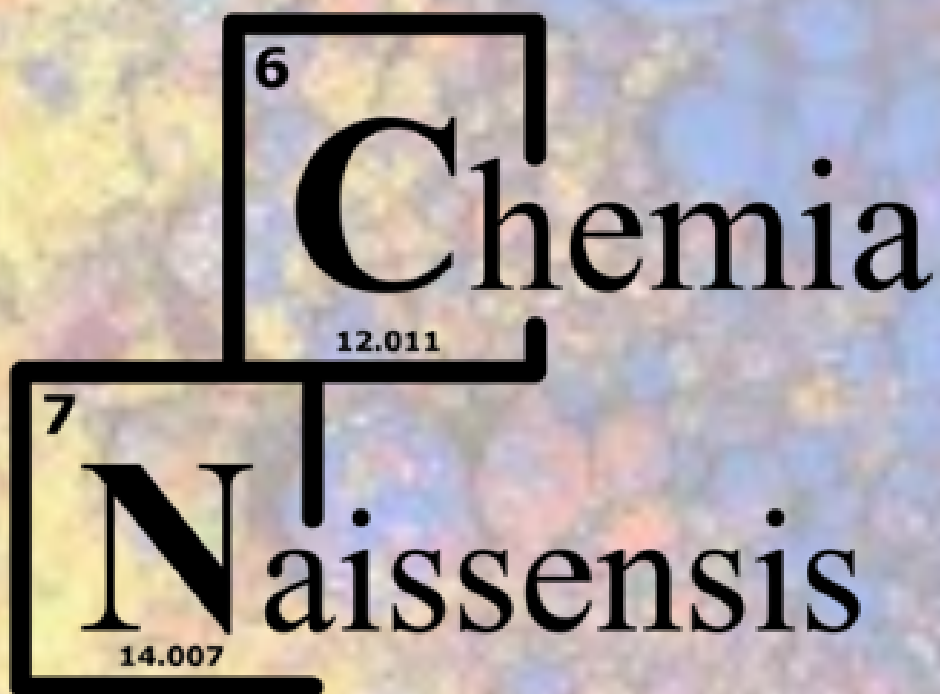
1- Ondokuz Mayıs Üniversitesi, Fakülte für Wissenschaften und Kunst, Lehrstuhl für Chemie, 55139, Kurupelit-Samsun, Türkei

2- Sinop Üniversitesi, Fakülte für Wissenschaften und Kunst, Lehrstuhl für Chemie, 57000, Sinop, Türkei

ABSTRACT

In dieser Studie wurde das elektrochemische Verhalten von Mordant-Farbstoff (CI 17135) in Britton-Robinson (BR)-Puffer (pH 2,0-12,0) unter Verwendung verschiedener voltammetrischer Techniken untersucht: Rechteckwellenvoltammetrie (SWV), zyklische Voltammetrie (CV), Differenzpulsvoltammetrie (DPV) und Gleichstromvoltammetrie (DCV). Das elektrochemische Verhalten des Farbstoffs wurde unter Verwendung einer Glaskohlenstoffelektrode (GCE) und einer Silberelektrode (SE) untersucht. Der breite Peak des Azofarbstoffs, der bei SW- und DP-Voltamogrammen auftrat, ist auf seine Adsorption an den Glasoberflächen der Kohlenstoff- und Silberelektrode zurückzuführen. Bei $\text{pH} < 9,5$ wurden zwei Reduktionspeaks beobachtet, und ein Reduktionspeak wurde bei $\text{pH} > 9,5$ für SVV- und DPV-Techniken an einer Glaskohlenstoffelektrode beobachtet. Nach den voltammetrischen Daten wurde ein elektrochemischer Reaktionsmechanismus des Azofarbstoffs an Glaskohlenstoff- und Silberelektroden vorgeschlagen.

Schlüsselwörter: Azoverbindung, Beizenfarbstoffe, Voltammetrie, Reaktionsmechanismus



ISSN 2620-1895